GEOLOGICAL INVESTIGATION OF LAND INSTABILITY BETWEEN KOHIMA AND ZHADIMA

SUPONGTEMJEN

DEPARTMENT OF GEOLOGY
NAGALAND UNIVERSITY

NAGALAND UNIVERSITY

October 2012

DECLARATION

I, Mr. Supongtemjen, hereby declare that the subject matter of this thesis is the record of work done by me, that the contents of this thesis did not form basis of the award of any previous degree to me or to the best of my knowledge to anybody else, and that the thesis has not been submitted by me for any research degree in any other University/Institute.

This is being submitted to the Nagaland University for the Degree of Doctor of Philosophy in Geology.

Candidate

Head

Supervisor

NAGALAND UNIVERSITY

Glenn T. Thong
Professor of Geology

☎/Fax : 0370-2240515
Mobile : 09436000479
E-mail : glen2t03@yahoo.com
nagalandslide@yahoo.com

Dated Kohima the 22nd October 2012

CERTIFICATE

The thesis presented by Mr. Supongtemjen, M.Sc., bearing Registration No. 274/2007 (24th November 2006) embodies the results of investigations carried out by him under my supervision and guidance.

I certify that this work has not been presented for any degree elsewhere and that the candidate has fulfilled all conditions laid down by the University.

(G.T. THONG)
Supervisor

PREFACE

Kohima, the capital of Nagaland is one of the oldest among the eleven districts of the state. Due to rapid growth of population and accelerated urbanization the Government of Nagaland has initiated further expansion of the township towards the north of the township. However, developmental activities are taking place without any scientific involvement.

Keeping this in mind, this study has been undertaken to develop a landslide hazard zonation (LHZ) map and make a risk assessment of some weak zones along the highway to provide mitigation measures. In this connection numerous maps have been generated using GIS applications, taking into consideration all geological aspects associated with landslides.

Extensive field surveys have been conducted to map geological structures, litho-units, groundwater condition, and land use / land cover. Satellite imagery is used to identify structural features and landslide incidences are marked with a hand-held GPS.

This study is carried out following the recommendations of the Bureau of Indian Standard that has been duly modified to suit the study area. All parameters that cause landslides in this area such as lithology, soil cover, structure, slope angle, groundwater condition, land use / land cover, etc. are used in this study. Most of the landslides in the area take place during the monsoon so attempts were made to correlate landslides with rainfall; however the exact temporal relation could not be derived due to paucity of landslide as well as rainfall data.

A LHZ map on 1:4000 scale is generated based on the results of the above mentioned parameters. Landslide incidences are overlaid on LHZ to study their relationship and validate results. Rock and slope mass rating of slope material in the slide areas have been estimated and kinematic analysis performed to understand the probable mode of failure. Data generated have been interpreted in terms of failure type and potential. Suitable recommendations have been made for such areas.

It is hoped that the concerned agencies will use the LHZ map as a base on which to start developmental activities and adopt the recommendations provided to enhance slope stability and reduce risk.

ACKNOWLEDGEMENT

Foremost thanks to my supervisor Prof. G.T. Thong, Department of Geology, Nagaland University for his constant guidance throughout my research work. He has been an inspiration in this scientific research through trials and adventure. I am grateful and remain indebted to Dr. Imtiwapang Aier, for his contribution and expertise in geotechnical analysis throughout this work.

I would like to extend my special thanks to Prof. S. Ibotombi and Dr. M. Pradipchandra Singh, Department of Earth Sciences, Manipur University for the point load test facilities.

I express my sincere thanks to Mrs. Azonuo Thong for her support and motherly treatment rendered towards me throughout the research work.

I owe my loving thanks to my parents and family members. Without their love, support, encouragement, and understanding it would not have been possible for me to finish this work.

(SUPONGTEMJEN)

LIST OF TABLES

LIST OF FIGURES

LIST OF PLATES

CONTENTS

CHAPTER 1

INTRODUCTION

Nagaland lies in the far northeastern part of the Indian subcontinent bordering the states of Assam in the west, Arunachal Pradesh in the north, and Manipur in the south. It shares an international boundary with Myanmar on the east. It lies between 93°19' & 95°15' east longitudes and 25°11' & 27°02' north latitudes. Nagaland came into existence as the 16th state of the Indian Union on 1st December 1963. It occupies an area of 16,579 sq km and, according to the 2011 census, has a population of 1980,602. The topography of this hilly state is very severe, comprising hilly ranges that break into a wide chaos of spurs and ridges, except for the low-lying alluvial tracts bordering the Assam valley. Mount Saramati with a height of 3,841 m is the highest peak in Nagaland; its range forms a natural barrier between Nagaland and Myanmar.

Geographically Nagaland represents part of a highly dissected major mobile belt of the westernmost morphotectonic unit of the Burmese Orogen. This belt continues to the north into the eastern Syntaxial Bend of the Himalaya which is believed to be still rising. To the east lay the central lowlands of Myanmar and on the west are the Karbi Anglong Precambrian massifs and Brahmaputra trough. The eastern margin represents part of the subducted Indian plate beneath that of the Burmese. This is a tectonically complicated and relatively young immature mountainous terrain. The subduction process that began during the Cretaceous is believed to be continuing till today (Nandy, 1976; Verma, 1985; Bhattacharjee, 1991). This geodynamically sensitive region is subject to intense and continuing tectonism that is responsible for large scale folding and faulting. This has caused extensive shearing, fracturing, jointing, and crumpling of the rocks. Various geomorphic processes have further weathered and eroded the weakened rocks leading to large scale slope instability.

Kohima is a hilly district of Nagaland that shares borders with Dimapur district in the west, Phek district in the east, Manipur state and Peren district in the south and

Wokha district in the north. One of the oldest among the eleven districts of the state, Kohima is the first seat of modern administration as the headquarters of Naga Hills District (then under Assam) with the appointment of G.H. Damant as Political Officer in 1879. When Nagaland became a full fledged state on 1st December 1963, Kohima was christened the capital of the state. The township of Kohima today has a population of 270,063.

Due to rapid growth in population and accelerated urbanization, the government of Nagaland has initiated further expansion of the township towards the north of the present township, along the NH 2 towards Zhadima. This part of the terrain is made up of Upper Cretaceous-Tertiary sedimentary rocks. These include the Disang and Barail, the former of Upper Cretaceous-Eocene age and the latter Oligocene. The Disang are dominantly shales with minor intercalations of sandstone and siltstone while the Barail are made up of thick bedded sandstones with minor alternations of thin papery shales.

Slope instability including landslides, is common in young terrain, particularly active mountain belts that are fragile and geodynamically sensitive due to intense tectonic activity. Landslides are responsible for loss of life, damage to property, disruption of communication and transportation systems, and destruction of natural resources. Landslides are downward and outward gravitational displacements of slope-forming materials including rock, soil, artificial fill, etc. due to shear failure. The material may move by falling, toppling, sliding, or spreading. Sliding may be sudden or through a prolonged period of time, with or without any apparent provocation. They occur when mobilizing forces exceed the resistive forces. Hence, landslides are intimately related to geo-environmental factors such as terrain morphology, geology, climate, land use, and vegetation. In subtropical and monsoonal climatic regions with hilly or mountainous topography, rainfall is generally the most common cause of landslides (Chen and Lee, 2002).

Slopes fail due to progressive external loading and deterioration of slope material (Zuoan et al., 2006). When hill slopes become steeper due to various geological reasons, a critical stage is attained leading to failure of such slopes at the slightest provocation, such as heavy rainfall. The stability of hill slopes is also directly or indirectly influenced by land use practices and land cover because these factors control the rate of weathering and erosion of the underlying formations. Deforestation and creation of arable land allows considerable water to seep into the soil which causes soil erosion and mass movements. Structures play an important role in instability, particularly in tectonically active terrain. The erosional processes that dissect geologic structures help loosen rock masses on slopes. Slope forming materials also have a direct bearing on landslide events. Hence, slopes are unstable and landslides fairly common in areas of jointed, faulted and intensely sheared rocks. This is particularly so where the dominant rocks are shale and mudstone that are intercalated with thin beds of sandstone. Due to intense shearing the shales are highly crumpled leading to partial or total weathering of the mass. Percolation of water into the unsaturated zone of sheared, crushed or crumpled rocks raises the groundwater table thereby leading to undesirable pore pressure and finally to destabilization of slopes.

Numerous landslide incidences and subsidence are noted in the region including the highways. Instability in the study area includes slumps, debris slides, rockslides, creep, rock topple, and subsidence. Instability commonly occurs during the monsoon. Cloudburst during the monsoon is responsible for major landslides in the region. Slope modification for developmental purposes and excavation for road widening has a negative impact on slope stability.

1.1 OVERVIEW OF THE STUDY AREA

1.1.1 Location of the area

The study area is located north of Kohima town and includes the Indira Gandhi Stadium in the south, New High Court Complex and Nagaland University Campus in the East (Fig. 1.1). A 12 km stretch of the NH 2 runs roughly north-south from the northern edge of Kohima Town to the Zhadima Junction through this area. This area is part of Survey of India (SoI) toposheet nos. 83 K/1 SW and K/2 NW and lies between north latitudes 25°41'21.19" & 25°45'57.28" and east longitudes 94°04'14.92" & 94°06'6.50". The area under investigation is approximately 13.90 sq km. For convenience of study and to display on larger scales the area is divided into two segments, viz., the northern and southern segments.

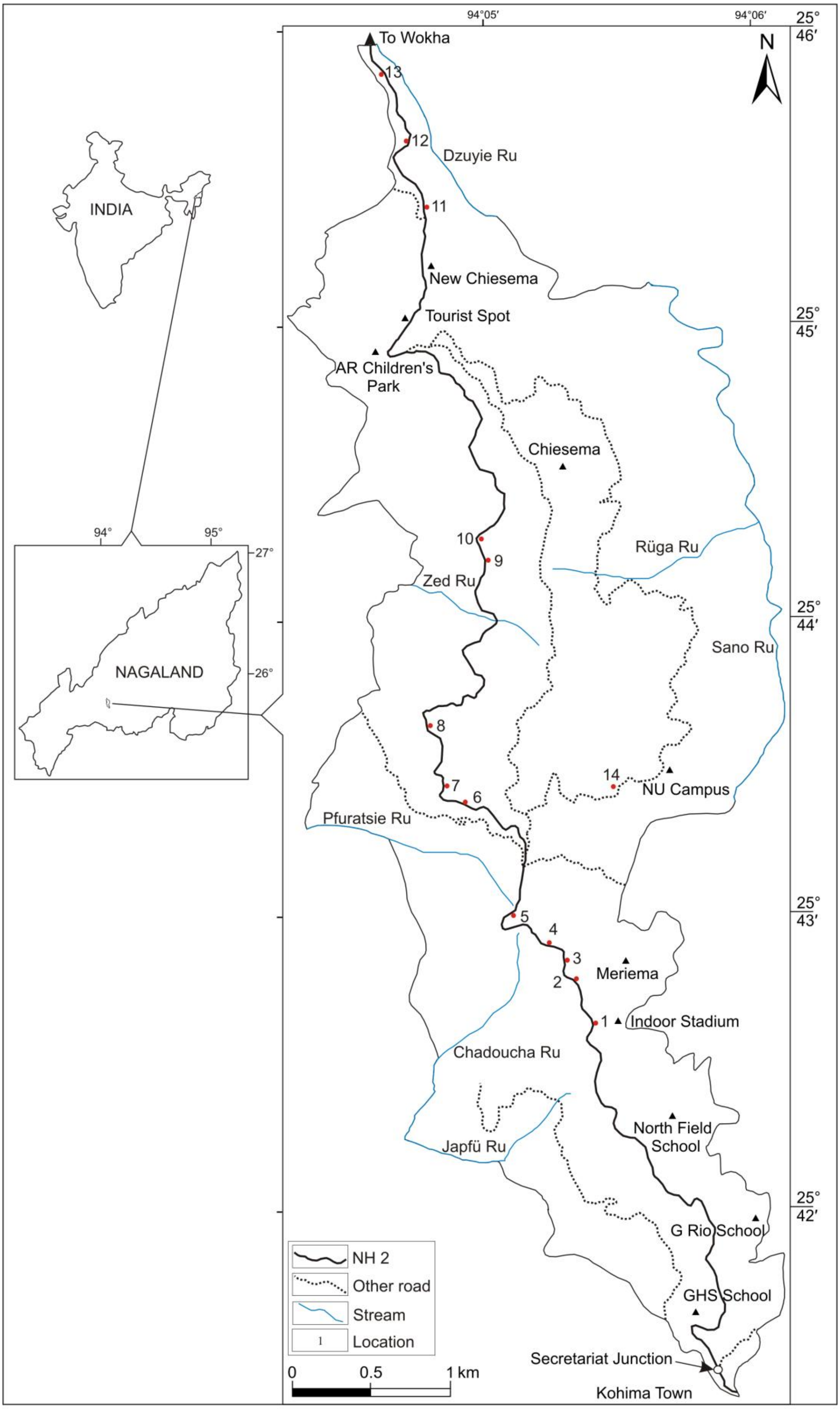

Fig. 1.1. Location Map

1.1.2 Accessibility

The study area is well connected to the neighbouring districts and the other northeastern states by a good network of roads. The NH 2, starting from Kohima in the south, runs through Wokha and Mokokchung in Nagaland and then through Mariani to Jhanji in Assam. The railhead and airport are located at Dimapur, about 70 km west of Kohima. An extensive network of roads connects the study area to numerous villages and other districts of the state.

1.1.3 Geomorphology

The study area is made up of low denuded hills of the Disang Group. Towards the north the Disang are capped by steeper ridges of Barail sandstones. The average altitude of Kohima Town is about 1444 m above mean sea level. The study area is not much affected by stream erosion. A Digital Elevation Model (DEM) of the area shows the rugged nature of the terrain (Fig. 1.2).

1.1.4 Climate

The area lies in the North Temperate Zone where summers are pleasantly warm and winters not too cold. Temperatures fall to about 5°C in January which is the coldest month of the year and rise to about 28°C in summer. This region receives abundant rainfall during the monsoon (Table 1.1). Heavy rainfall, storms, and cloudbursts are commonly noted during the period. The monthly maximum amount of rainfall recorded in this area is 689.4 mm in August 1993. The average annual rainfall recorded in Kohima town from 1981 to 2010 ranges from 1069.6 mm to 2620.8 mm.

1.1.5 Drainage

This area is cut across by a large number streams which dry up during the winter months. However some seepage ponds contain water even in the dry season. The major streams in this area are the Dzuyie Rü, Rüga Rü, Sano Rü, Japfü Rü, Chadoucha Rü, Hapuma Rü, Zed Rü, Pfuratsie Rü, and Dzüza Rü (Fig. 1.3). This area is characterised by parallel and trellis drainage patterns indicating structural control of the streams. Some areas also exhibit local dendritic patterns in the Disang dominated portions indicating homogeneity of the rocks.

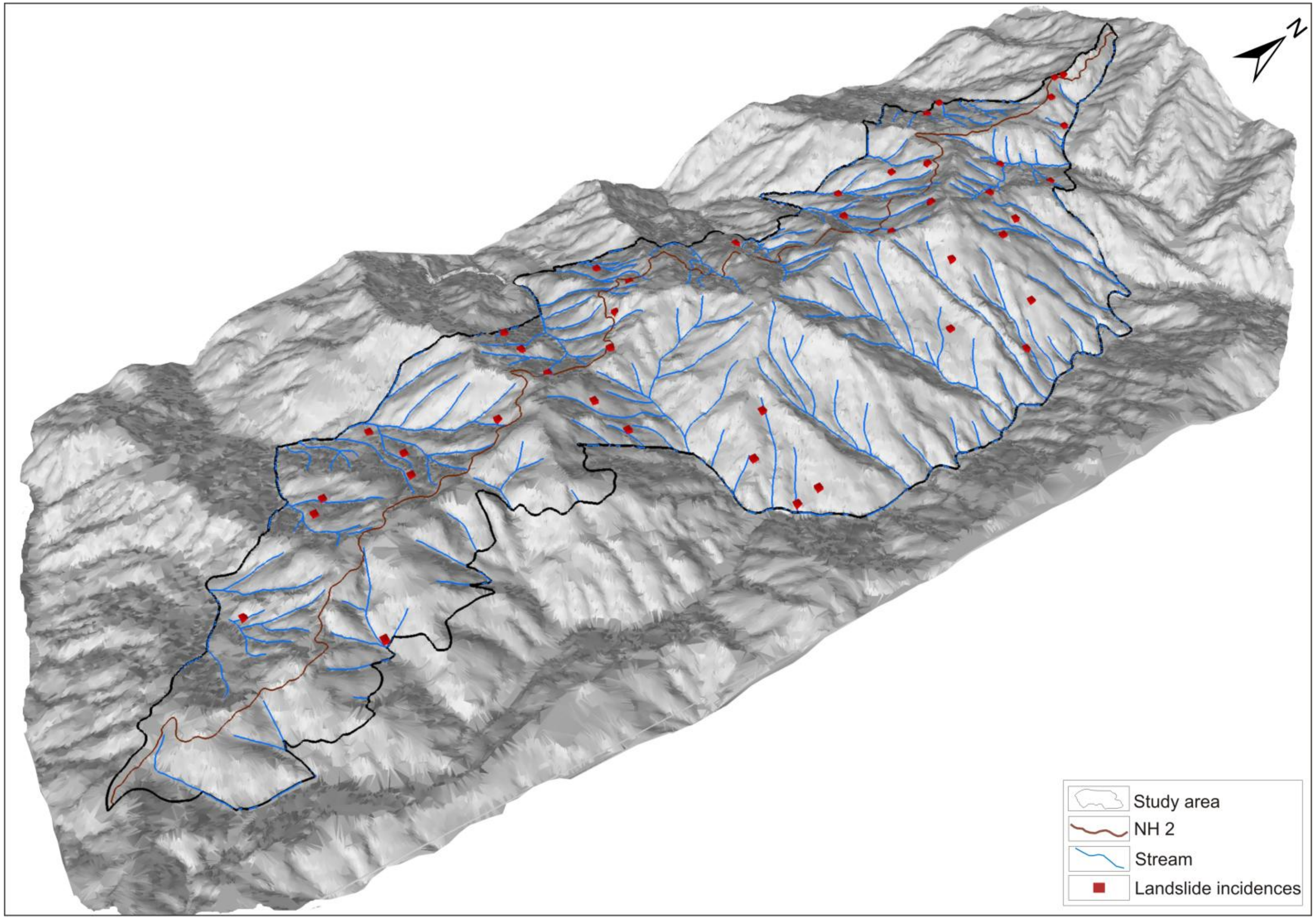

Fig. 1.2. Digital elevation model

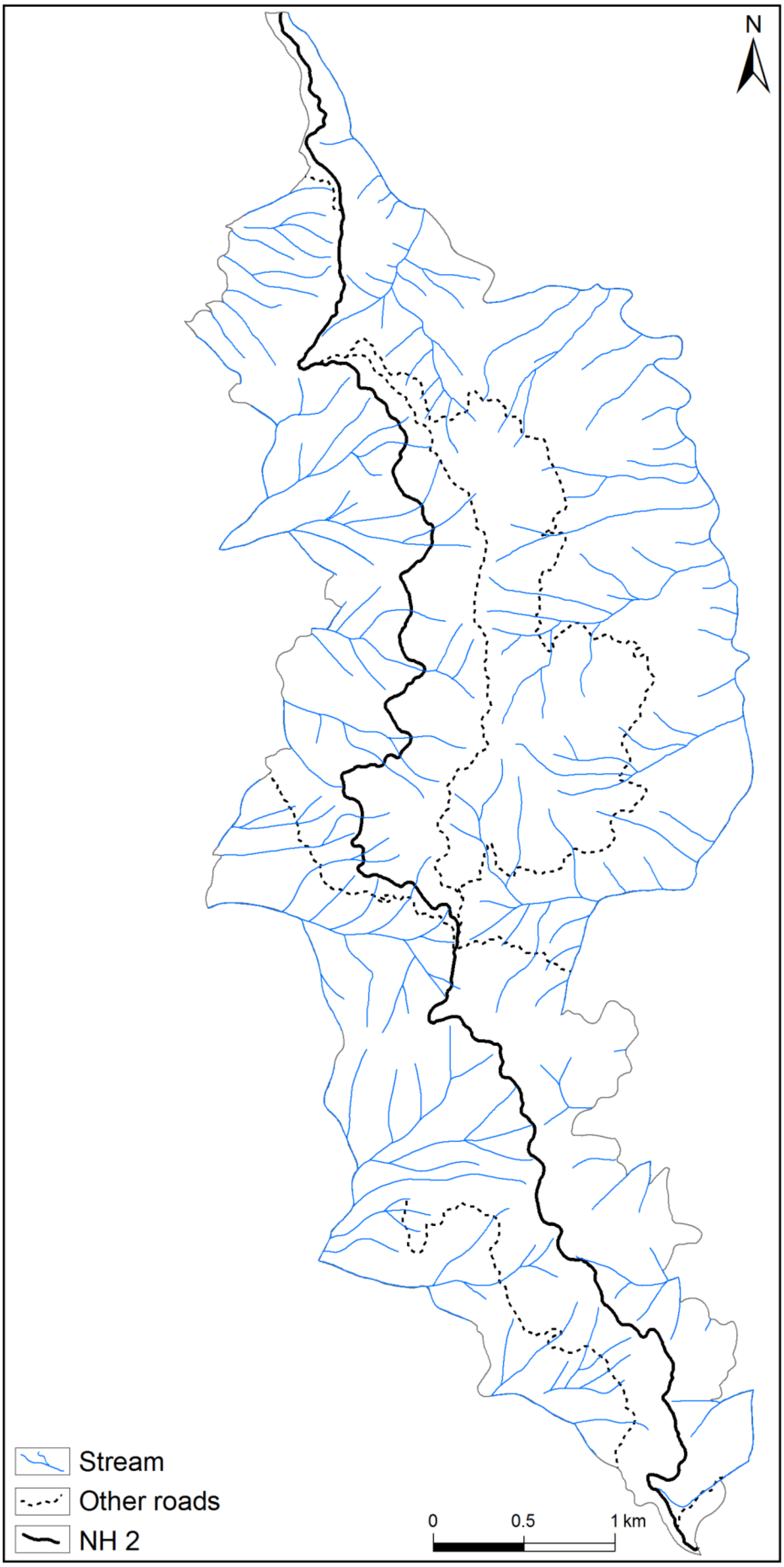

Fig. 1.3. Drainage map

Table 1.1. Rainfall data

(Meteorological Observatory, Kohima)

Year	Minimum (month) mm	Maximum (month) mm	Total Annual mm
1981	7.0 (December)	402.8 (July)	1575.7
1982	6.3 (December)	394.5 (July)	1648.8
1983	11.3 (January)	353.5 (July)	1720.3
1984	14.6 (January)	517.7 (June)	1627.5
1985	6.5 (November)	393.1 (August)	1075.6
1986	8.6 (January)	260.8 (August)	1514.3
1987	3.3 (December)	394.0 (July)	1507.2
1988	3.4 (January)	365.3 (July)	1632.7
1989	5.8 (November)	358.0 (August)	1729.7
1990	32.9 (November)	558.9 (July)	2114.6
1991	5.6 (November)	417.2 (June)	2291.9
1992	7.2 (March)	669.6 (July)	2466.9
1993	18.0 (January)	689.4 (August)	2616.1
1994	3.4 (January)	480.4 (June)	1950.0
1995	6.8 (January)	501.8 (September)	1768.8
1996	0.0 (January)	454.1 (August)	1571.9
1997	1.5 (November)	262.4 (August)	1242.2
1998	0.8 (December)	289.1 (August)	1384.2
1999	0.5 (February)	403.8 (August)	1778.0
2000	0.0 (December)	547.2 (August)	1958.2
2001	0.0 (December)	360.0 (June)	1731.2
2002	10.0 (December)	335.4 (July)	1577.3
2003	5.2 (November)	358.4 (August)	1866.6
2004	0.3 (December)	505.8 (July)	1871.8
2005	2.7 (December)	322.9 (August)	1599.3
2006	0.0 (January)	298.7 (June)	1338.4
2007	0.0 (January)	416.5 (August)	2003.7
2008	0.0 (December)	394.4 (June)	1999.1
2009	0.0 (January)	388.8 (August)	1436.4
2010	1.4 (January)	530.0 (July)	2000.6

1.1.6 Flora and fauna

The study area is covered by a large variety of indigenous shrubs and small trees. The vegetative cover in the area is more or less moderate. The area contains faunal species such as various insects, bees, snails, frogs, etc. and some poisonous and non-poisonous snakes and lizards. The mammals include porcupine, squirrel, rats, mongoose, etc. Some small fish are found in the streams and numerous species of birds like sparrow, bulbul, etc. are noted. Common pests such as mosquitoes and flies are abundant in the jungles.

1.1.7 Soil and outcrops

The soil cover in the area including rock and soil debris is variable in thickness and range from less than 3 m to more than 15 m at places. Soil exposures are commonly pale brownish to pale gray in colour. They are dark gray, soft, and loamy in areas that are damp and covered by vegetation. The area is rich in outcrops. These outcrops are a result of erosion by streams, landsliding, faulting, recent hill-slope widening for roads and other developmental activities, etc.

1.1.8 Lithology

The study area is made up dominantly of shale with some sandstone. The shale belonging to the Disang contains minor alternations of sandstone and siltstone. The younger Barail are made up dominantly of sandstone which form outliers in the region. In the study area the Barail sandstones make up the ridge crests traversing the entire area. The Disang are made up of abundant shales which are, at places splintery. The shales are highly crumpled and partially to completely weathered in many places. Landslides frequently occur in the shale dominated areas.

1.1.9 Structure

This area is disturbed due to active tectonism. These disturbances are reflected in the rocks, particularly the Disang which are folded, fractured, jointed, faulted, and sheared. Satellite imagery shows the presence of numerous lineaments. Some lineaments are of local extent whereas others are regionally extensive. The rocks are affected by three to four sets of joints that generally trend NW-SE, WNW-ESE, and NE-SW (Fig. 1.4). Along the NW-SE planes normal faults and tensile fractures may be noted. Synthetic shearing will take place along the WNW-ESE direction. NE-SW is the regional trend along which thrusting of rocks take place. The shear zones are areas that are continuously affected by instability, particularly during the monsoon.

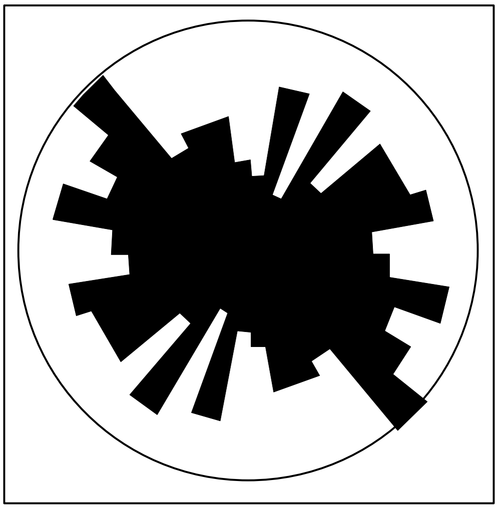

Fig. 1.4. Rosette of Joints

1.1.10 Land cover and land use practice

The highway is flanked both on the uphill and downhill sides by small patches of forests, fallow land, and cultivated tracts, besides a few small villages. The cultivated tracts include areas under terrace cultivation along both sides of the highway.

1.2 OBJECTIVES

The study area lies immediately north of Kohima town, the capital of Nagaland. Keeping in mind the interest of the Urban Development Department in the present study area and its surroundings for expansion of the township, this study has been taken up. The NH 2 that runs through this area was previously very narrow, but being upgraded to national highway status, the process of conversion to four-lane has begun. This has led to acute instability of the road at numerous places, including the study area. Hence, studies have been taken up in this area to:

i) determine the factors responsible for instability including geoenvironmental parameters such as slope, lithology, structure, groundwater, and land use / land cover;

ii) create a spatial database using Geographic Information System (GIS) techniques and construct thematic maps using SoI toposheets on 1:25000 scale, satellite imagery of IRS-1D (PAN+LISS III merged), P6 (PAN), and field studies;

iii) generation of a Landslide Hazard Evaluation Factor (LHEF) rating scheme for each of the geo-environmental parameters and then consolidating them for determination of the Total Estimated Hazard (TEHD);

iv) construct a large-scale Landslide Hazard Zonation (LHZ) map for the area on 1:4000 scale;

v) determine mechanical properties of rocks in weak zones;

vi) provide mitigation measures for such areas.

CHAPTER 2

GEOLOGY OF NAGALAND

2.1 GEOLOGICAL SETTING

Nagaland forms a part of the northern extension of the Indo-Myanmar Range (IMR) that links the Arunachal Himalaya on the north to the Andaman and Nicobar Islands in the south. This region is representative of some Cretaceous-Tertiary orogenic upheavals that form a fairly young and mobile belt of the earth. The stratigraphic framework of Nagaland modified after Mathur and Evans (1964), Directorate of Geology & Mining (1978), and Ghose et al. (2010) is shown in table 2.1.

The IMR is an arc-shaped tectonic belt that is convex towards the west. This IMR is thought to be northern prolongation of the Indonesian island arc. It links up with the eastern end of the Himalayas probably along the Tidding Suture Zone. The IMR is divided longitudinally into three segments (Brunnschweiler, 1974). From north to south they are represented as Naga Hills, Chin Hills, and Arakan-Yoma Hills.

Naga Hills

The Naga Hills, trending approximately NE-SW, represents the northernmost segment of the IMR. It terminates against the continental mass of the Mishmi Block/Hills (Soibam, 1998). The Naga-Patkai Hills of Nagaland and northern part of Manipur principally constitutes this segment. Brunnschweiler (1974) classified this region into three major lithostratigraphic units such as the Naga Metamorphic Complex, Naga Hills Flysch, and Upper Chindwin Molasse of the Chindwin Basin. Acharyya (1986) described the geological and tectonic setting of this segment of IMR in two distinct longitudinal belts. They include the Central Naga Hills Paleogene flysch sediments and the Naga-Chin Hills ophiolite belt.

Table 2.1. Stratigraphy of Nagaland

Age	Group	Litho-formations: Outer and Intermediate Hills		Litho-formations: Eastern Hills
Recent - Pleistocene		Alluvium and high level terraces		
	Dihing	Boulder beds		
		--------Unconformity---------		
Mio-Pliocene	Dupi Tila	Namsang Beds		
		--------Unconformity---------		
Miocene	Tipam	Girujan Clay Tipam Sandstone		
	Surma	Upper Bhuban Lower Bhuban		
		--------Unconformity---------		
Oligocene	Barail	Renji	Tikak Parbat	Jopi / Phokphur Formation Tuffaceous shale, sandstone, greywacke, grit and conglomerate. Minor limestone and carbonaceous matter
		Jenam	Baragolai	
		Laisong	Naogaon	
Upper Cretaceous - Eocene	Disang	Upper		
		Lower		Shale/slate/phyllite with calcareous lenses in basal sections and invertebrate and plant fossils in upper sections with brine springs
		-------Base not seen-------		-------Fault/Thrust-------
Upper Jurassic - Upper Cretaceous	**Ophiolite Complex**			**Zepuhu Formation** Marine sediments (shale, phyllite, greywacke, iron-rich sediments, chert and limestone with radiolaria and coccoliths), volcanics (basalt, spilite, volcaniclastics), metabasics greenschist, glaucophane schist/ glaucophane-bearing metachert, eclogite), layered cumulate sequence (peridotite, pyroxenite, gabbroids, plagiogranite, anorthosite), and peridotite tectonite and serpentinite associated with deposits of podiform chromite and nickeliferous magnetite, minor Cu-Mo sulphides associated with late felsic intrusions and some dolerite dykes
				------Fault/Thrust-------
Pre-Mesozoic (?)	Naga Metamorphic Complex			**Nimi Formation** Weakly metamorphosed limestone, phyllite, quartzite and quartz-sericite schist Naga Metamorphics Mica schist, granitoid gneiss and feldspathic metagreywacke with tectonic slices of ophiolite in variable dimensions

Chin Hills

The Chin Hills lies between the Naga Hills on the north and Arakan-Yoma segment in the south. This unit is principally composed of flysch sediments with minor igneous and metamorphic rocks. On the southern part, a group of schistose rocks known as Kanpetlet schists, overthrusts the lower Tertiary unmetamorphosed shales and sandstones with conglomeratic layers to the west. Brunnschweiler (1974) described this segment of the IMR without ophiolite but with exotics in the flysch sediments. This could probably be the basis on which the two segments, the Naga Hills and Chin Hills were separated.

Arakan-Yoma Range

This segment lies on the south of the Chin Hills and comprise relatively low hills and the coastal areas of Myanmar. The tectonic setting of this segment of is more or less same as the other two segments; however the general strike of the tectonic lineaments is NNW-SSE. Ophiolite rocks, although relatively less, are found on the eastern side as small outcrops.

2.2 STRATIGRAPHY

The Naga-Patkai Hills is a tectonically complex area that is made up of igneous, sedimentary, and metamorphic rocks that range in age from Pre-Mesozoic (?) to Recent. The Tertiary sediments make up the bulk of the rocks in Nagaland while the igneous, some sedimentary and most metamorphic are confined to the eastern fringe of Nagaland.

Naga Metamorphic Complex

This complex is part of the eastern fringe of Nagaland and represents a detached portion of the Pre-Tertiary Burmese continental crust that is probably of Pre-Mesozoic age (Directorate of Geology & Mining, 1978). The complex comprises a cover of meta-sediments which are primarily members of calc-psammopelitic sequences. The main litho-units of the Naga Metamorphics comprise mica schist, granitoid gneiss, and feldspathic metagreywacke with tectonic slices of ophiolite of variable dimensions. These occur as a klippe above a thrust plane dipping east and overlying the younger mélange zone. This formation is overlain by the Nimi

Formation that consists of interbands of phyllite, quartzite, limestone, and quartz-sericite schist.

Zepuhu Formation

This formation represents part of the dismembered Ophiolite Complex of Nagaland. This is a NE-SW trending linear belt that is about 90 km in length and varies from 5 to 15 km in breadth. The Zepuhu Formation lies between the Nimi Formation in the east and the Disang Group on the west. It is characterized by dismembered tectonic slices of serpentinite, cumulates, and volcanics. The associated pelagic sediments include chert and limestone which are interbedded with volcanic rocks. Chert is usually bedded and radiolarian bearing. Fossil assemblages from the limestone suggest an Upper Cretaceous-Lower Eocene age. The ophiolite suite of rocks is unconformably overlain by ophiolite derived volcano-clastics and an open marine to paralic sedimentary cover which has been designated as the Phokphur Formation.

Jopi / Phokphur Formation

This formation, considered equivalent to the Barail, comprises tuffaceous shale, sandstone, greywacke, grit, and conglomerate. Minor limestone and carbonaceous matter are noted in the rocks.

Disang Group

The Disang Group of rocks is the oldest of the Tertiary in Nagaland. This group comprises flysch sediments (Directorate of Geology & Mining, 1978). They range in age from Upper Cretaceous to Eocene. These rocks are found over more than half the surface area of Nagaland. They consist of thick monotonous sequences of splintery shale (Mallet, 1876). The splintery nature of the Disang is practically due to the intersection of bedding and a prominent fracture cleavage (Soibam, 1998). This group is divided into two distinct formations, a basal argillaceous and an upper arenaceous horizon designated as Lower and Upper Disang formations respectively (Sinha et al., 1982).

These rocks occupy the intermediate hill region in the Inner Fold Belt of Nagaland and are confined to the east of the Disang Thrust. The Disang consists of well-bedded, splintery, dark grey shale intercalated with fine grained, well cemented, and thin flaggy sandstones. The sandstones are just a few centimetres thick at the base but become very prominent near the top. The Disang gradually pass upward and laterally into the Barail.

The shales are finely laminated and occasionally, curved or concentric. Ferruginous concretions and nodules are noted in areas of red soils. Brine and sulphur springs and iron pyrite are also common. At places the Disang are carbonaceous and intercalated with massive shale and/or fine grained sandstone. These rocks are commonly crumpled and squeezed to a very high degree. The Disang are occasionally penetrated by thin quartz veins and serpentinized intrusions. Metamorphism is noted towards the east in the form of hard, glossy, dark greyish to blue slates. They grade into talcose and chloritic phyllite and schist further east. The Disang also include black slate, quartzite, limestone, and coloured slates (Oldham, 1883; Goswami, 1960) along the eastern parts of Nagaland and Manipur. These rocks abut against an igneous body further southeast which may be a projection of the parent rock of the Arakan-Yoma.

Due to the presence of discontinuities, secondary porosity is increased considerably in these rocks which further enhance weathering. Weathering of shale is brought about by two main processes namely, air breakage and the dispersion of colloidal material (Badger et al., 1956). As a result, talus and scree form at the base of slopes and thick columns of soil are developed on slopes, consequently rendering the Disang dominated areas vulnerable to various forms of slope failure, including landslides.

Barail Group

The Barail is essentially an arenaceous suite of flysch sediments named after the Barail Range in the North Cachar Hills of Assam. These rocks of Upper Eocene-Oligocene age conformably overlie the Disang. The Barail comprise thick sequences of sandstones intercalated with thin papery shale. They are found scattered all over Nagaland, being exposed in the southern and eastern parts and western margin of Nagaland. Along the east some of the highest peaks of the state like Saramati and its range are located.

In the south and southwest of Nagaland the Barail may be divided into three formations including Laisong, Jenam, and Renji. In the northern intermediate hills of Nagaland they are recognized as Tikak Parbat, Baragolai, and Naogaon formations.

The Laisong Formation comprises very hard, grey, thin bedded sandstones alternating with hard, sandy shale. Occasionally, massive sandstones with intercalations of carbonaceous shale and thin streaks of coal are also encountered. The Jenam is made up predominantly of massive sandstones with intercalations of shale, sandy shale and calcareous and iron stained shale. The Renji extends beyond the south and southwest borders of Nagaland into Manipur and Assam. The Renji sandstones are massive, hard, ferruginous, and very thick bedded and intercalated with minor shale. This formation forms a very thick forested range with high peaks such as Japfü (3015 m) in southern Nagaland. These rocks are of marine to estuarine origin, are confined to the schuppen belt along the western margin of Nagaland where they are intermittently exposed as inliers due to strike faulting. They exhibit a number of sedimentary structures such as ripple marks, load casts, flute marks, and current bedding but however, lack in fossils.

Rocks of the Naogaon Formation are extensively exposed as high ranges in the north-eastern parts of Nagaland. Towards the south these rocks branch out into strips, one such branch extending into northern Manipur. The Naogaon sandstones are hard, grey, thin bedded, and fine to medium grained and intercalated with some shale and carbonaceous shale. Concretionary structures are occasionally noted. Towards the south of Nagaland the sandstones are thick and massive with thin shale partings. The Tikak Parbat and Baragolai formations are made up of sandstone, shale, carbonaceous shale, and coal. The Tikak Parbat contains workable coal reserves.

Surma Group

These rocks unconformably overlying the Barail consist of Lower Miocene molasse. They comprise alternations of well-bedded sandstone, shaly sandstone, mudstone, sandy shale, and thin beds of conglomerate. The rocks are exposed on the western margin of Nagaland in the schuppen belt as long narrow strips. They gradually thin out toward the north. The Surma are subdivided into the Bhuban and Boka Bil formations, the former characterised by the presence of some conglomerates.

Tipam Group

The Tipam Group of molasse sediments unconformably overlies the Surma. This Mio-Pliocene group includes the older Tipam Sandstone and the younger Girujan Clay. These formations are exposed along the western fringe of Nagaland in the schuppen belt as long, narrow strips due to strike faulting. The Tipam Sandstone Formation comprises massive sandstones that are highly friable and contain subordinate clay and shale. The sandstones are generally coarse grained, occasionally gritty and ferruginous. They are commonly green in colour due to the presence of chlorite but are found to be weathering to different shades of brown. The Girujan Clay Formation is essentially argillaceous, consisting of bluish-gray mottled clay, sandy clay and subordinate sandstone.

Namsang Beds

The Namsang Beds belong to the Dupi Tila Group. They lie unconformably over the Girujan Clay. These beds have been assigned to Mio-Pliocene age. They consist of sandstone, pebbles of lignite, conglomerate, grit, mottled clay, and lenticular seams of lignite. They are also confined to the schuppen belt.

Dihing Group

The Namsang Beds are unconformably overlain by the Dihing Group of Plio-Pleistocene age. This group consists of an unconsolidated mass of Barail boulders and pebbles interspersed with clay and soft sand. These deposits are found in a few patches in the schuppen belt.

Alluvium and High-level Terraces

Alluvium and high-level terraces are found in many parts of Nagaland. The high-level terraces are dominantly boulder beds with coarse sand, gravel, and clay at various levels above the present rivers. The older alluvium occupies the northeastern tract of the Naga-Patkai ranges while the newer alluvium covers the western border of Nagaland. The older alluvium is composed mainly of cobbles and boulders with considerable amount of clay, silt, and sand. The younger alluvium occurs as recent alluvial deposits of rivers and streams. They are principally composed of dark gray to black clay, silt, and sand deposits.

2.3 MAJOR STRUCTURAL UNITS

The major structural features of Northeast India are probably due collision of the India subcontinent with Eurasia. When Gondwanaland rifted, the eastern margin of the Indian Peninsula was positioned at latitude 50°S and was oriented in an E-W direction (Chatterjee and Hotton, 1986). Since the Cretaceous, the Indian plate has moved northward and the eastern continental passive margin rotated 20° in a clockwise direction (Gordon et al., 1990) until it collided with Eurasia during Late Eocene. This theory is supported by palaeomagnetic studies of the Indian rocks (McElhinny, 1973) and oceanic magnetic anomalies (McKenzie and Sclater, 1971). The remarkable correlation between high seismicity, depth of foci, and large negative isostatic anomalies to the east of the Arakan-Yoma suggest that the subduction processes are still continuing (Verma, 1985).

The major structural units of Nagaland owe their origin to the above stresses. The major lineaments with general NE-SW trends imply NW-SE compression directions. Hence, all compressional structures such as reverse faults and folds are parallel to the regional NE-SW trend. Normal faults, tensile fractures, and some joints have developed parallel to the NW-SE compression direction. The crustal rocks of this mobile belt have suffered much squeezing which has led to large-scale surface deformation. This region has suffered three deformational episodes, viz., F_1, F_2, and F_3 corresponding to three orogenic events of the rising Himalayas. F_1 represents an early Alpine-Himalayan event. The surface rocks of Nagaland do not show imprints of this orogenic movement. F_2, representing a Late Alpine-Himalayan event, has produced large NE-SW, low to moderately plunging asymmetric open folds and four to five major NE-SW thrust planes. The F_3 Pliocene-Quaternary open folds are small with NW-SE / WNW-ESE trends that are moderately to highly plunging and partially asymmetrical. The F_2 and F_3 deformations are post-collisional features (Roy and Kacker, 1986). F_3 movements that are continuing today are responsible for the neotectonic features of the region.

Nagaland is geologically very complicated from the tectonic and structural points of view. Based on the morphotectonic elements, Nagaland can be longitudinally divided from west to east into three distinct units, namely the “Belt of Schuppen”, the “Inner Fold Belt” and the “Ophiolite Complex” (Goswami, 1960; Mathur and Evans, 1964;

Directorate of Geology & Mining, 1978). All these major structures have NE-SW trends.

Belt of Schuppen

This belt runs along the northwestern margin of Nagaland and is defined by a narrow linear belt of imbricate thrust slices that follow the boundary of the Assam Valley alluvium along the flanks of the Naga Hills. It is postulated that this belt comprises eight or possibly more overthrusts along which the Naga Hills have moved northwestward relative to the Foreland Spur (Evans, 1964). The total horizontal movement of all the thrusts together is estimated to be over 200 km. This schuppen belt is delineated on the east by the Haflong-Disang Thrust and on the west by the Naga Thrust which has an en-echelon disposition. Sediments ranging in age from Eocene to Oligocene and Plio-Pleistocene along with the total absence of the Disang Group characterize this belt.

Inner Fold Belt

It occupies the central part of the Naga Hills and extends up to the Pangsu Pass in Arunachal Pradesh. A large spread of Disang rocks with isolated outliers of Barail characterizes the geological setting of this belt. The Palaeogene rocks that have been folded into a series of anticlines and synclines are confined within the Haflong-Disang Thrust to the west and ophiolite belt to the east. The Inner Fold Belt is characterized by two major synclinoria, the Kohima Synclinorium in the south and Patkai Synclinorium on the north.

Ophiolite Complex

The litho-tectonic framework suggests convergence of plates whereby the Indian plate thrusted below that of the Burmese (Shan Massif) eastward forming the Indo-Myanmar Range along the Ophiolite Complex of Nagaland (Directorate of Geology & Mining, Nagaland, 1978). In their analysis of the ophiolite belt of Nagaland, Chattopadhyay et al. (1993) have indicated that the drainage is mainly structurally controlled. The ophiolite suite mainly comprises basic and ultrabasic intrusive as well as extrusive rocks besides a number of exotic blocks. The associated sedimentary rocks include limestone, chert, shale, sandstone, and conglomerate. This suite is thrusted over the younger Disang sediments on the west, while to the east these rocks and their sedimentary envelope are overthrusted at places by the Naga Metamorphics or their equivalents.

CHAPTER 3

METHODOLOGY

The problem of slope instability and LHZ for this study takes into account the topography, lithology, structure, groundwater conditions, and land use and land cover for which data is generated and thematic maps are prepared in a GIS platform. Thematic maps on the above factors are superimposed to provide the essential data for the LHZ maps.

The present studies involve two major components of data products - spatial and non-spatial / attribute data. Spatial data are the basic topographical properties of location, dimension, and shape. Locations are stored in terms of a coordinated system and each feature location is represented in a unique way. The data are represented on maps or in GIS as point, line, or area features. Spatial data for topographic maps are collected from land surveys, Remote Sensing (RS), and Global Positioning System (GPS). The two models that represent the spatial component of geographic information are vector and raster models. The vector-based method are mainly used for digital mapping and resource inventories while raster-based methods are more concerned with spatio-temporal modeling in environmental application.

Non-spatial / attribute data describes the characteristic of spatial features in terms of records, fields, and keys. Characteristic of a feature contains a measurement or value for the feature. Attributes can be labels, categories, or numbers. They can be dates, standardized values, or field or other measurements. Such data are managed in a table containing descriptive attributes for a set of geographic features, usually arranged so that each row represents a feature and each column represents one attribute. Each cell in a column stores the value of that column's attributes for that row's features. Attribute data in the present work consists of field and collateral data. Field data is acquired through field surveys by recording all information of landslide events and related geological evidence. Collateral data includes meteorological information (Fig. 3.1).

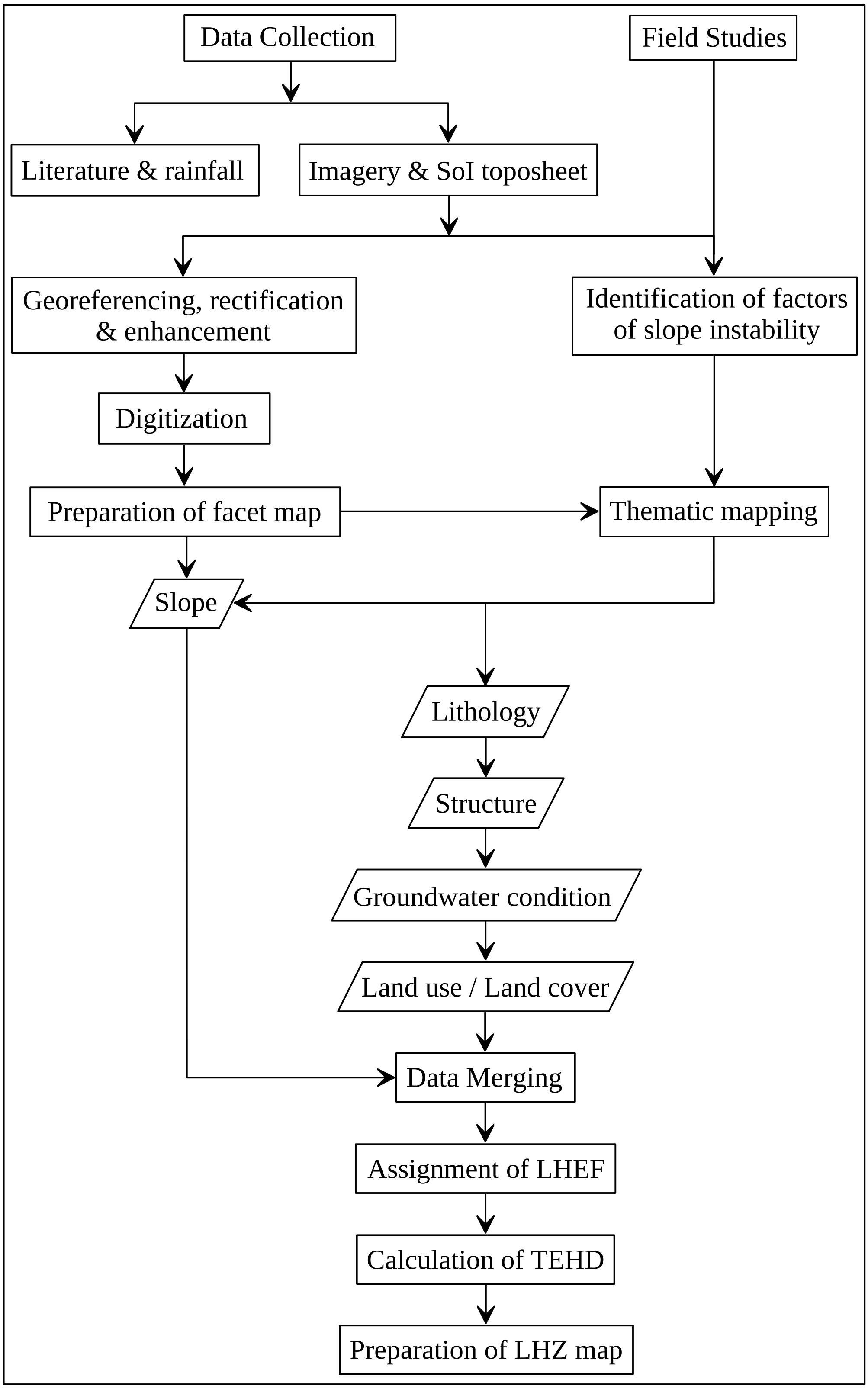

Fig. 3.1. Flow chart for LHZ mapping

SoI toposheet on 1:25,000 scales is used for mapping. Slope angles are directly calculated from the toposheet. IRS-1D (PAN+LISS III merged) data on 1:50,000 scales are used for identification of structural features and mapping. A GPS is used for mapping landslide incidences including recent and old slide, besides subsidence in the area. Detailed fieldwork is conducted for determination of lithology, structure, and land use and land cover. A Silva compass is used for measurement of dips and strikes of beds and joints. Rainfall data is obtained from the Directorate of Soil and Water Conservation (2010).

The toposheet of the area are scanned to produce a raster file of the study area. These are georeferenced using geographic coordinates in ArcGIS 9.2. A sufficient number of well distributed ground control points is selected both on the toposheet and corresponding imagery to perform image registration. All contours at 10 m interval are then digitised in ArcGIS. Additional contours at 1 m interval are generated and superimposed onto the existing contours. This data is used to generate a DEM of the area. Nakamura et al. (2001) and Chi Kwang-Hoon et al. (2002) carried out landslide stability analysis and prediction modeling using DEM. DEMs help visualize surface features and permit evaluation of terrain conditions in 3D perspective. The DEM generated represents the spatial variation in altitude and shows the distribution of landslides.

Pre-field thematic maps are verified in the field and modifications made where necessary. The data obtained are used to generate the LHZ maps on 1:4,000 scales. Landslide incidences are plotted on all thematic maps to understand the role played by each geoenvironmental factor. Landslide incidences are also plotted on the LHZ maps for validation of results.

The Department of Science & Technology (1994) has prescribed a methodology after the works of Anbalagan (1992) which the Bureau of Indian Standards (1998) recommended for use. This methodology is taken into consideration for construction of the various thematic and LHZ maps.

3.1 DEMARCATION OF FACETS

The study area is divided into a number of facets (Fig. 3.2). These facets are parts of hill slopes having nearly consistent slope angles and directions and are prepared from the toposheet. Gullies, stream channels, ridges, spurs, and variations in contour spacing, depending on the topography, are used as boundaries for each facet. Each facet denotes the smallest mappable unit and forms the basis for mapping. The facet boundaries are digitised over the georeferenced toposheet in ArcGIS and stored as polygonal features. Each facet is represented by these polygons and the area of a polygon entity is automatically calculated from the geodatabase in ArcGIS. Numbers are assigned for the facets beginning from the south and ending at the north. The area has been divided into 225 facets.

3.2 LANDSLIDE HAZARD EVALUATION FACTOR RATING SCHEME

The LHEF rating scheme of Anbalagan (1992) is a numerical system governed by the major causative factors of slope instability which helps determine landslide vulnerability of a slope. The factors governing LHEF rating are slope morphometry, lithology, relationship of structural discontinuities with slope, groundwater condition, and land use and land cover. External factors like cloudburst and earthquake are not included in this rating scheme even though they trigger slope failure and affect large areas at places as they cannot be calculated accurately. The maximum LHEF rating scheme for the various factors are determined on the basis of their estimated significance in inducing instability. In this study following Anbalagan’s scheme, a maximum value of 9, as given below, is assigned for the TEHD.

Contributory Factors	Maximum LHEF Rating
Slope angle	2.0
Lithology	2.5
Structure	2.0
Groundwater condition	1.0
Land use & Land cover	1.5
Total	9.0

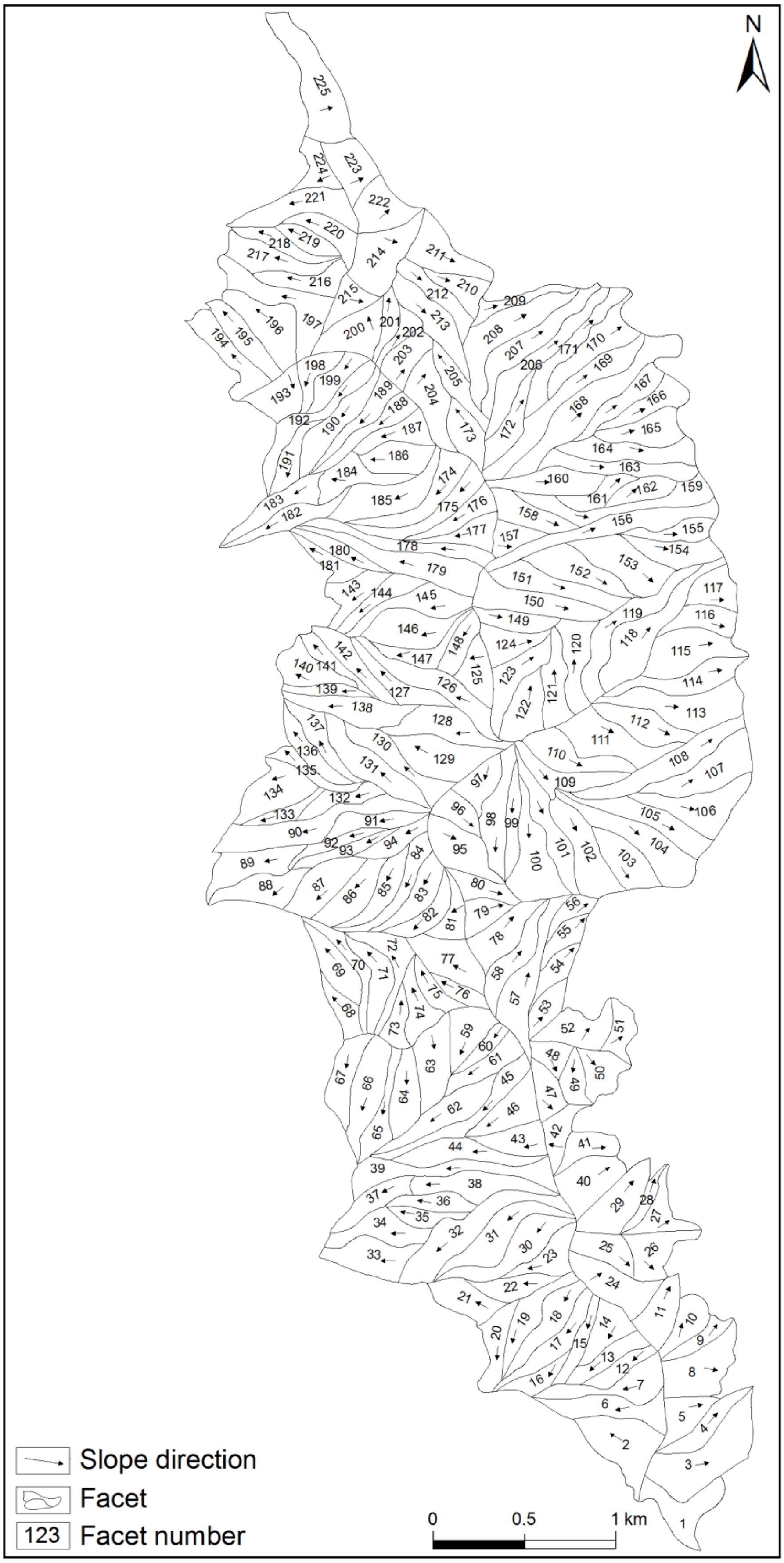

Fig. 3.2. Facet map

3.3 SLOPE ANGLE

Slopes are important criteria in any landslide analysis. It is estimated that more than 80 percent landslide events have occurred on slopes greater than 30°. However, the relationship between slope and landslide is intimately dependent on lithology. Hence, landslides may occur on gentler slopes as well. Slope angles for each facet are determined by counting the number of contours in a facet and measuring the length of the facet. This is given by the formula $\tan \theta = BC/AB$, where AB is the length of the facet and BC is the altitude difference in a facet. The slope map is prepared on the basis of frequency of occurrence of particular angles of slopes which may be categorised under five heads. Slopes and corresponding ratings are given below.

Slope angles	Category	Rating
0° - 15°	Very gentle slope	0.5
16° - 25°	Gentle slope	0.8
26° - 35°	Moderately steep slope	1.2
36° - 45°	Steep slope	1.7
> 45°	Very steep slope	2.0

3.4 LITHOLOGY

Mechanical properties of rocks depend on their composition and the way they have been affected by tectonism and weathering. Weathering greatly reduces their shearing resistance. The sedimentary rocks found in the area are vulnerable to weathering and erosion which thus makes them prone to landslides. Soils are of varied nature and their strengths depend on composition, grain size, permeability, thickness, etc. These rocks are classified into several litho-units which are given ratings as below.

Lithologic units	Rating
Sandstone with minor shale	0.5
Shale	1.0
Shale with minor sandstone	1.5
Crumpled shale; partially weathered shale	2.0
Weathered shale; loose debris	2.5

3.5 STRUCTURE

The area is highly disturbed due to active tectonism. These disturbances are reflected in the rocks in the form of folds, joints, fractures, and faults. Planes of weakness such as bedding, joints, fractures, faults, etc. largely determine slope stability. Faults, joints, shear zones, and fractures are common in the rocks of the study area. They play a major role in promoting instability, individually or in varying combinations. The attitude of bedding or joint planes in relation to slope is an important criterion for determination of slope stability. Anbalagan (1992) gives three relationships based on which ratings are assigned to each facet.

(i) Extent of parallelism between the directions of the discontinuity or the line of intersection of two discontinuities and the slope.

(ii) The steepness of the dip of discontinuity or the plunge of the line of intersection of the two discontinuities.

(iii) The difference in the dip of the discontinuity or the plunge of the line of intersection of the two discontinuities to the inclination of the slope.

3.6 GROUNDWATER CONDITION

The area is made up dominantly of shale, much of which are fractured and crumpled. Water seepage into the subsurface is high during the monsoon. These waters seep out at various levels along hill slopes during this period. Groundwater in hilly terrain does not have a uniform flow pattern because they are generally channelled along structural discontinuities of rocks. The evaluation of observations of the behaviour of groundwater on hill slopes is not possible over large areas. Therefore, in order to make a quick appraisal, the nature of surface indications of the behaviour of groundwater will provide valuable information on the stability of hill slope for hazard mapping proposes Anbalagan (1992). Surface indications are categorised and corresponding ratings are given below.

Category	Rating
Dry	0.0
Damp	0.2
Wet	0.5
Dripping	0.8
Flowing	1.0

3.7 LAND USE AND LAND COVER

The stability of hill slopes is also influenced to a great extent by land use practices and type of land cover. Land use refers to the use of land for human activity while land cover refers to the natural cover in an area. These factors control the rate of weathering of underlying rocks and erosion of the surface. The land use / land cover map for the study area has been prepared using the following broad classification with ratings for each category. Terrace cultivation has been awarded the highest rating due to the fact that water retention in such zones is very high thereby leading to slope instability in the region. Data derived from satellite imagery using tonal and textural characteristics were subsequently verified in the field.

Category	Rating
Populated land	0.65
Dense vegetation	0.80
Moderate vegetation	1.00
Sparse vegetation	1.20
Terrace cultivation	1.50

3.8 TOTAL ESTIMATED HAZARD

LHEF ratings for individual causative factors including categories are calculated facet-wise. The ratings for all factors are then added up to obtain the TEHD. Thus, TEHD = ratings of slope morphometry + lithology + structure + groundwater condition + land use / land cover. It indicates the facet-wise net probability of instability. A rating of 9 will indicate the maximum value of TEHD.

3.9 LANDSLIDE HAZARD ZONATION

Landslide hazard zonation is a division of land surface into areas, and the relative ranking of these areas according to degrees of actual or potential hazard from landslides on slopes. Zonation from scientific research does not generally imply legal restrictions, but can be useful to those people who are charged with land management, by providing them with information that is indispensable for planning and regulation purposes (Parise, 2002). LHZ maps aid in identifying and delineating landslide prone areas thereby leading to minimization or avoidance of high instability risks. Such maps can play a significant role in minimizing loss to life and property while delineating zones conducive for development. The LHZ map of the study area is generated on the basis of the distribution of the TEHD values following Anbalagan (1992). The different categories of hazard for designated TEHD values are as follows:

TEHD Values	Description of Zones
< 3.15	Very low hazard
3.15 - 4.50	Low hazard
4.60 - 5.40	Moderate hazard
5.50 - 6.75	High hazard
> 6.75	Very high hazard

3.10 ROCK AND SLOPE MASS RATING

Studies of fresh-cut slopes along this highway enable an understanding of stability conditions in the area. Fifteen major slides and two subsidences in the area are studied in detail. Remedial and/or mitigation measures are provided for these areas in addition to general mitigation measures. Thirty to forty rock samples are collected from each location and analysed using a Point Load Index Tester (PLIT). Averages are taken of these samples to determine their strengths.

The present study is based on the slope mass rating (SMR) of Romana (1985) which is basically evolved from the rock mass rating (RMR), a rock mass classification of Bieniawski (1979). The RMR is computed by adding rating values for five parameters including strength of intact rock, rock quality designation, spacing and condition of discontinuities, and water inflow through discontinuities (Table 3.1). Rock mass classes determined from total ratings are given in (Table 3.2).

Table 3.1. Classification parameters and ratings (after Bienawski, 1979)

Parameters		Ranges of values				
1. Strength of intact rock material (MN/m^{-2})	Point load strength index	>10	4-10	2-4	1-2	
	Uniaxial compressive strength	>200	100-200	50-100	25-50 10-25 3-10 1-3	
Rating		15	12	7	4 2 1 0	
2. Drill core quality RQD (%)		90-100	75-90	50-75	25-50	<25
Rating		20	17	13	8	3
3. Spacing of joints		>3 mm	1-3 mm	0.3-1 mm	50-300 mm	<50 mm
Rating		30	25	20	10	5
4. Condition of joints		Very rough surface; not continuous; no separation	Slightly rough surface; separation <1mm; hard joint wall rock	Slightly rough surface; separation <1mm; soft joint wall rock	Slickenside surface; gouge <5mm; thick; joints open; 1.5mm; continuous	Soft gouge <5m; joints open; 1.5m; continuous
Rating		25	20	12	6	0
5. Groundwater	Inflow per 10 m tunnel length ($1min^{-1}$)	None	<25	25-125	>125	
	Ratio of joint water pressure/major principal stress	0	0.0-0.2	0.2-0.5	0.5	
	General conditions	Completely dry	Moist (interstitial water)	Water under moderate pressure	Severe water problem	
Rating		10	7	4	0	

Table 3.2. Rock mass classes

Rating	100-81	80-61	60-41	40-21	<20
Class No	I	II	III	IV	V
Description	Very good rock	Good rock	Fair rock	Poor rock	Very poor rock

The strength parameters of the rocks are measured using point load testing machine. The point load strength index I_s is calculated from the values obtained in the point load tester using the following relation:

$$I_s = P/D^2$$

Where P - pressure obtained at failure

D - diameter of sample

The rock quality designation index (RQD) was developed by Deere et al. (1967) to provide a quantitative estimate of rock mass quality from drill core logs. Palmström (1982) estimated RQD from the number of joints per unit volume given by the following equation:

$$RQD = 115 - 3.3\ J_v$$

Where J_v is the sum of the number of joints per unit length for all joint sets known as the volumetric joint count.

The condition of joint is inferred from the inherent surface smoothness or unevenness and waviness relative to the plane of the joint. Joint roughness can be felt by touch and is recognized in the field as very rough, rough, slightly rough, smooth, polished and slickensided surfaces. Joint roughness can be estimated numerically from the joint roughness coefficient (JRC). The JRC is estimated (Table 3.3) by comparing the appearance of a discontinuity surface with standard profile (Barton and Choubey, 1977).

Table 3.3. Joint roughness profiles and corresponding JRC values

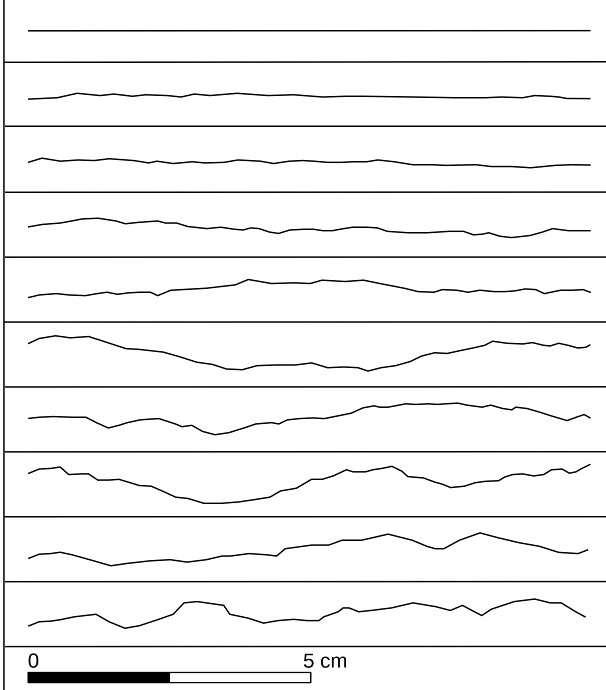

(profile)	JRC = 0-2
(profile)	JRC = 2-4
(profile)	JRC = 4-6
(profile)	JRC = 6-8
(profile)	JRC = 8-10
(profile)	JRC = 10-12
(profile)	JRC = 12-14
(profile)	JRC = 14-16
(profile)	JRC = 16-18
(profile)	JRC = 18-20

Groundwater condition is one of the important parameters for the assessment of stability conditions of a slope. Visual observations are made for estimating the groundwater conditions for the present work and accordingly their rating are estimated. The algebraic sum of these five parameters gives the RMR values for a particular slope facet. For slope stability assessment, stereographic analysis of discontinuities is carried out for determining the mode of failure and adjustment ratings. The adjustment ratings F_1, F_2, and F_3 for joints are evaluated depending on joint trend (α_j), slope face trend (α_s), joint dip angle (β_j), and slope angle (β_s) as suggested by Romana (1985). The value of F_4 is taken corresponding to natural slopes.

The SMR is obtained from the RMR by adding a factorial adjustment factor depending on the joint-slope relationship and adding a factor for the natural slope. Here,

$$SMR = RMR + (F_1 x F_2 x F_3) + F_4$$

1) F_1 depends on parallelism between strikes of joints and slope faces. Values range from 1.00 to 0.15. These values match the relationship $F_1=(1\text{-}SinA)^2$, where A denotes the angle between the strikes of slope faces and joints.

2) F_2 refers to joint dip angle in the planar mode of failure. Its value ranges from 1.00 to 0.15 and matches the relationship $F_2=tg^2Bj$, where Bj denotes the joint dip angle. For the toppling mode of failure F_2 remains 1.00.

3) F_3 reflects the relationship between slope face and joint dips.

4) F_4 denotes the adjustment factor for the method of excavation that has been fixed empirically.

The adjustment rating and stability classes are represented in Tables 3.4 and 3.5.

Table 3.4. SMR rating system (after Bienawski, 1989)

Case	Very favorable	Favorable	Fair	Unfavorable	Very unfavorable
P I αi-αs I T I αi-αs-180 I P/T F_1	>30° 0.15	30°-20° 0.40	20°-10° 0.70	10°-5° 0.85	<5° 1.00
P I βi I P F_2 T F_2	<20° 0.15 1	20°-30° 0.40 1	30°-35° 0.70 1	35°-45° 0.85 1	45° 1.00 1
P βi-βs P βi+βs T F_3	>10° >110° 0	10°-0° >110°-120° -6	0° >120° -25	0°-(-10°) -50	<-10° -60
Method	Natural slope	Pre-splitting	Smooth blasting	Regular blasting	Deficient blasting
F4	+15	+10	+8	0	-8

P = plane failure αs = slope dip direction αi = joint dip direction
T = toppling failure βs = slope dip βi = joint dip
SMR = RMR+(F_1xF_2xF_3)+F_4

Table 3.5. SMR classes (after Romana, 1985)

Class No	**V**	**IV**	**III**	**II**	**I**
SMR	0-20	21-40	41-60	61-80	81-100
Description	Very poor	Poor	Fair	Good	Very good
Stability	Very unstable	Unstable	Partially stable	Stable	Fully stable
Failures	Large planar or soil-like	Planar or large wedge	Some joints or many wedge	Some blocks	None
Support	Re-excavation	Extensive corrective	Systematic	Occasional	None

3.11 KINEMATIC ANALYSES

Kinematics refers to the study of movement without reference to the force producing it. Kinematic analyses which is purely geometric, examines which mode of slope failure are possible in a jointed rock mass. Angular relationships between discontinuities and slope surfaces are applied to determine the potential and modes of failures (Kliche, 1999). Kinematic analyses have been performed for determination of possible failure mode along fresh-cut slopes of the NH 2 and the approach road to the Nagaland University. About 150 to 200 joint trends are taken from each location and plotted in GEOrient software (R.J. Holcombe, University of Queensland, Australia) to construct polar density and contour diagrams to determine the dominant joint sets that control instability. These are used to generate stereographic projections to ascertain type of failure mode. Data generated from joint projections are used for kinematic analyses using Markland's test (Markland, 1972) that was modified by Hocking (1976), Cruden (1978), and Hoek and Bray (1981). Using this method the probable mode of failure at each location in the study area is determined.

CHAPTER 4

LITERATURE REVIEW

INTRODUCTION

Works on the Geology of Nagaland and landslides studies are very inadequate because of its remoteness, inaccessibility, and rationally, socio-political issues. The earliest literature was established and discussed by Oldham (1883) on the geology of Kohima and parts of northern Manipur. Pascoe (1912) described the geology between Dimapur and Saramati. The Tertiary succession of Assam including the tectonics of Nagaland was reported in the works of Evans (1932). Mathur and Evans (1964) studied the stratigraphy, structure, and conditions of deposition of the Tertiary sediments of Upper Assam and Nagaland. Sarmah (1989) studied the Disang and Barail sediments of Kohima. Agarwal and Shukla (1996), in their investigations of the ophiolite complex, concluded that drainage is mainly structurally controlled with most rivers flowing along a multitude of lineaments trending NE-SW and NW-SE. Pillai et al. (2008) discussed the identification, distribution, and significance of clay minerals in the Disang shale of Kohima and concluded that the Disang flysch are clastic sediments that were derived from complex sources. The sediments were possibly derived as a result of severe weathering and rapid erosion from orogenic sources where climatic conditions were humid. Aier et al. (2011a) gave a detailed account on geomorphic evolution of Medziphema intermontane basin and Quaternary deformation in the schuppen belt of Nagaland.

Landslides are unpredictable natural calamities that damage properties and vital infrastructure every year and adversely affect human lives. Landslides commonly occur due to extreme natural events such as volcanic eruption, earthquake, etc. The unique combination of active but diverse tectonic setting, high rates of weathering, and abundant rainfall aggravated by human interference in the form of rapid urbanization, development of infrastructure, and deforestation adversely affect the fragile ecosystems of mountainous terrain. Most hilly terrain is subject to slope failure due to various geological causes. Landslides are amongst the most rapid of all mass movements and pose very great hazards in mountainous terrain (Sharma et al., 1996). Slope failure may be triggered by a number of external factors such as intense rainfall, ground vibrations due to earthquakes, subsurface water level changes, storm waves and rapid stream erosion (Dai et al., 2002). Aier et al. (2009a) opine that the load and vibrations due to heavy vehicles along weak slopes may also have a minor role in leading to slope failure.

Sondhi (1941) first studied landslides in Nagaland along the Dimapur-Manipur road. Sharda and Bhambay (1980) prepared geotechnical and slope classification maps of Kohima town. In their effort they conducted environmental and geotechnical / geoscientific studies of the area. Anand (1988) gave a general account of landslides between Chumukedima and Mao. The Directorate of Geology and Mining (1990) studied landslides in the Alempang Ward of Mokokchung town. Lotha (1994) investigated some landslides of Kohima paying particular attention to the Chiepfütsiepfe slide of Kohima. Bhattacharjee et al. (1998) studied land instability along parts of NH 39. The Central Road Research Institute (2000a) commented on the weak zones between Chumukedima and Maram. The Directorate of Geology and Mining (2001) conducted geohydrological, geotechnical, and geoenvironmental studies of Mokokchung town and reported that slope instability and soil erosion in the township was due to unplanned and uncontrolled construction while developmental activity is of great concern and a threat to environmental equilibrium. A preliminary geological report of the Mao slide of Manipur with mitigation measures for the BRO was submitted by Thong et al. (2004). Aier et al. (2005) investigated the Lalmati slide to provide mitigation measures. Walling et al. (2005) suggested mitigation measures for the Chiepfütsiepfe slide of Kohima. The Directorate of Geology and Mining (2005) investigated landslides that occurred on 25th June 2005 in Mokokchung town. Aier and Thong (2006) reported on the major subsidence at the Lumami Campus of the Nagaland University, Zunheboto. Thong et al. (2006a) and Thong et al. (2006b) submitted detailed project reports on their investigations of land instability along part of the NH 39 and Kohima town. Thong et al. (2007) reported on the 179 km slide along the NH 39. Aier et al. (2009b) gave a detailed account on SMR and kinematic analyses along part of NH 61, Nagaland. Aier et al. (2011b) investigated instability at Merhülietsa of Kohima town.

Landslides are natural hazards that may damage natural resources and properties, and disrupt communication systems. They are occasionally also responsible for loss of lives. It is therefore very important to identify their causes and assess their impact so that appropriate remedial and/or mitigation measures can be worked. Landslides are comparatively less studied than the other geological hazards such as earthquakes, volcanoes, and floods and are not given due importance in many regions. However, in many other areas landslide research is receiving increased support from governmental agencies due to growing awareness.

Landslides are down-slope movements of rock debris or earth masses due to failure along curved or planar surfaces due to gravity when material lose their shearing strengths, with or without the aid of excess water. Landslides occur when the driving/mobilizing forces exceed the resisting forces. However, if the shearing strength of the soil can adequately counter this tendency then the slope is stable. Landslides occur suddenly or through a prolonged period of time, which may be with or without any apparent provocation. Landslides are commonly influenced by factors such as slope angle, relief of the area, lithology, structure, drainage, groundwater conditions, etc. According to their mode and genesis they may be broadly divided into two subdivisions, viz., natural and anthropogenic. Naturally induced landslides are caused by neotectonic activities such as earthquakes and reactivation of faults and thrusts, water action, and denudational processes acting on the surface of the earth. Man-induced landslides are due to human intervention related to urbanisation, deforestation, mining, public utility activities, etc.

Numerous terminologies are used for mass movements of varied nature, each with its own distinct characteristic. Some are slow movements that are imperceptible in short durations but are characterised by surface expressions whereas others are rapid. Creep is a type of slope movement in which viscous soil and rock materials move down slowly. Slide can be defined as landslides in which the failed masses move along a planar or curved surface with a perceptible rate. Fall is the abrupt downward movement of loosened material or solid rock from vertical slope / cliffs. Flows are movements of unconsolidated material in the plastic or fluid state. Subsidence refers to the vertical downward movement of unconsolidated material without any horizontal flow. Complex landslides are a combination of two or more of the above mentioned types of failure. Caine and Mool (1982) observed that most landslides are complex hybrids between several classes. Varnes (1984) and Crozier (1986) classified landslides into two basic types. The first category of landslides includes those due to mechanical causes while the second category includes those due to changes in the physical or chemical properties of soils.

Landslide hazard zonation is a division of land surface into smaller areas, and the relative ranking of these areas according to the degree of potential to landsliding. Blanc and Cleveland (1968) used lithology and slope to generate landslide zonation maps for parts of California. Nilsen and Brabb (1972) used landslide debris besides geological formations and slope ranges to prepare a landslide zonation map of the San Francisco Bay region. Landslide zonation has been carried out on both regional and local scales in different parts of India which include construction and superimposition of thematic maps that supposedly correspond to contributing causative factors and are interpreted either manually (Anbalagan, 1992; Pachauri and Pant, 1992; Gupta et al., 1993; Sarkar et al., 1995; Mehrotra et al., 1996) or by GIS-based techniques (Gupta and Joshi, 1990; Nagarajan et al., 1998; Saha et al., 2002; Kanungo et al., 2006). Some of the factors responsible for landslides in the mountainous belt extending from the Himalaya in the north and northeast to the Arakan-Yoma range in the southeast including Nagaland and Manipur are steep slopes, toe erosion by swift flowing streams and rivers, heavy rainfall, loss of vegetation, mining, and unplanned urbanization. In the recent past rapid growth in population and developmental activities have taken place to such an extent that the environment has been considerably damaged. This has given rise to more risks due to the natural hazard. Thapliyal (1998) states that manmade disasters can be averted to some extent but with increasing degradation of the environment the frequency and magnitude of natural disasters have increased manifold. Dai et al. (2002) insist that analysis and assessment are important tools in addressing uncertainty inherent in landslide hazards due to degradation in recent years. Mantovani et al. (1996), Cardinali et al. (2002), and van Westen et al. (2003) carried out geomorphological approaches for estimation of landslide hazards and risks. Tiziano (2003) contributed to the monitoring and planning for slope stabilization.

Landslides and other forms of mass wasting are very common in Nagaland because of its tectonic setting comprising the Arakan-Yoma ranges that is characterized by extremely steep, rugged, and weak slopes. Some research on landslides has recently begun in the state which includes hazard zonation mapping and kinematic analysis. Aier (2005) investigated instability along the NH 39 between Chumukedima and Kohima and prepared a LHZ map of the section and proposed some mitigation measures. Walling (2005) studied instability in Kohima town and prepared a LHZ map using RS and GIS for the same and recommended mitigation measures for some weak zones. Hiese (2005) prepared a landslide risk map of Kohima town and its surroundings. Sothu (2008) studied instability along the NH 150 between Kohima and Chakhabama and provided mitigation measures for road stability along some shear zones. Nokmatongba et al. (2011) gave an appraisal of a debris slide in the Artang Ward of Mokokchung town.

A landslide may occur as consequence of changes in landforms. It may also be because of gravitational forces which are always acting on soils and aided by increased buoyancy; under such conditions soils, which were formerly stable on steep slopes, become less stable and slide. Gray (1973), Swanson and Dyrness (1975), and Swanston and Swanson (1977) blame forest destruction and road construction for initiating landslides. Bhandari (1987) blames man for his interference in the ecosystem. Valdiya (1987) blames unscientific road construction as causing destructive landslides as most roads are poorly planned and very badly constructed. Sahai (1993) opines that weak lithology, unfavourable slopes, poor vegetative cover, and abnormal rainfall together cause landslides. Thick deposits of unconsolidated material on steep hill slopes, adverse lithological and hydrogeological conditions, and anthropogenic activities such as road cutting, construction of heavy structures, etc. are responsible for many major landslides (Kumar et al., 1995). While Cruden and Varnes (1996) opine that landslides are caused by geological, geomorphological, and human processes, Petley and Reid (1999) have indicated that landslides are inevitable where mountain chains are being uplifted.

Moghaddas and Ghafoori (2007) studied landslides in the Albroz Mountain Range of Iran and classified them as deep and shallow slides. Investigations of these landslides showed that lithology, geological structure, weathering, and toe erosion of slopes are important factors that favor the occurrences of landslides whereas earthquakes, intense rainfall, and road construction are the main triggering factors. Akgun et al. (2008) stress that both urbanized and cultivated areas result from heavier modifications of the original landscape and the instability phenomena could be triggered by such modifications. Ramasamy and Muthukumar (2008) came out with a methodology involving advanced concepts available in GIS. GIS layers were generated for important contributing geosystems like lineament density, geomorphology, drainage density, slope, regolith, land use / land cover, etc. Landslide data was integrated with the various datasets and based on frequency of landslide occurrence threshold values for each geosystem were identified.

4.1 Slope

Slopes are naturally unstable unless they have been stabilized through geologic time. There are many ways in which slopes may fail depending on the angle of slope, water content, type of earth material involved, and local environmental factors such as ground temperature and climate. Brabb et al. (1972) and Nilsen and Brabb (1972) are of the opinion that the evaluation of any region should include an analysis of slope stability characteristics of the terrain and incorporate factors such as soil characteristics, degree of slope, bedrock, seismic triggering of landslides, etc. Nilsen et al. (1976) subscribes to the idea of a combination of various factors as responsible for landslides which may occur due to sudden or gradual changes on a slope. The factors may be soils and surface deposits, types and properties of underlying bedrock, angle and direction of slope, amount of rainfall, type of vegetation, placement of cuts and fills, types of construction, and the presence of ancient landslide deposits. Accurate mapping of ancient deposits and slides in conjunction with other factors such as slope angles, bedrock, etc. can yield significant data for analyses of slope stability. It is observed that there is a delicate balance of different factors for slope stability. Fujita et al. (1976) and Fujita (1980) view landslide incidences as closely associated with inclination of slopes. Slopes are generally gentle to moderate, with a tendency to become steeper near valleys. Emelyanova (1977) is of the opinion that lithology and structure play a vital role in the development and disposition of slopes and instability pattern in any area. Veder and Hilbert (1980) conclude that a landslide will develop at the toe of a slope as soon as the driving forces exceed the resisting forces with average shear strength. Diverse combinations of these factors give rise to a variety of slopes marked by favourable and unfavourable terrain conditions (Shah and Jadhav, 1987). The safety factor for a slope is the ratio of the sum of resisting forces that act to prevent failure to the sum of the driving forces that tend to cause failure (Piteau and Peckover, 1989). Two important characteristics of hill slopes are slope and geology (Galster and Laprade, 1991). Slope instability hazard assessment should be based on the analysis of terrain conditions at palaeoslide sites (van Westen, 1993). Slope instability processes are the product of geomorphological, geological, and hydrological conditions, the modification of these conditions induced by geodynamic processes and human activities, vegetation and land use practices, and the frequency and intensity of precipitation and seismicity (Soeters and Westen, 1996). The Central Road Research Institute (2000b) is of the opinion that instability of slopes is due to the complex interaction of factors such as geotechnical, geological, hydrological, climatic, and human activities. The impact of slope instability on landscape evolution has been hampered by heterogeneity in lithology, climate, and tectonic forces common to many active tectonic regions (Roering et al., 2004).

Slope failure takes place when the critical slope angle is exceeded. This angle depends on the frictional properties of slope material and increases slightly with the size and angularity of fragments. Based on observations it is estimated that eighty one percent of landslide events have occurred on slopes that are greater than 30°. Debris flows can occur on slopes greater than 30° (Terzaghi, 1950).

Sharma et al. (1996) observed that slopes are a combination of highly irregular surfaces that cannot be described by a simple mathematical expression. It is also observed that slopes are generally transitional in nature. Therefore a complete understanding of their behaviour is very difficult. Hence the stability of a slope will depend on the forces that tend to resist failure compared with those that tend to cause failure. It is a known fact that shearing stresses will build up with increase in the inclination and height of sloping surfaces and failure will occur when shearing stresses exceed the shearing strength of the slope forming material. The amount of shearing and fracturing and the attitude of beds or joints with relation to slope geometry are important criteria in determining slope stability conditions. The instability of slopes, whether it be outward or downward movements, are mostly influenced by forces such as huge accumulations of debris in the head regions of slides and diminishing resistance to sliding due to reduction in shear strength. This is usually attributed to high pore-water pressure and large slope deformations (Central Road Research Institute, 2000a). Choubey and Lallenmawia (1987) state that failure of natural slopes clears the surface off vegetation and other soil cover thereby exposing the surface to further erosion by surface and subsurface waters. Thigale et al. (1998) insist that slope metamorphosis due to anthropogenic activity is a vital factor in slope instability. Increase in moisture content induces slope failure, though moisture content need not be a target for monitoring Towhata (2007). Jakob (2000) found that landslides initiating on open slopes were more frequent than landslides initiating on the sides or headwall of steep, deeply incised, and confined mountain channels.

Climatic condition plays a vital role in slopes stability. Landslides occur frequently due to climatologic and geologic conditions with high tectonic activities (Raj et al., 2011). It is seen that incessant rainfall often acts as a triggering factor for slope failure. High rainfall may affect natural slopes and disturb slopes differently. Water enters pores and cracks of slope material and causes swelling which ultimately leads to decrease of shearing strength where cracks may develop (Nishida et al., 1979; Crozier, 1989). Such slopes may suddenly lose their stability due to loss of shearing strength though they may have remained stable over very long periods. Kumar et al. (1995) investigated slides between Rampur and Wangtu in Himachal Pradesh and found that major slides occur in the middle slopes while Piteau and Peckover (1989) are of the opinion that concave slopes tend to be more stable than those that are convex. They state that convex slopes cut in mountainous terrain for highways or any other developmental purposes are often more unstable. Dortch et al. (2008) studied the nature and timing of large landslides in the Himalaya and Trans-Himalaya of northern India and concluded that the temporal association between the occurrence of large landslides and enhanced monsoon precipitation suggests that the latter plays an important role in triggering large landslides. Heavily fractured bedrock and varying lithologies can enable an enhanced monsoon rainstorm to trigger large landslides. Enhanced precipitation may also have removed transiently stored material in the channel and undercut rock-slopes causing destabilization.

Landslides may occur in a geomorphic hollow and naturally lead to set a recovery process into motion. Hence it is necessary to estimate the rate of infilling of previous landslide scars for slope stability simulations. Infilling of hollows may span a period of several decades to several tens of millennia (Shimokawa, 1984; Reneau et al., 1986; DeRose, 1996). The infilling process is a complex set of hydrologic, geomorphic, and biological feedbacks that consist of surface wash, frost heave, dry ravel, slumping around the headwall, small landslides, inputs of woody debris, bioturbations, and soil creep. Infilling is generally rapid at first, dominated by inputs of sediment and wood, and progressively slower as sloughing and erosion give way to chronic processes such as soil creep.

4.2 Lithology

Natural slopes are made up of various types of rocks and soils; the physical characteristics of these rocks or soil formations play a significant role in slope instability. It has been widely documented that lithology greatly influences the occurrence of landslides, because lithological and structural variations often lead to a difference in strength and permeability of rocks and soils. The mineral assemblage and strength of the constituent minerals are important rock properties that affect stability. If the mineral constituents or strength of the bonds between the minerals are weak, the rocks tend to be fragile and become more unstable. Weathering greatly reduces the shearing resistance of rocks. While the planes of weakness within rock masses determine the stability of rock slopes to a great extent, their physical and mechanical properties are a function of the attitude, geometry, and spatial distribution of these planes. However, basic behavioural differences exist between rocks and soils. A rock mass is a heterogeneous and discontinuous medium composed essentially of different solid blocks that are separated by discontinuities. Therefore failure in rock masses tends to follow pre-existing discontinuities and do not occur throughout the intact rock to any great extent unless the rock is weak or incompetent. Hence, the shear strength of a rock mass is determined largely by the presence of discontinuities. On the other hand a soil mass is a relatively homogenous and continuous medium composed of loose particles. Failure in soil tends to occur within the soil mass and the direction of failure does not depend on variations of soil properties.

Veder and Hilbert (1980) insist that clays are important in the study of landslides because their cohesiveness and shear strength fall in the presence of water. They attribute loss of shear strength in clayey soils to the water absorption and resultant swelling of clays and ion exchange whereby loosely bonded clay minerals are replaced by others. The two processes may accelerate each other as they frequently interact. It is seen that because of superimposition of layers of rocks after sedimentation, clay minerals become dehydrated, compacted, and consolidated. Absorption and adsorption may also result in the removal of load water. It is also seen that water flows between platelets and causes an increase in volume, which subsequently reduces the bonding forces between particles. When there is a constant water source, water will flow in and out of clayey and sandy soils which may cause movements. The fine particles may not be washed out but the whole viscous mass may slowly creep downhill to the extent of several millimetres a day. Terzaghi (1950) is of the opinion that where silt is interbedded with sand or clay with silt, water percolating through the coarser permeable units gets trapped above the fine grained units; hence loss of shearing strength will result. Comegna et al. (2007) pointed out that the most widespread landslide type in clays is flow and that mudslides consist of softened clay which has a water content that is much higher than the parent formation. Materials forming mudslides completely lose their original structure and get highly destructured and softened. Mixtures of clay (matrix) and litho relicts (lumps) of the parent formation as rock fragments are also widespread in soils.

Clay deposits are generally less affected by discontinuities compared to rocks. However they are weakened by the presence of fine fissures. When fissures are even a few centimetres wide the slope may become unstable and slide down due to developmental activities. According to Ter-Stepanian (1974), Gudehus et al. (1976) and Blight (1977), slides in narrowly fissured clays take place as soon as the shear stresses exceed the average shear strength of the material. Occasionally, well consolidated clays may develop many small cracks and fissures which form an interconnecting network that may also affect stability. There are also occasions where clays possess well defined joints. These joints influence the nature and trend of landslides. Discontinuities seen in clays often act as water passages, which in turn softens up the mass. This leads to loss of cohesion and promotes chances of failure. It is noted that in clay deposits landslides are usually deep seated rotational failures.

4.3 Structure

It has been widely recognized that geologic and tectonic structures greatly accentuate the stability of slopes. Structures such as joints, faults, etc. play an important role in the deformation of rocks. However, according to Kandpal and Pant (1995) they are important only if they occur along the slopes or ridges of local topography. The strength of rocks may be reduced due to the presence of bedding planes, joints, or faults. Faults and joints are the most prominent of geological discontinuities that affect slope stability. Joint systems often cause more trouble in slopes than faults. The seepage of water along joints, faults, and bedding planes has been found to be more responsible for the occurrence of rock slides than the other causes combined. Increase in moisture content in joints filled with clay can cause considerable swelling pressure which may lead to rock falls and rock slides. Geological discontinuities like thrusts, faults, fractures, and joints reduce rock mass strength and result in marginal instability of slopes (Donati and Turrini, 2002). The deterioration of strength is more severe closer to the discontinuities and decreases away from such structural features. It is also noted that the frequency of landslides is greater near thrust zones and decreases progressively away.

Landslides are common phenomena in intensely fractured, faulted, and sheared areas. Weak geological structures such as folds, faults, joints, bedding, cleavage, foliation, lineation, etc. have aided slope failure in most regions affected by instability. Alternations of strata of variable strengths that are affected by geologic structures are favourable for slope movement. The attitude of bed or joint planes in relation to slope is an important criterion for determination of slope stability. Mehrotra et al. (1993) opine that instability increases proportionally as the strike of the discontinuities approaches that of the slope. Sharma et al. (1996) have indicated that secondary discontinuities also play an important role in slope failure. They also state that high incidences of discontinuities cause more instability.

Crosta et al. (2003) state that more than one soil horizon is usually evident at landslide scar sites. The failure surface is located, in most cases, at the contact between layers with contrasting physico-mechanical properties. Typical stratigraphic settings of terraced areas are represented by upper loose horizons with varying degree of anthropogenic reworking lying on compacted glacial or glacio-fluvial deposits, or on colluvial debris. Hence, the presence of deeper and more compacted horizons influence the depth of the foundations chosen for construction of dry retaining walls. Complex stratigraphic settings are evident at some scar sites. They are related to the natural spatial variability of soils and to the repeated sequence of reworking that the upper horizons suffered during the realisation and modification of terraces.

Fractures, fissures, joints, faults, and shear zones are very pronounced in the study area. These factors play a major role in promoting instability, individually or in varying combinations. Choubey and Lallenmawia (1989) opine that though tectonic structures are commonly responsible for slope failure, they have been given very little importance in landslide investigations. Aier (2005) opine that abundant and closely-spaced lineaments such as joints and faults in any area ensures severe erosion and slope failure. The degree of fracturing and shearing and the attitude of bedding or joint planes in relation to slope geometry are important criteria for determination of slope stability. If the orientation of a joint plane favours potential slope failure, the effects of other properties are generally unimportant. Aier et al. (2011b), in their analyses of the Merhülietsa slide, conclude that the slope-forming material, mostly crumpled and weathered shale, have suffered shear failure due to heavy rainfall along the tectonically active Sarmah fault.

4.4 Groundwater condition

Precipitation is a major source of groundwater. During monsoon most parts of the study area are highly saturated with the water table rising to appreciable heights. Groundwater in hilly terrain does not have a uniform flow pattern because they are generally channelled along structural discontinuities of rocks. An evaluation of the behaviour of groundwater on hill slopes is not possible over large areas. Therefore, in order to make a quick appraisal the nature of surface indications of the behaviour of groundwater will provide valuable information on the stability of hill slope for hazard mapping proposes Anbalagan (1992). The study area is made up dominantly of shale, much, of which are fractured, weathered, and crumpled. Water seepage into the subsurface is high during the monsoon. These waters seep out at various levels along hill slopes during this period. The drainage system can also cause high amounts of slope saturation leading to reduction in shear strength and thereby augment chances of slope failure. Sartori et al. (2003) state that groundwater circulation within networks of joints act as triggering mechanisms by effects of chemical alteration and water pressure.

Veder and Hilbert (1980) are of the opinion that a consolidated soil may swell only if hydrostatic pressure increases and earth pressure remains constant. It is seen that an increase of water pressure in soils may lead to water absorption. Bartarya and Valdiya (1989) and Mathewson and Clary (1997) opine that change in flow of underground water may lead to build-up of pore water pressure over a period of time and may cause a decrease in shear resistance, ultimately triggering landslides. Piteau and Peckover (1989) have shown that fluctuating water tables can also contribute markedly to the alteration and periodic changes in the mechanical properties of rocks. They have also stressed that knowledge of the controlling influences such as texture, stratigraphy, and structure on factors such as flow, permeability, recharge, and storage capacity are also important while giving consideration to environmental factors such as variations in climatic conditions that result in periods of either high or low recharge or other variations in groundwater conditions. It is also seen that the decisive factors for water absorption and proportionate loss of strength is the difference between the effective consolidation pressure and the pressure of water in contact with silty clays or clayey soils. Alteration of rocks can also be caused by moisture in such a way that its increase can cause high swelling pressures in certain clay minerals which may occur in joints either as infilling or as products of alteration. This may lead to rock falls or rock slides. A thorough knowledge of the hydrogeology of the region is thus necessary as pore-water pressure in joints is responsible for rock slides. Water on slopes affects stability by increasing the pore-water pressure in joints (Terzaghi, 1962; Muller, 1964; Serafim, 1968). Varshney et al. (1987) pointed out that the flow of water through fissures exerts a lateral pressure on the rock mass which is proportional to differential head. Slide affected areas and slopes usually have unconsolidated overburden and disturbed bedrock which allow easy access to percolating waters to saturate the slope-forming material and cause instability.

Keefer (1999) also analyzed the long-term effects of earthquakes, which may modify the characteristics of drainage basins. Erosion and transport of the landslide material may then finally result in creation of new alluvial fans, increasing also the potential of debris flows or water flows over time. Starkel (1972) states that at the contact between the regolith and bedrock the wet clays act as lubricants. At margins of landslides infiltration is even higher due to the presence of numerous cracks and joints. This reduces the shear strength of the rocks by displacing air and building up pore pressure on the regolith. In the regolith and deeply jointed bedrocks, water from precipitation or surface runoff normally has a very high infiltration rate. Rapid urbanization with haphazard developmental activities is the root cause of many landslides. Construction of highways without proper scientific studies and planning has taken its toll in slide related disturbances. Road cutting in areas of unfavourable dips of beds and strikes, will disrupt the natural slope as well as disturb the drainage system running along the slopes. In such kinds of areas underground water as well as surface water should be effectively drained off at various levels so that water finds a passage to get through the soil and rock mass.

4.5 Land use and land cover

Stability of hill slopes is greatly influenced by land use practices and type of land cover. These factors control erosion of the surface and rate of weathering of underlying rocks. Under normal conditions, if the soil is well covered, erosive activities are comparatively less. The rate of erosion is higher if the cover is less or lacking. However, it is notable that availability of forests and trees are not the answer for land stability. Deforestation brings about erosion and soil movement but its impact on creeping slopes is a matter of debate Gray (1973). Investigations indicate that instability may be brought about by deforestation Crozier and Vaughan (1990). Crozier (1989) is of the opinion that slope angles and height appear to be below the critical limits for mass movement on forested and unpopulated slopes. Because of the exploitation of natural vegetation for human needs has caused a gradual decline in the extent of their coverage. Deforestation and the creation of arable land may allow considerable water from rainfall to seep into the soil and ultimately leads to slope modification. It also removes top soil thus augmenting the process of erosion by surface waters flowing along slopes. Brown and Sheu (1975), on experimental observation conclude that removal of large heavy trees which also eliminates wind action on the vegetative cover, improves stability.

Bishop and Stevens (1964) and Swanston (1974) state that in shallow-depth landslides that are confined to the root zone, the apparent cohesion of slope material are reduced with the gradual decay of tree roots following deforestation. Zaruba and Mencl (1969) state that vegetative-type conversion commonly involves the changing of an area from trees and brush to a grass cover. Roots of plants play a vital role in enhancing stability of soil or rocks. This is done so by the physical consolidation through a network of roots and by drying out of surface layers. Swanston and Dyrness (1973), O'Loughlin (1974), and Burroughs and Thomas (1977) demonstrate the stabilizing effect of tree-root networks. It is found that the peak and residual shearing resistances increases two and four times respectively due to root networks. Lopez-Tello (1977) reports an increase of 33 percent of the safety factor for a 10 m high cut-slope in clay when covered with vegetation having a root density of 5000 kg/ha. Wu and Swanston (1980) noted a significant increase in the frequency of landslides in shallow soils on hillside slopes of south eastern Alaska following timber harvest. This phenomenon relates to the loss of root strength and evapo-transpiration stress that follows the cutting of the trees. Vegetated areas, especially dense with strong and large root systems, help in improving stability of slopes (Greenway, 1987). Vegetation provides both hydrological and mechanical effects that generally are beneficial to the stability of slopes. In contrast, barren areas and fallow lands destabilize slopes. Schuster (1997) opines that landslides affect topography, forests and grasslands, and natural habitats. Where such slides are controlled, a certain plant species, *Alprus nepalenses*, is found in abundance (Directorate of Geology and Mining, 1996).

Jakob (2000), while studying the impact of logging on landslide activity at Clayoquot Sound, British Columbia concluded that the frequency of landslides in logged terrain is nine times higher than in undisturbed forest. An exponential increase in landslide frequency within the area logged was observed on a large watershed scale. Debris slides and debris flows are the most frequently occurring mass movements, initiating mostly from road fill failures and from within cut blocks.

Conklin (1957) states that jhumming is a nomadic mode of cultivation. Jhum refers to unplanned shifting cultivation with an abrupt change in location. Arunachalam (1998) is of the opinion that where the accumulation of detrital matter is increased with increasing jhum cycling period, the water holding capacity and soil moisture content shows a significant increase. Some of the causes for instability of land or increase in landslides are poor drainage, toe erosion by streams, road construction activity including repeated back cutting, and recurring debris slides in the colluvium of slopes which destroy the vegetative cover. According to Mehrotra et al. (1993) human activity disturbs the natural balance of the environment which leads to destabilisation of slopes. Land use for various human activities and the amount of forest cover available controls the stability of slopes. Heavy constructions and other detrimental activities have also become a menace to the environment. There is very limited scope for extension of agricultural land to cope up with increasing pressure of population. As a result pressure on forested and other restricted areas is gradually increasing.

4.6 Rainfall

Rainfall-triggered landslides are part of a natural process of hill slope erosion that can result in catastrophic loss of life and extensive damage to property in mountainous, densely populated areas (Larsen, 2008). The relationship between climate and landslides has attracted the interest of numerous researchers because rainfall is the most frequent landslide-triggering factor in many regions in the world (Corominas, 2001). Many attempts have been made worldwide to establish relationships between rainfall and landslides (Pichler, 1957; Barata, 1969; Endo, 1970; Vargas, 1971; Guidicini and Iwasa, 1977). Most statistical analysis of rainfall and landsliding has developed to produce some sort of threshold beyond which a landslide occurs. The different methods of analysis mostly rely on attempting to define the relationship between the intensity and duration of precipitation with the incidence of landsliding (Ibsen and Casagli, 2004). Campbell (1975) identifies an intensity threshold above which landslides occur. Nilsen et al. (1976) have equally ascertained an intensity/storm threshold, stipulating that failures are even more likely to occur if the storm takes place after a particularly rainy period. Crozier (1996), Reichenbach et al. (1998), and Guzzetti et al. (2007) commented that a threshold may define rainfall, soil moisture, or hydrological conditions that, when reached or exceeded, are likely to trigger landslides. Caine (1980) collected a worldwide set of rainfall data recorded near reported sites of landslide occurrences and derived a rainfall-landslide threshold. The rainfall intensity-duration (ID) values were plotted in logarithmic coordinates and it was established that with increased rainfall duration, the minimum average intensity likely to trigger shallow slope failures decreases linearly, in the range of durations from 10 minutes to 35 days.

The different factors that control landslides such as steepness of slopes, soils, and vegetation are also affected by the amount, type, and yearly distribution of precipitation. High intensity rainfall generally leads to increased landslide activity. Nilsen and Turner (1975) established that dry periods probably reduce the effects of the previous precipitation on the landslide-generating capabilities of succeeding storms. The largest number of landslides will occur during and after long periods of relatively continuous rainfall. Nilsen et al. (1976) estimated that during periods of very intense rainfall abundant landslides generally occur, although the time sequence and amount of the annual rainfall vary greatly at any particular place, and the effect of these factors complicates the relation between rainfall and landsliding. Extreme rainfall often triggers landslides, sometimes with a considerable delay, pointing to a decrease in the shearing strength of the soil due to swelling (Veder and Hilbert, 1980). Jworchan and Nutalaya (1994) state that the addition of water on slopes due to rainfall triggers landslides. During the early months of the rainy season, higher rainfall intensities are required to activate landslides as compared to the later months. Landslides occur more easily when the ground is wetted and the water table is high. Areas with high mean annual rainfall are generally associated with abundant landslides. The alternating effect of wet and dry spells during the rainy season is another important factor affecting landslides. Abundance of water during the monsoon combines with it to cause debris flows. The majority of landslide incidences in India fall in the category of rainfall-induced landslides, especially in areas subject to limited periods of intense monsoon but that which remain dry during the rest of the year (Central Road Research Institute, 2000a).

The infiltration from rainfall accompanied by subsurface flow from upslope contributing areas (Beven and Kirkby, 1979; Montgomery and Dietrich, 1994; Acharya et al., 2006) saturates the soil around the toe of the flume and then triggers landslides. Brand (1981) has explained the mechanism of rain-induced failure in unsaturated residual soils. Abdullah and Ali (1994) and Chenniah et al. (1994) determined the safety factor for unsaturated residual soil slopes considering pore-water pressure. Zhang et al. (2000) have said that the mechanism by which rainstorms can lead to slope instability in the unsaturated zone in weathered rock profiles include percolation into the unsaturated part of a slope resulting in rise of groundwater tables. Corominas et al. (2003) studied rainfall triggers of landslides in the Spanish Eastern

Pyrenees and state that in slopes covered with pervious colluvium and weathered bedrock formations, high intensity short-lasting rainfall is able to trigger debris slides, debris flows, and rock falls. Only high intensity rains allow concentration and build-up of pore-water pressures that lead to slope failure. Campbell (1975) and Crozier (1999) established that sufficient antecedent rainfall is necessary to bring the regolith up to field capacity (the soil moisture beyond which gravity drainage will ensue) such that future rainfall may produce positive pore-pressures and trigger landslides. However, Emmanuel et al. (2004) concluded that landslides are not triggered until about 860 mm of rain have fallen during the monsoon.

The behavior of shallow and deep landslides is probably related to infiltration processes, namely the different pressure head responses to rainfall controlled by soil characteristics, slip surface depths, and effective hydraulic diffusivities (Iverson, 2000). Zezere et al. (2005) studied the shallow and deep landslides induced by rainfall in the Lisbon region of Portugal and concluded that shallow translational soil slips are related to intense rainfall periods ranging from 1 to 15 days, while deep slope movements like translational slides, rotational slides, and complex and composite slope movements occur in relation to longer periods of less intense rain, lasting from 30 to 90 days. Intense rainfall is responsible for the rapid growth of pore pressure and loss of apparent cohesion of thin soils, resulting in failure within the soil material or at the contact with the underlying impermeable bedrock. Long duration, less intense rainfall periods allow the steady rise of the groundwater table and the occurrence of deep failures through the reduction of shear strength of affected materials. Dahal et al. (2008) made a comparative analysis of contributing parameters for rainfall-triggered landslides in the Lesser Himalayan slopes of Nepal and found that shallow and highly mobile landslides in zero-order basins or topographic hollows are mainly triggered by transient pore-water pressure in response to intense monsoon rainfall and bedrock seepage. Tsai and Wang (2010) adopted four representative rainfall patterns that include uniform, advanced, intermediate, and delayed rainfalls for examination of influences of rainfall patterns on shallow landslides due to dissipation of matric suction. Results show that not only the occurrence of shallow landslides but also the failure depth are affected by rainfall pattern. A rainfall duration threshold for landslide occurrence exists in a rainfall event with larger than the minimum landslide triggering rainfall amount and decreases to a constant with increase in rainfall amount. Delayed rainfall has the largest rainfall duration threshold for landslide occurrence followed by intermediate rainfall, whereas uniform rainfall possesses the least rainfall duration threshold for landslide occurrence. Therefore, the occurrence of shallow landslides could be misevaluated if the rainfall pattern is not taken into account.

Heavy monsoon downpours account for most of the major landslides in Nagaland. As the study area falls within a small geographic unit, the rainfall event does not vary significantly and thus, the temporal probability is expected to be the same. Cloudbursts are a common occurrence in Nagaland. It has been noted that cloudbursts, particularly those occurring well into the rainy season, or those following prolonged wet spells, have been the cause for some of the most damaging landslides in this region (Kemas et al., 2004; Thong et al., 2004; Aier, 2005). Sengupta et al. (2009) and Anbarasu et al. (2010) studied the mechanism of activation of the Lanta Khola landslide in the Sikkim Himalaya and concluded that there is some correlation between the amount of rainfall and slide movement. The area receives very high rainfall, and slide activity is characteristically triggered during the monsoon, usually only after cloudbursts. Aier et al. (2009a) made a geotechnical assessment of the Mehrülietsa slide along NH 39 at Kohima and concluded that very heavy rainfall was the triggering factor for the landslide.

4.7 Seismicity

Earth vibrations weaken slopes thereby causing their failure by reducing the factor of safety of slope material. These factors causing slope failure include the intensity and duration of shaking, the type of slope, slope geometry and its geotechnical characteristics, local geological details, and existing pore-water pressure due to seepage, impounded water, or other conditions. The role of seismicity as a triggering mechanism should be studied for historic landslide events (Thigale, 1999). Many large landslides have been triggered by earthquakes (Schuster and Highland, 2001). Varnes (1978) and Brabb (1984) gave two basic assumptions required in the verification of landslide-susceptibility calculation models. One is that landslides are related to spatial factors such as topography, geology, and land cover and the other is that future landslides will be triggered by a specific impact such as seismic shock or heavy rainfall. Malamud et al. (2004) opine that landslide events are generally associated with a trigger such as an earthquake, a large storm, a rapid snowmelt, or a volcanic eruption. A landslide event may include a single landslide or many thousands and can be quantified by the frequency-area distribution of the triggered landslides. However, ground surface acceleration alone is a poor measure of the effect of shaking on slope stability (National Institute of Disaster Management, 2009).

According to Keefer (1984) and Rodriguez et al. (1999) landslides may be triggered by earthquakes of magnitude 4 or larger. Havenith and Bourdeau (2010) state that while most of the giant rockslides have been triggered by large magnitude seismic events ($M \geq 7$) in the Central Asian Mountain regions, loess earth-flows may be triggered by smaller earthquakes or even by climatic factors alone. Sassa (1996) observed that seismic landslide occurrence is strongly dependent on the proximity of the fault rupture. Wen et al. (2004) noted that the locations of most of large landslides are very close to major fault zones. From the Kashmir earthquake in 2005 Petley et al. (2006) noted that close to the fault rupture there was a high incidence of landslides triggered by the earthquake and that the distribution of these landslides appeared to be very asymmetric, with most of the landslides being located on the hanging wall on the northeastern side of the fault. For the same event Sato et al. (2007) further noted that more than one third of the landslides occurred within 1 km of the active fault.

Dadson et al. (2004) analyzed the co- and post-seismic geomorphic impact of the 1999 Chi-Chi event in Taiwan. In addition to the 20,000 landslides immediately triggered by the earthquake, they found that co-seismic weakening of substrate material had caused increased landsliding during subsequent typhoons. Further, they observed that most of the co-seismically produced landslide material was transported towards the rivers and noticed an increased sediment concentration during storms after the earthquake. Papathanassiou et al. (2005) observed that the most characteristic co-seismic effects were typical ground failures like rock falls, soil liquefaction, ground cracks, and slope failures.

Gurung et al. (2011) noted from stability studies of the Laprak Landslide of Nepal that a dry season earthquake should not be expected to trigger future movement whereas a wet season earthquake could exacerbate the effects of high pore-water pressures and produce sliding with even low factors of safety. Although a dry season earthquake with the same acceleration might not trigger landslide movement, it may still result in collapse of or damage to unreinforced stone buildings.

India stands highly vulnerable to seismic hazards owing to the burgeoning population and extensive developmental investments. In the past the country has experienced several devastating earthquakes namely Shillong (1897), Kangra (1905), Assam (1950), Bihar-Nepal (1934), Latur (1993), Jabalpur (1997), Chamoli (1999), Bhuj (2001), and Kashmir (2005) (Nath et al., 2008). The north-eastern region of India has been struck by more than 40 earthquakes with magnitudes greater than 6 in the last century of which two earthquakes with magnitudes greater than 8 have occurred in 1897 and 1950. Verma (1985) is of the opinion that repeated earthquakes in this region caused by intermittent tectonic stress releases indicate that the orogenic movements are still in progress. Froehlich et al. (1992) maintain that high density of joints in rocks is probably connected with high seismicity of any region. This would also support large scale mass wasting. Nagaland falls in the Zone-V category with an expected maximum magnitude greater than 8. It is therefore very important to take seismicity into consideration while studying landslides. However, data pertaining to earthquakes and their effects on surface instability are lacking.

CHAPTER 5

THEMATIC MAPPING

INTRODUCTION

Maps based on themes such as slope, lithology, structure, groundwater, and land use / land cover are generated for the study area, about 13.90 sq km, which has been divided into 225 facets.

The forms of instability in the study area include old and recent slides. The few subsidences noted are not mapped as they are confined to road sections that are built across shear and crushed zones. Vibrations due to movement of heavy vehicles along such weak planes that are saturated with groundwater are probably the cause of these subsidences.

5.1 Slope angle

This area comprises five categories of slope (Fig. 5.1a). These include are very gentle, gentle, moderately steep, steep, and very steep slopes. Very gentle slopes cover an area of 1.09 sq km which is 7.84% of the total area, gentle slopes occupy 8.3 sq km and represent 59.71% of the area, moderately steep slopes which cover 4.08 sq km represent 29.35%, steep and very steep slopes cover an area of 0.4 and 0.03 sq km which is 2.88% and 0.22% respectively. Ratings for different categories of slope are assigned (Table 5.1). Table 5.2 shows the frequency of landslides on the various slope categories. The pie chart indicates slope angle distribution (Fig. 5.1b).

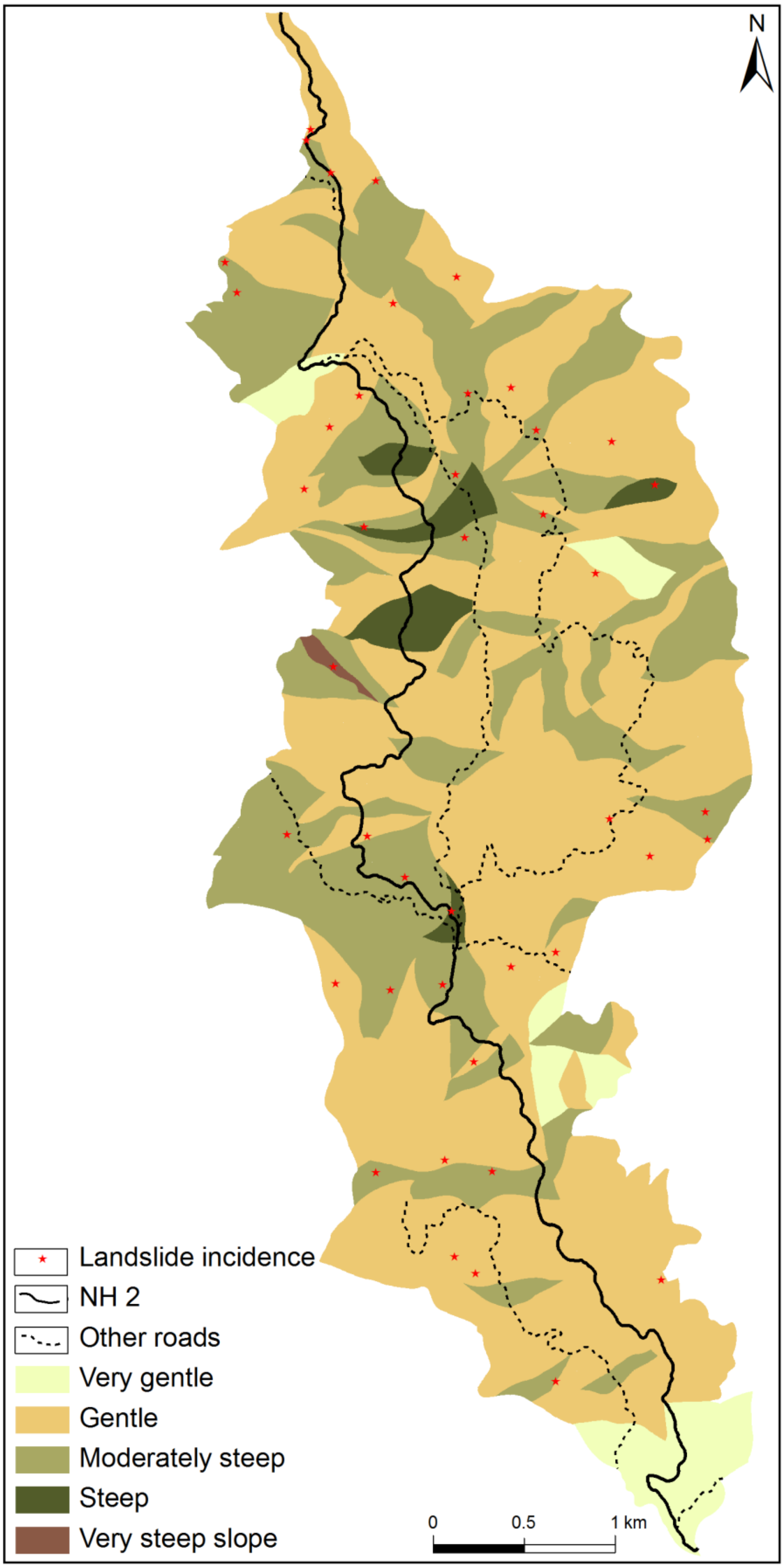

Fig. 5.1a. Slope morphometric map

Table 5.1. Observations, LHEF & TEHD

Facet No	Slope (2.0)		Lithology (2.5)		Structure (2.0)	Groundwater (1.0)		Land use / Land cover (1.5)		TEHD (9.0)	LHZ
1	Very gentle	0.5	Partially weathered shale	2.0	1.35	Dry	0.0	Populated land	0.7	4.55	MH
2	Very gentle	0.5	Partially weathered shale	2.0	1.35	Dry	0.0	Populated land	0.7	4.55	MH
3	Very gentle	0.5	Partially weathered shale	2.0	1.35	Dry	0.0	Populated land	0.7	4.55	MH
4	Very gentle	0.5	Partially weathered shale	2.0	1.35	Dry	0.0	Populated land	0.7	4.55	MH
5	Very gentle	0.5	Partially weathered shale	2.0	1.35	Dry	0.0	Populated land	0.7	4.55	MH
6	Gentle	0.8	Loose debris	2.5	2.00	Damp	0.2	Terrace cultivation	1.5	7.00	VHH
7	Gentle	0.8	Shale with minor sandstone	1.5	1.55	Damp	0.2	Populated land	0.7	4.75	MH
8	Gentle	0.8	Shale with minor sandstone	1.5	1.55	Damp	0.2	Populated land	0.7	4.75	MH
9	Gentle	0.8	Partially weathered shale	2.0	1.55	Dry	0.0	Populated land	0.7	5. 05	MH
10	Gentle	0.8	Partially weathered shale	2.0	1.55	Dry	0.0	Populated land	0.7	5. 05	MH
11	Gentle	0.8	Shale with minor sandstone	1.5	1.55	Dry	0.0	Moderate vegetation	1.0	4.85	MH
12	Moderately steep	1.2	Crumpled shale	2.0	0.85	Damp	0.2	Moderate vegetation	1.0	5.25	MH
13	Gentle	0.8	Partially weathered shale	2.0	1.55	Dry	0.0	Moderate vegetation	1.0	5.35	MH
14	Gentle	0.8	Partially weathered shale	2.0	1.55	Dry	0.0	Moderate vegetation	1.0	5.35	MH
15	Gentle	0.8	Loose debris	2.5	1.30	Dry	0.0	Terrace cultivation	1.5	6.10	HH
16	Moderately steep	1.2	Loose debris	2.5	1.30	Dry	0.0	Terrace cultivation	1.5	6.10	HH
17	Gentle	0.8	Crumpled shale	2.0	1.55	Dry	0.0	Moderate vegetation	1.0	5.35	MH
18	Gentle	0.8	Crumpled shale	2.0	1.55	Dry	0.0	Moderate vegetation	1.0	5.35	MH
19	Gentle	0.8	Crumpled shale	2.0	0.85	Dry	0.0	Moderate vegetation	1.0	4.35	LH
20	Gentle	0.8	Crumpled shale	2.0	0.85	Dry	0.0	Moderate vegetation	1.0	4.35	LH
21	Gentle	0.8	Crumpled shale	2.0	1.75	Dry	0.0	Dense vegetation	0.8	5.35	MH
22	Moderately steep	1.2	Crumpled shale	2.0	1.55	Dry	0.0	Moderate vegetation	1.0	5.35	MH
23	Gentle	0.8	Crumpled shale	2.0	1.55	Dry	0.0	Dense vegetation	0.8	5.15	MH
24	Gentle	0.8	Crumpled shale	2.0	1.55	Dry	0.0	Dense vegetation	0.8	5.15	MH
25	Gentle	0.8	Crumpled shale	2.0	1.55	Dry	0.0	Moderate vegetation	1.0	5.35	MH

26	Gentle	0.8	Loose debris	2.5	1.30	Dry	0.0	Terrace cultivation	1.5	6.10	HH
27	Gentle	0.8	Crumpled shale	2.0	1.55	Dry	0.0	Moderate vegetation	1.0	5.35	MH
28	Gentle	0.8	Crumpled shale	2.0	1.55	Dry	0.0	Moderate vegetation	1.0	5.35	MH
29	Gentle	0.8	Crumpled shale	2.0	1.55	Dry	0.0	Dense vegetation	0.8	5.15	MH
30	Gentle	0.8	Weathered shale	2.5	2.00	Dry	0.0	Terrace cultivation	1.5	6.80	VHH
31	Gentle	0.8	Weathered shale	2.5	2.00	Dry	0.0	Moderate vegetation	1.0	6.30	HH
32	Gentle	0.8	Loose debris	2.5	1.30	Dry	0.0	Terrace cultivation	1.5	6.10	HH
33	Gentle	0.8	Partially weathered shale	2.0	1.55	Dry	0.0	Moderate vegetation	1.0	5.35	MH
34	Gentle	0.8	Partially weathered shale	2.0	1.55	Dry	0.0	Moderate vegetation	1.0	5.35	MH
35	Gentle	0.8	Partially weathered shale	2.0	1.55	Dry	0.0	Moderate vegetation	1.0	5.35	MH
36	Gentle	0.8	Partially weathered shale	2.0	1.55	Dry	0.0	Moderate vegetation	1.0	5.35	MH
37	Gentle	0.8	Weathered shale	2.5	2.00	Dry	0.0	Moderate vegetation	1.0	6.30	HH
38	Moderately steep	1.2	Weathered shale	2.5	2.00	Dry	0.0	Moderate vegetation	1.0	6.30	HH
39	Moderately steep	1.2	Loose debris	2.5	2.00	Wet	0.5	Terrace cultivation	1.5	7.70	VHH
40	Gentle	0.8	Weathered shale	2.5	2.00	Dry	0.0	Moderate vegetation	1.0	6.30	HH
41	Gentle	0.8	Crumpled shale	2.0	1.55	Dry	0.0	Moderate vegetation	1.0	5.35	MH
42	Moderately steep	1.2	Weathered shale	2.5	2.00	Dry	0.0	Moderate vegetation	1.0	6.70	HH
43	Gentle	0.8	Weathered shale	2.5	2.00	Dry	0.0	Moderate vegetation	1.0	6.30	HH
44	Gentle	0.8	Weathered shale	2.5	2.00	Wet	0.5	Terrace cultivation	1.5	7.30	VHH
45	Gentle	0.8	Weathered shale	2.5	0.85	Dry	0.0	Moderate vegetation	1.0	5.15	MH
46	Gentle	0.8	Crumpled shale	2.0	1.55	Dry	0.0	Moderate vegetation	1.0	5.35	MH
47	Very gentle	0.5	Partially weathered shale	2.0	1.35	Dry	0.0	Populated land	0.7	4.55	MH
48	Very gentle	0.5	Partially weathered shale	2.0	1.35	Dry	0.0	Populated land	0.7	4.55	MH
49	Gentle	0.8	Crumpled shale	2.0	1.55	Dry	0.0	Moderate vegetation	1.0	5.35	MH
50	Very gentle	0.5	Partially weathered shale	2.0	1.35	Dry	0.0	Populated land	0.7	4.55	MH
51	Gentle	0.8	Crumpled shale	2.0	1.55	Dry	0.0	Moderate vegetation	1.0	5.35	MH
52	Moderately steep	1.2	Partially weathered shale	2.0	1.55	Dry	0.0	Populated land	0.7	5.40	MH
53	Very gentle	0.5	Partially weathered shale	2.0	1.35	Dry	0.0	Populated land	0.7	4.55	MH
54	Gentle	0.8	Loose debris	2.5	1.30	Dry	0.0	Terrace cultivation	1.5	6.10	HH

55	Gentle	0.8	Loose debris	2.5	2.00	Wet	0.5	Terrace cultivation	1.5	7.30	VHH
56	Moderately steep	1.2	Shale with minor sandstone	1.5	2.00	Dry	0.0	Moderate vegetation	1.0	5.70	HH
57	Gentle	0.8	Weathered shale	2.5	2.00	Dry	0.0	Moderate vegetation	1.0	6.30	HH
58	Gentle	0.8	Weathered shale	2.5	2.00	Dry	0.0	Moderate vegetation	1.0	6.30	HH
59	Moderately steep	1.2	Shale with minor sandstone	1.5	1.30	Dry	0.0	Sparse vegetation	1.2	5.20	MH
60	Gentle	0.8	Weathered shale	2.5	1.30	Dry	0.0	Terrace cultivation	1.5	6.10	HH
61	Moderately steep	1.2	Crumpled shale	2.0	1.00	Dry	0.0	Moderate vegetation	1.0	5.20	MH
62	Gentle	0.8	Weathered shale	2.5	2.00	Dry	0.0	Moderate vegetation	1.0	6.30	HH
63	Gentle	0.8	Weathered shale	2.5	2.00	Dry	0.0	Sparse vegetation	1.2	6.50	HH
64	Gentle	0.8	Weathered shale	2.5	2.00	Dry	0.0	Sparse vegetation	1.2	6.50	HH
65	Gentle	0.8	Crumpled shale	2.0	1.45	Dry	0.0	Sparse vegetation	1.2	5.45	HH
66	Gentle	0.8	Crumpled shale	2.0	1.45	Dry	0.0	Sparse vegetation	1.2	5.45	HH
67	Gentle	0.8	Crumpled shale	2.0	1.45	Dry	0.0	Sparse vegetation	1.2	5.45	HH
68	Gentle	0.8	Crumpled shale	2.0	1.55	Dry	0.0	Moderate vegetation	1.0	5.35	MH
69	Gentle	0.8	Loose debris	2.5	2.00	Wet	0.5	Terrace cultivation	1.5	7.30	VHH
70	Moderately steep	1.2	Crumpled shale	2.0	1.55	Damp	0.2	Moderate vegetation	1.0	5.95	HH
71	Moderately steep	1.2	Loose debris	2.5	2.00	Wet	0.5	Terrace cultivation	1.5	7.70	VHH
72	Moderately steep	1.2	Crumpled shale	2.0	1.55	Damp	0.2	Moderate vegetation	1.0	5.95	HH
73	Gentle	0.8	Crumpled shale	2.0	1.50	Dry	0.0	Moderate vegetation	1.0	5.30	MH
74	Gentle	0.8	Crumpled shale	2.0	1.45	Dry	0.0	Sparse vegetation	1.2	5.45	HH
75	Moderately steep	1.2	Crumpled shale	2.0	1.55	Damp	0.2	Moderate vegetation	1.0	5.95	HH
76	Moderately steep	1.2	Crumpled shale	2.0	1.00	Dry	0.0	Moderate vegetation	1.0	5.20	MH
77	Moderately steep	1.2	Crumpled shale	2.0	1.55	Damp	0.2	Moderate vegetation	1.0	5.95	HH
78	Gentle	0.8	Crumpled shale	2.0	1.55	Dry	0.0	Moderate vegetation	1.0	5.35	MH
79	Gentle	0.8	Weathered shale	2.5	2.00	Damp	0.2	Sparse vegetation	1.2	6.70	HH
80	Gentle	0.8	Weathered shale	2.5	2.00	Damp	0.2	Moderate vegetation	1.0	6.50	HH
81	Steep	1.7	Weathered shale	2.5	2.00	Wet	0.5	Moderate vegetation	1.0	7.70	VHH
82	Moderately steep	1.2	Loose debris	2.5	2.00	Wet	0.5	Terrace cultivation	1.5	7.70	VHH
83	Moderately steep	1.2	Crumpled shale	2.0	1.55	Wet	0.5	Moderate vegetation	1.0	6.25	HH

84	Moderately steep	1.2	Crumpled shale	2.0	1.55	Wet	0.5	Sparse vegetation	1.2	6.45	HH
85	Moderately steep	1.2	Crumpled shale	2.0	1.55	Wet	0.5	Sparse vegetation	1.2	6.45	HH
86	Moderately steep	1.2	Crumpled shale	2.0	1.55	Wet	0.5	Moderate vegetation	1.0	6.25	HH
87	Moderately steep	1.2	Weathered shale	2.5	2.00	Dry	0.0	Moderate vegetation	1.0	6.70	HH
88	Moderately steep	1.2	Weathered shale	2.5	2.00	Dry	0.0	Moderate vegetation	1.0	6.70	HH
89	Moderately steep	1.2	Weathered shale	2.5	2.00	Damp	0.2	Dense vegetation	0.8	6.70	HH
90	Moderately steep	1.2	Loose debris	2.5	2.00	Wet	0.5	Terrace cultivation	1.5	7.70	VHH
91	Gentle	0.8	Crumpled shale	2.0	1.55	Damp	0.2	Dense vegetation	0.8	5.35	MH
92	Gentle	0.8	Crumpled shale	2.0	1.55	Damp	0.2	Dense vegetation	0.8	5.35	MH
93	Moderately steep	1.2	Crumpled shale	2.0	1.55	Damp	0.2	Moderate vegetation	1.0	5.95	HH
94	Moderately steep	1.2	Shale with minor sandstone	1.5	1.55	Damp	0.2	Moderate vegetation	1.0	5.45	HH
95	Gentle	0.8	Shale with minor sandstone	1.5	1.00	Dry	0.0	Sparse vegetation	1.2	4.50	LH
96	Gentle	0.8	Shale with minor sandstone	1.5	1.00	Dry	0.0	Sparse vegetation	1.2	4.50	LH
97	Gentle	0.8	Shale with minor sandstone	1.5	1.00	Dry	0.0	Sparse vegetation	1.2	4.50	LH
98	Gentle	0.8	Weathered shale	2.5	2.00	Damp	0.2	Sparse vegetation	1.2	6.70	HH
99	Gentle	0.8	Weathered shale	2.5	2.00	Dry	0.0	Sparse vegetation	1.2	6.50	HH
100	Gentle	0.8	Weathered shale	2.5	2.00	Dry	0.0	Sparse vegetation	1.2	6.50	HH
101	Gentle	0.8	Loose debris	2.5	2.00	Damp	0.2	Sparse vegetation	1.2	6.70	HH
102	Gentle	0.8	Crumpled shale	2.0	1.35	Dry	0.0	Sparse vegetation	1.2	5.35	MH
103	Gentle	0.8	Crumpled shale	2.0	1.35	Dry	0.0	Sparse vegetation	1.2	5.35	MH
104	Gentle	0.8	Crumpled shale	2.0	1.35	Dry	0.0	Sparse vegetation	1.2	5.35	MH
105	Gentle	0.8	Crumpled shale	2.0	1.35	Dry	0.0	Sparse vegetation	1.2	5.35	MH
106	Moderately steep	1.2	Crumpled shale	2.0	1.55	Damp	0.2	Terrace cultivation	1.5	6.45	HH
107	Gentle	0.8	Weathered shale	2.5	2.00	Damp	0.2	Sparse vegetation	1.2	6.70	HH
108	Gentle	0.8	Crumpled shale	2.0	1.55	Dry	0.0	Moderate vegetation	1.0	5.35	MH
109	Gentle	0.8	Weathered shale	2.5	2.00	Damp	0.2	Sparse vegetation	1.2	6.70	HH
110	Gentle	0.8	Weathered shale	2.5	2.00	Damp	0.2	Sparse vegetation	1.2	6.70	HH
111	Moderately steep	1.2	Weathered shale	2.5	2.00	Wet	0.5	Sparse vegetation	1.2	7.40	VHH
112	Gentle	0.8	Weathered shale	2.5	2.00	Damp	0.2	Sparse vegetation	1.2	6.70	HH

113	Gentle	0.8	Weathered shale	2.5	2.00	Damp	0.2	Sparse vegetation	1.2	6.70	HH
114	Gentle slope	0.8	Weathered shale	2.5	2.00	Damp	0.2	Sparse vegetation	1.2	6.70	HH
115	Moderately steep	1.2	Weathered shale	2.5	2.00	Dry	0.0	Moderate vegetation	1.0	6.70	HH
116	Moderately steep	1.2	Sandstone with minor shale	0.5	1.10	Dry	0.0	Moderate vegetation	1.0	3.80	LH
117	Moderately steep	1.2	Sandstone with minor shale	0.5	1.50	Dry	0.0	Moderate vegetation	1.0	4.20	LH
118	Gentle	0.8	Weathered shale	2.5	2.00	Damp	0.2	Moderate vegetation	1.0	6.50	HH
119	Moderately steep	1.2	Sandstone with minor shale	0.5	1.20	Dry	0.0	Moderate vegetation	1.0	3.90	LH
120	Gentle	0.8	Weathered shale	2.5	2.00	Damp	0.2	Moderate vegetation	1.0	6.50	HH
121	Moderately steep	1.2	Weathered shale	2.5	2.00	Dry	0.0	Moderate vegetation	1.0	6.70	HH
122	Gentle	0.8	Weathered shale	2.5	2.00	Dry	0.0	Sparse vegetation	1.2	6.50	HH
123	Moderately steep	1.2	Weathered shale	2.5	2.00	Wet	0.5	Moderate vegetation	1.0	7.20	VHH
124	Gentle	0.8	Weathered shale	2.5	2.00	Damp	0.2	Moderate vegetation	1.0	6.50	HH
125	Gentle	0.8	Crumpled shale	2.0	1.55	Dry	0.0	Moderate vegetation	1.0	5.35	MH
126	Gentle	0.8	Crumpled shale	2.0	1.55	Dry	0.0	Moderate vegetation	1.0	5.35	MH
127	Gentle	0.8	Crumpled shale	2.0	1.55	Dry	0.0	Dense vegetation	0.8	5.15	MH
128	Gentle	0.8	Crumpled shale	2.0	1.55	Dry	0.0	Moderate vegetation	1.0	5.35	MH
129	Moderately steep	1.2	Weathered shale	2.5	2.00	Dry	0.0	Moderate vegetation	1.0	6.70	HH
130	Gentle	0.8	Weathered shale	2.5	1.30	Dry	0.0	Terrace cultivation	1.5	6.10	HH
131	Gentle	0.8	Weathered shale	2.5	2.00	Damp	0.2	Dense vegetation	0.8	6.30	HH
132	Gentle	0.8	Crumpled shale	2.0	1.55	Dry	0.0	Moderate vegetation	1.0	5.35	MH
133	Moderately steep	1.2	Weathered shale	2.5	2.00	Dry	0.0	Moderate vegetation	1.0	6.70	HH
134	Moderately steep	1.2	Weathered shale	2.5	2.00	Dry	0.0	Moderate vegetation	1.0	6.70	HH
135	Gentle	0.8	Crumpled shale	2.0	1.55	Dry	0.0	Dense vegetation	0.8	5.15	MH
136	Gentle	0.8	Crumpled shale	2.0	1.55	Dry	0.0	Dense vegetation	0.8	5.15	MH
137	Gentle	0.8	Crumpled shale	2.0	1.55	Dry	0.0	Dense vegetation	0.8	5.15	MH
138	Gentle	0.8	Crumpled shale	2.0	1.55	Dry	0.0	Moderate vegetation	1.0	5.35	MH
139	Moderately steep	1.2	Weathered shale	2.5	2.00	Dry	0.0	Moderate vegetation	1.0	6.70	HH
140	Moderately steep	1.2	Weathered shale	2.5	2.00	Dry	0.0	Moderate vegetation	1.0	6.70	HH
141	Very steep slope	2.0	Crumpled shale	2.0	1.55	Damp	0.2	Moderate vegetation	1.0	6.75	HH

142	Moderately steep	1.2	Crumpled shale	2.0	1.20	Dry	0.0	Moderate vegetation	1.0	5.40	MH
143	Gentle	0.8	Weathered shale	2.5	1.30	Dry	0.0	Terrace cultivation	1.5	6.10	HH
144	Gentle	0.8	Loose debris	2.5	1.30	Dry	0.0	Terrace cultivation	1.5	6.10	HH
145	Steep	1.7	Crumpled shale	2.0	1.55	Damp	0.2	Moderate vegetation	1.0	6.45	HH
146	Steep	1.7	Crumpled shale	2.0	1.55	Damp	0.2	Moderate vegetation	1.0	6.45	HH
147	Gentle	0.8	Crumpled shale	2.0	1.55	Dry	0.0	Moderate vegetation	1.0	5.35	MH
148	Moderately steep	1.2	Weathered shale	2.5	2.00	Dry	0.0	Moderate vegetation	1.0	6.70	HH
149	Moderately steep	1.2	Shale	1.0	1.55	Damp	0.2	Moderate vegetation	1.0	4.95	MH
150	Gentle	0.8	Sandstone with minor shale	0.5	1.30	Dry	0.0	Sparse vegetation	1.2	3.80	LH
151	Gentle	0.8	Weathered shale	2.5	2.00	Damp	0.2	Sparse vegetation	1.2	6.70	HH
152	Gentle	0.8	Weathered shale	2.5	2.00	Damp	0.2	Sparse vegetation	1.2	6.70	HH
153	Very gentle	0.5	Weathered shale	2.5	1.30	Wet	0.5	Terrace cultivation	1.5	6.30	HH
154	Moderately steep	1.2	Weathered shale	2.5	2.00	Dry	0.0	Moderate vegetation	1.0	6.70	HH
155	Gentle	0.8	Crumpled shale	2.0	1.55	Dry	0.0	Moderate vegetation	1.0	5.35	MH
156	Gentle	0.8	Crumpled shale	2.0	1.55	Dry	0.0	Dense vegetation	0.8	5.15	MH
157	Gentle	0.8	Crumpled shale	2.0	1.55	Dry	0.0	Moderate vegetation	1.0	5.35	MH
158	Moderately steep	1.2	Crumpled shale	2.0	1.55	Wet	0.5	Sparse vegetation	1.2	6.45	HH
159	Gentle	0.8	Crumpled shale	2.0	1.55	Dry	0.0	Moderate vegetation	1.0	5.35	MH
160	Moderately steep	1.2	Weathered shale	2.5	2.00	Dry	0.0	Moderate vegetation	1.0	6.70	HH
161	Moderately steep	1.2	Weathered shale	2.5	2.00	Dry	0.0	Dense vegetation	0.8	6.50	HH
162	Steep	1.7	Weathered shale	2.5	2.00	Wet	0.5	Terrace cultivation	1.5	8.20	VHH
163	Gentle	0.8	Weathered shale	2.5	2.00	Damp	0.2	Sparse vegetation	1.2	6.70	HH
164	Gentle	0.8	Crumpled shale	2.0	1.55	Dry	0.0	Moderate vegetation	1.0	5.35	MH
165	Gentle	0.8	Loose debris	2.5	1.30	Dry	0.0	Terrace cultivation	1.5	6.10	HH
166	Gentle	0.8	Crumpled shale	2.0	1.55	Dry	0.0	Moderate vegetation	1.0	5.35	MH
167	Gentle	0.8	Crumpled shale	2.0	1.55	Dry	0.0	Dense vegetation	0.8	5.15	MH
168	Gentle	0.8	Loose debris	2.5	1.30	Damp	0.2	Terrace cultivation	1.5	6.30	HH
169	Moderately steep	1.2	Crumpled shale	2.0	1.55	Damp	0.2	Moderate vegetation	1.0	5.95	HH
170	Moderately steep	1.2	Crumpled shale	2.0	1.55	Damp	0.2	Moderate vegetation	1.0	5.95	HH

171	Gentle	0.8	Crumpled shale	2.0	1.55	Damp	0.2	Dense vegetation	0.8	5.35	MH
172	Gentle	0.8	Crumpled shale	2.0	1.55	Damp	0.2	Dense vegetation	0.8	5.35	MH
173	Moderately steep	1.2	Weathered shale	2.5	2.00	Dry	0.0	Dense vegetation	0.8	6.50	HH
174	Moderately steep	1.2	Loose debris	2.5	2.00	Wet	0.5	Terrace cultivation	1.5	7.70	VHH
175	Steep	1.7	Loose debris	2.5	2.00	Wet	0.5	Terrace cultivation	1.5	8.20	VHH
176	Steep	1.7	Loose debris	2.5	2.00	Wet	0.5	Terrace cultivation	1.5	8.20	VHH
177	Moderately steep	1.2	Weathered shale	2.5	2.00	Damp	0.2	Dense vegetation	0.8	6.70	HH
178	Moderately steep	1.2	Crumpled shale	2.0	0.85	Damp	0.2	Dense vegetation	0.8	5.05	MH
179	Gentle	0.8	Crumpled shale	2.0	1.55	Dry	0.0	Dense vegetation	0.8	5.15	MH
180	Moderately steep	1.2	Weathered shale	2.5	2.00	Dry	0.0	Dense vegetation	0.8	6.50	HH
181	Moderately steep	1.2	Weathered shale	2.5	2.00	Dry	0.0	Dense vegetation	0.8	6.50	HH
182	Gentle	0.8	Weathered shale	2.5	2.00	Damp	0.2	Moderate vegetation	1.0	6.50	HH
183	Gentle	0.8	Weathered shale	2.5	2.00	Wet	0.5	Dense vegetation	0.8	6.60	HH
184	Moderately steep	1.2	Weathered shale	2.5	2.00	Dry	0.0	Dense vegetation	0.8	6.50	HH
185	Gentle	0.8	Partially weathered shale	2.0	1.50	Dry	0.0	Moderate vegetation	1.0	5.30	MH
186	Steep	1.7	Sandstone with minor shale	0.5	1.20	Dry	0.0	Dense vegetation	0.8	4.20	LH
187	Moderately steep	1.2	Crumpled shale	2.0	1.55	Wet	0.5	Moderate vegetation	1.0	6.25	HH
188	Moderately steep	1.2	Crumpled shale	2.0	1.55	Wet	0.5	Moderate vegetation	1.0	6.25	HH
189	Moderately steep	1.2	Crumpled shale	2.0	1.55	Wet	0.5	Moderate vegetation	1.0	6.25	HH
190	Gentle	0.8	Loose debris	2.5	1.30	Dry	0.0	Terrace cultivation	1.5	6.10	HH
191	Gentle	0.8	Crumpled shale	2.0	1.55	Dry	0.0	Moderate vegetation	1.0	5.35	MH
192	Gentle	0.8	Weathered shale	2.5	2.00	Damp	0.2	Moderate vegetation	1.0	6.50	HH
193	Very gentle	0.5	Partially weathered shale	2.0	1.35	Dry	0.0	Populated land	0.7	4.55	MH
194	Moderately steep	1.2	Partially weathered shale	2.0	1.55	Dry	0.0	Populated land	0.7	5.40	MH
195	Moderately steep	1.2	Partially weathered shale	2.0	1.55	Wet	0.5	Sparse vegetation	1.2	6.45	HH
196	Moderately steep	1.2	Partially weathered shale	2.0	1.55	Wet	0.5	Dense vegetation	0.8	6.05	HH
197	Moderately steep	1.2	Partially weathered shale	2.0	1.55	Wet	0.5	Dense vegetation	0.8	6.05	HH
198	Very gentle	0.5	Partially weathered shale	2.0	1.35	Dry	0.0	Populated land	0.7	4.55	MH
199	Gentle	0.8	Crumpled shale	2.0	1.55	Wet	0.5	Moderate vegetation	1.0	5.85	HH

200	Gentle	0.8	Weathered shale	2.5	2.00	Damp	0.2	Dense vegetation	0.8	6.30	HH
201	Gentle	0.8	Weathered shale	2.5	2.00	Damp	0.2	Dense vegetation	0.8	6.30	HH
202	Gentle	0.8	Weathered shale	2.5	2.00	Damp	0.2	Dense vegetation	0.8	6.30	HH
203	Gentle	0.8	Weathered shale	2.5	2.00	Damp	0.2	Moderate vegetation	1.0	6.50	HH
204	Gentle	0.8	Weathered shale	2.5	2.00	Damp	0.2	Moderate vegetation	1.0	6.50	HH
205	Moderately steep	1.2	Weathered shale	2.5	2.00	Dry	0.0	Moderate vegetation	1.0	6.70	HH
206	Gentle	0.8	Loose debris	2.5	2.00	Wet	0.5	Terrace cultivation	1.5	7.30	VHH
207	Gentle	0.8	Crumpled shale	2.0	1.55	Damp	0.2	Dense vegetation	0.8	5.35	MH
208	Moderately steep	1.2	Crumpled shale	2.0	1.55	Damp	0.2	Moderate vegetation	1.0	5.95	HH
209	Gentle	0.8	Crumpled shale	2.0	1.55	Dry	0.0	Moderate vegetation	1.0	5.35	MH
210	Gentle	0.8	Weathered shale	2.5	2.00	Wet	0.5	Terrace cultivation	1.5	7.30	VHH
211	Gentle	0.8	Weathered shale	2.5	2.00	Wet	0.5	Terrace cultivation	1.5	7.30	VHH
212	Moderately steep	1.2	Weathered shale	2.5	2.00	Dry	0.0	Dense vegetation	0.8	6.50	HH
213	Moderately steep	1.2	Weathered shale	2.5	2.00	Dry	0.0	Moderate vegetation	1.0	6.70	HH
214	Moderately steep	1.2	Partially weathered shale	2.0	1.55	Dry	0.0	Populated land	0.7	5.45	HH
215	Gentle	0.8	Crumpled shale	2.0	1.35	Dry	0.0	Sparse vegetation	1.2	5.35	MH
216	Gentle	0.8	Sandstone with minor shale	0.5	1.20	Damp	0.2	Moderate vegetation	1.0	3.70	LH
217	Gentle	0.8	Sandstone with minor shale	0.5	1.10	Damp	0.2	Moderate vegetation	1.0	3.60	LH
218	Gentle	0.8	Shale with minor sandstone	1.5	1.35	Dry	0.0	Moderate vegetation	1.0	4.65	MH
219	Gentle	0.8	Crumpled shale	2.0	1.55	Dry	0.0	Moderate vegetation	1.0	5.35	MH
220	Moderately steep	1.2	Crumpled shale	2.0	1.55	Wet	0.5	Sparse vegetation	1.2	6.45	HH
221	Gentle	0.8	Crumpled shale	2.0	1.55	Wet	0.5	Sparse vegetation	1.2	6.05	HH
222	Moderately steep	1.2	Weathered shale	2.5	2.00	Dry	0.0	Moderate vegetation	1.0	6.70	HH
223	Gentle	0.8	Weathered shale	2.5	2.00	Damp	0.2	Moderate vegetation	1.0	6.50	HH
224	Moderately steep	1.2	Weathered shale	2.5	2.00	Wet	0.5	Sparse vegetation	1.2	7.40	VHH
225	Gentle	0.8	Crumpled shale	2.0	1.55	Dry	0.0	Moderate vegetation	1.0	5.35	MH

Table 5.2. Frequency of landslide incidences on slope

Category	Area		Landslide		Frequency
	km^2	%	No	%	No/km^2
Very gentle	1.09	7.84	-	-	-
Gentle	8.30	59.71	20	46.50	2.41
Moderately steep	4.08	29.35	19	44.19	4.66
Steep	0.40	2.88	3	6.98	7.50
Very steep	0.03	0.22	1	2.33	33.33

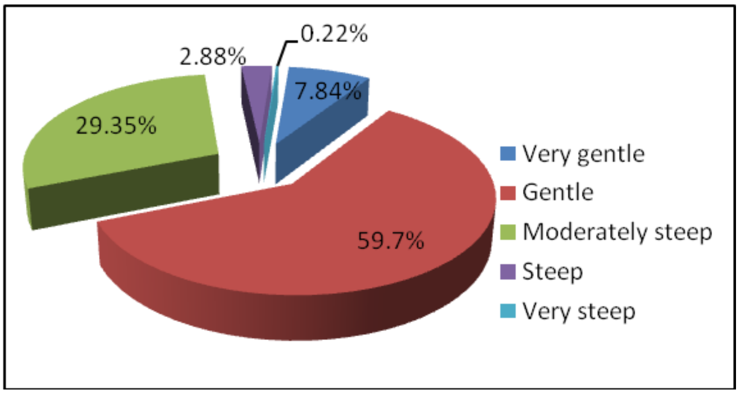

Fig. 5.1b. Distribution of slopes

5.2 Lithology

Seven classes of litho-units are noted in this segment (Fig. 5.2a) and ratings for the various litho-units are given in Table 5.1. The first class is represented by sandstone with minor shale that occupies an area of 0.75 sq km and which is 4.40% of the total area. The second litho-unit consists of shale which occupies 0.04 sq km which is 0.29% of the area. The third class comprises shale with minor sandstone covering an area of 0.26 sq km representing 1.87%. The fourth litho-unit comprising crumpled shale covers an area of 4.97 sq km which is 35.78%. The fifth litho-unit consisting of partially weathered shale covers 1.65 sq km which accounts for 11.88%. The sixth class represent weathered shale covering an area of 4.80 sq km which is 34.56% of the area and the last litho-unit consists of loose debris which covers 1.42 sq km which is 10.22% of the total area. The following chart (Table 5.3) shows the frequency of landslides in the various litho-units. The pie chart shows the distribution of the various litho-units (Fig. 5.2b).

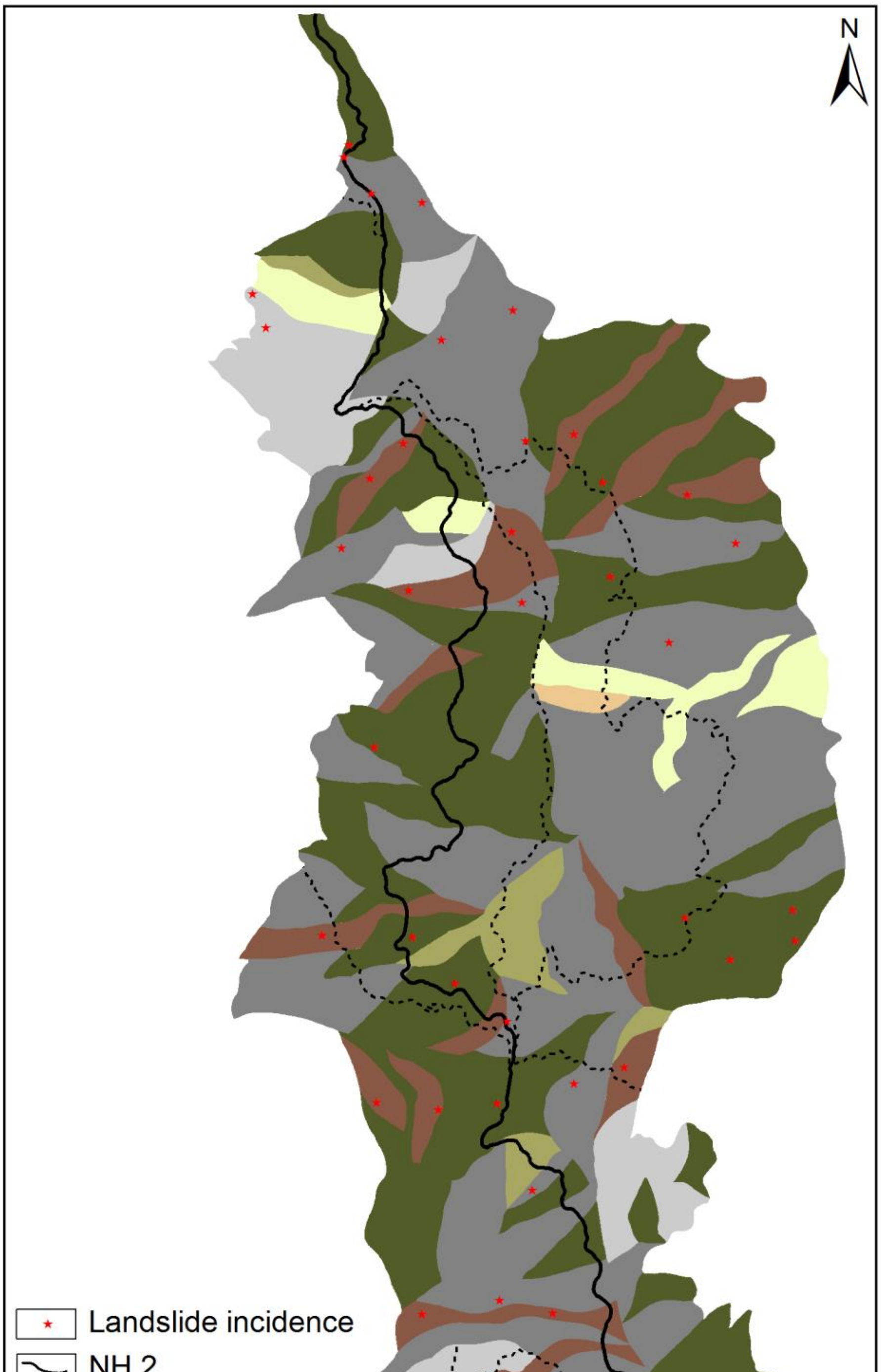

Fig. 5.2a. Lithological map

Table 5.3. Frequency of landslide incidences on lithology

Category	Area		Landslide		Frequency
	km^2	%	No	%	No/km^2
Sandstone/minor shale	0.75	5.40	-	-	-
Shale	0.04	0.29	-	-	-
Shale/minor sandstone	0.26	1.87	-	-	-
Crumpled shale	4.97	35.78	11	25.58	2.21
Partially weathered shale	1.65	11.88	2	4.65	1.21
Weathered shale	4.80	34.56	15	34.88	3.13
Loose debris	1.42	10.22	15	34.88	10.56

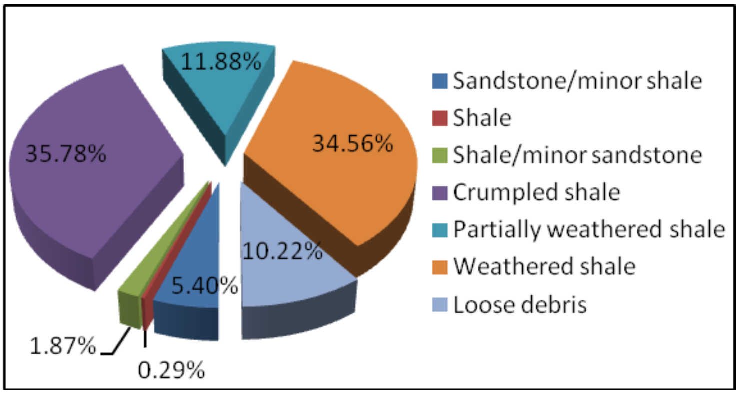

Fig. 5.2b. Distribution of litho-units

5.3 Structure

Structure is an important parameter in determining landslide characteristics. The structural elements in the study area include bedding planes, three to four sets of joints, faults, and shear zones. The direction and inclination of slopes and disposition of structural discontinuities are important relationships in an understanding of slope stability. The risk of failure increases when a discontinuity or the line of intersection of two discontinuities is parallel to a slope. Probability of failure also increases with increasing dip of discontinuity or the plunge of the line of intersection of two discontinuities. The failure potential also remains high if the inclination of the slope is more than the dip of discontinuity or the plunge of the line of intersection of two discontinuities. Discontinuities of interest in this area include joint planes. The ratings for the various facets of this area are given in Table 5.1. Sixteen faults traversing the study area are mapped using satellite imagery (Fig. 5.3). Five of these trend NE-SW, five almost N-S, while one trends NNW-SSE along the entire study area. Another fault trends along a NNE-SSW direction whereas the other four trend E-W.

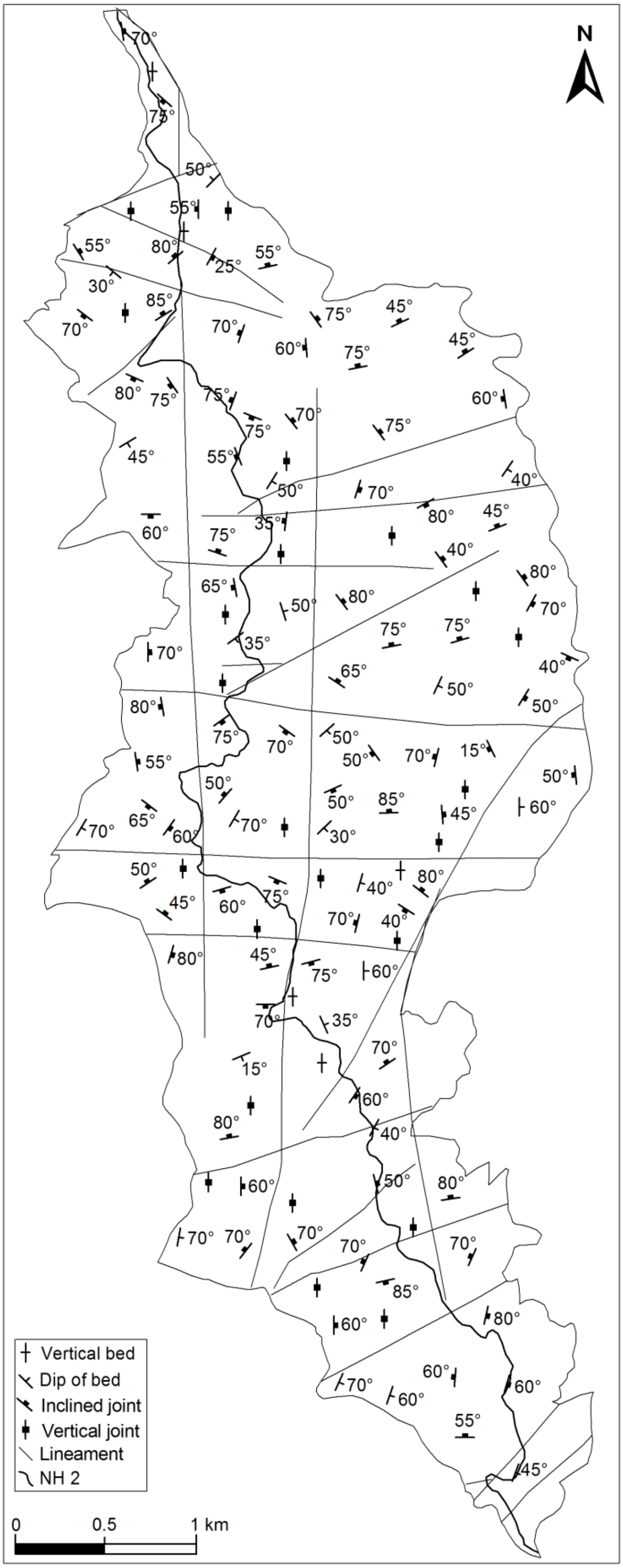

Fig. 5.3. Structural Map

5.4 Groundwater condition

Surface indications of groundwater provide valuable information because observations of groundwater activity on hill slopes are not possible over large areas. Three categories of groundwater conditions are noted in this area (Fig. 5.4a) including dry, damp, and wet for which ratings are assigned (Table 5.1). Dry conditions are noted in 8.18 sq km which is 58.85% of the total area. Damp and wet groundwater conditions cover 3.57 and 2.15 sq km which represent 25.68% and 15.47% respectively. The following chart (Table 5.4) portrays the frequency of landslides on groundwater condition. A pie chart shows the distribution of various categories of groundwater condition (Fig. 5.4b).

Table 5.4. Frequency of landslide incidences on groundwater condition

Category	Area		Landslide		Frequency
	km^2	%	No	%	No/km^2
Dry	8.18	58.85	15	34.88	1.83
Damp	3.57	25.68	8	18.60	2.24
Wet	2.15	15.47	20	46.51	9.30

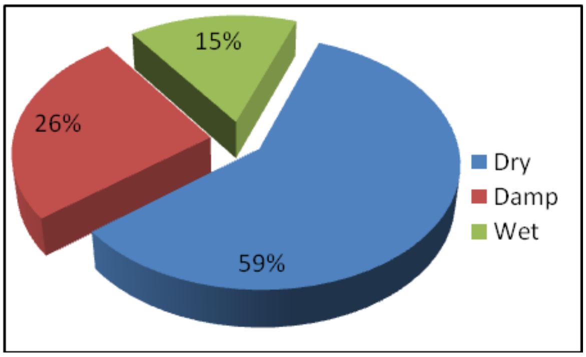

Fig. 5.4b. Distribution of groundwater condition

5.5 Land use / land cover

Land use and land cover of the area have been classified under five categories (Fig. 5.5a). The first class comprises populated land which covers an area of 1.18 sq km and represents 8.49% of the total area. The second class comprises dense vegetation which occupies 14.03% of the area, covering 1.95 sq km. The third class includes moderate vegetation which accounts for 43.88% and covering an area of 6.10 sq km. The fourth class consisting of those areas with sparse vegetation occupy 2.67 sq km which is 19.21% of the area. The fifth class comprises terrace cultivations covering

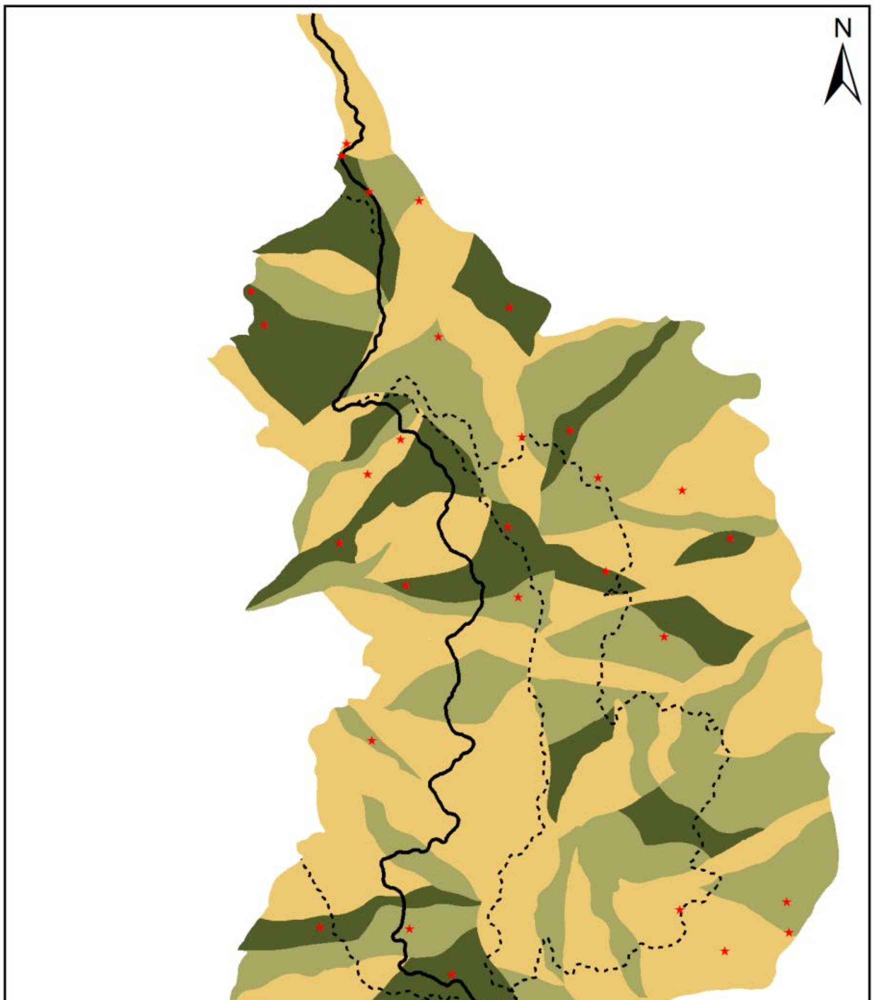

Fig. 5.4a. Groundwater map

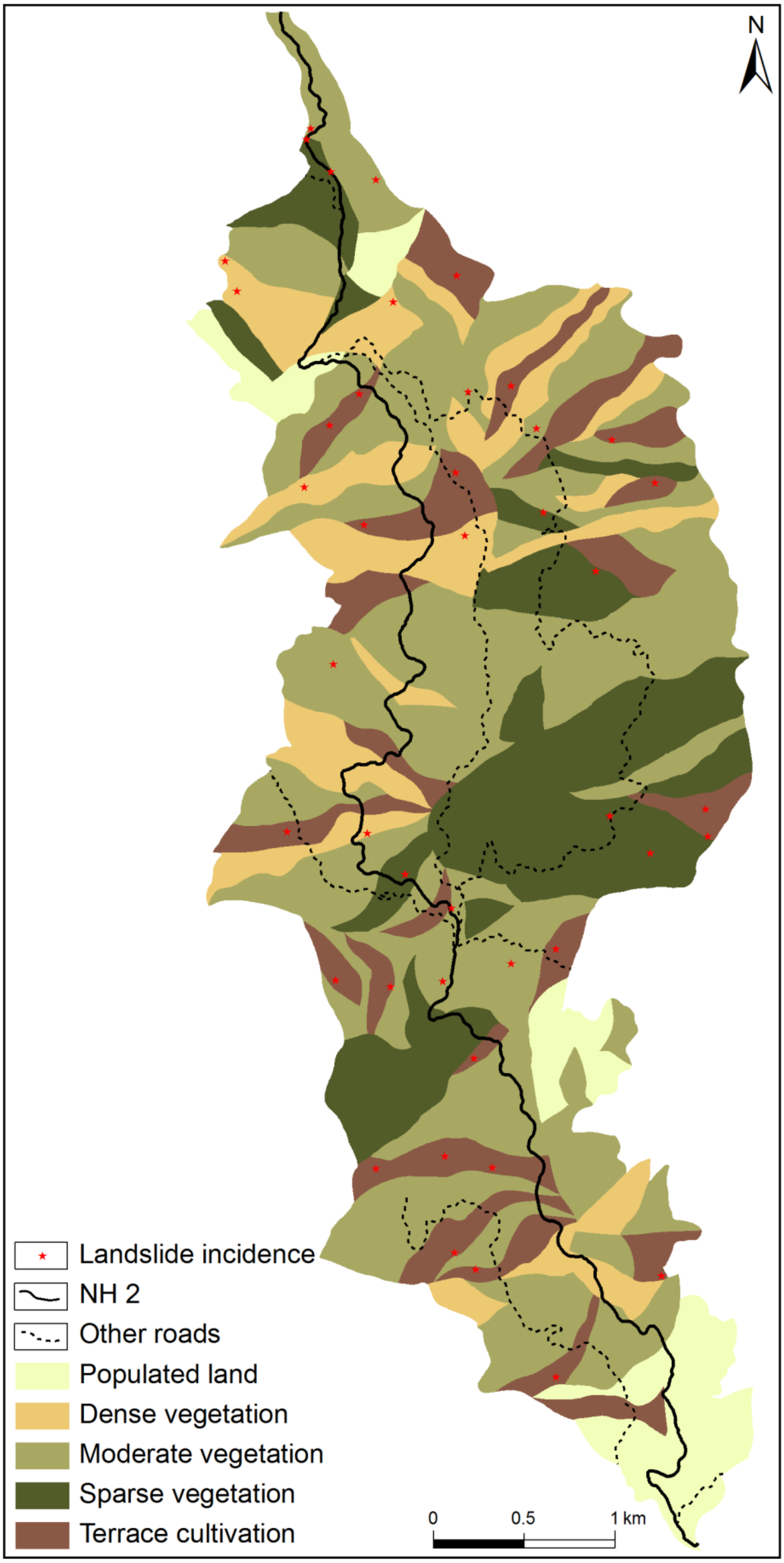

Fig. 5.5a. Land use / land cover map

14.39% of the area covering 2.00 sq km. Ratings for land use and land cover categories are given in Table 5.1. The following chart (Table 5.5) portrays the frequency of landslides on land use / land cover. A pie chart (Fig. 5.5b) portrays distribution of land use and land cover categories.

Table 5.5. Frequency of landslide incidences on land use / land cover

Category	**Area**		**Landslide**		**Frequency**
	km^2	**%**	**No**	**%**	**No/km^2**
Populated land	1.18	8.49	-	-	-
Dense vegetation	1.95	14.03	6	13.95	3.08
Moderate vegetation	6.10	43.88	8	18.60	1.31
Sparse vegetation	2.67	19.21	7	16.28	2.62
Terrace cultivation	2.00	14.39	22	51.16	11.00

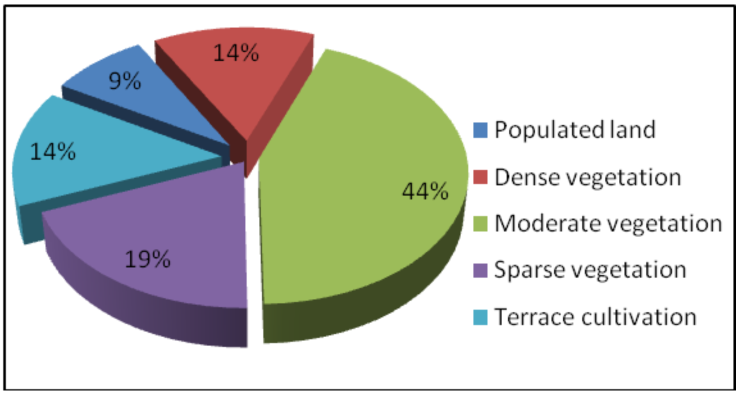

Fig. 5.5b. Distribution of various classes of land use / land cover

CHAPTER 6

LANDSLIDE HAZARD ZONATION

6.1 INTRODUCTION

Landslides and other forms of surface instability are common in mountainous terrain and have stirred major challenges to many researchers for hazard studies in the country. Landslide hazard zonation is a division of land surface into areas, and the relative ranking of these areas according to degrees of actual or potential hazard from landslides on slopes. LHZ maps aid in identifying and delineating landslide prone areas thereby leading to minimization or avoidance of high instability risks. Such maps are useful in that they provide data regarding stability of areas and can play a significant role in minimizing loss to life and property while delineating zones conducive for development. According to Bhandari (1984) graded landslide hazard maps are required among various other things by developmental planners as tools for efficient management of landslide prone areas as also for forecasting catastrophic landslides. Zonation from scientific research does not generally imply legal restrictions, but can be useful to those people who are charged with land management, by providing them with information that is indispensable for planning and regulation purposes (Parise, 2002).

Several workers attempted LHZ mapping using different methods and approaches in an effort to give a scientific basis for the causative factors, which directly or indirectly influence slope instability. The main purpose of various data integration techniques or models is to combine spatial data from diverse sources together to describe and analyze interactions, to make prediction with models, and to provide support to decision makers. Today RS and GIS with the help of computers have changed the scenario. GIS is an ideal tool capable of handling large amounts of data and their upgrading and analysis. Its expansion has led to rapid development of landslide hazard assessment methods (Aleotti and Chowdhury, 1999). Generally, landslide hazard is usually assessed based on statistical analyses, a physically based or deterministic approach.

Statistical approach

This statistical approach deals with the role of each factor which is determined on the basis of observed relations with past and present landslide distribution. The combinations of factors that have led to landslides in the past are determined statistically and quantitative predictions are made for areas presently free of landslides but where similar conditions exist. In bivariate statistical analysis each factor map is combined with the landslide distribution map and weighing values based on landslide densities are calculated for each parameter class. One such method is the information value method (Yin and Yan, 1988; Sridevi and Sarkar, 1993). In multivariate statistical analysis all the relevant factor maps are sampled either on a grid basis or in morphometric units. For each of the sampling units, the presence or absence of landslides is also determined. The resulting matrix can then be analysed using discriminant analysis, or multiple regression analysis (Carrara, 1983). Chung et al. (1995) presented multivariate statistical models for assessing landslide hazards. Other statistical methods, such as the use of information models and fuzzy set theory were also applied in this context (Yin and Yan, 1988; Juang et al., 1992; Jade and Sarkar, 1993). Raj et al. (2011) introduced LHZ using the Relative Effect (RE) method in southeastern Nilgiris. This method determines the RE of each unit, such as surface geology, slope morphometry, climatic conditions, and land use and land cover by calculating the ratio of the unit portion in coverage and landslide.

Heuristic approach

In this approach landslide influencing factors such as lithology, structure, slope morphometry, land use and land cover, drainage density, etc. are ranked and weighted according to their assumed or expected importance in causing mass movements. This is normally based on prior knowledge available to experts on various causes of landslides in the area of investigation and knowledge is dependent on the experience of the expert. Abella and van Westen (2008) used the heuristic model by analyzing the different landforms and the causative factors for landslides. The model is based on weights assigned by expert judgment and organized in a number of components such as slope angle, internal relief, slope shape, geological formation, active faults, distance to drainage, distance to springs, geomorphological subunits, and existing landslide zones. Gahgah et al. (2009) assessed GIS based LHZ and studied landslide relevant factors related to their influence in landslide occurrence using the heuristic method. Landslide factors such as lineaments, soil map, lithology, roads, drainage pattern, and rainfall together with slope angle and elevation from DEM. All these parameters, which are vital for landslide hazard assessment, are integrated into GIS for data processing.

Deterministic approach

This approach is applicable for site-specific problems where the geomorphological and geological conditions are fairly homogeneous over the entire study area. The advantage of this approach is that validity of the geotechnical approach using the infinite slope model depends on landslide geometry, geotechnical properties of sliding material, and groundwater parameters, allowing the calculation of quantitative values of stability in terms of factor of safety (Jelínek and Wagner, 2007). He concludes that the method can be applied for an individual landslide in large scale. However, detailed knowledge of the area must be ensured. It is necessary to bear in mind that input data and parameterization of the primary geotechnical model play a key role in successful analysis. The proposed approach can be useful in identifying relatively unstable parts within the studied area and also to predict potential for slope instability if the mechanism of landslide is correctly defined.

LHZ has been attempted in a wide variety of environments and using diverse approaches. The different methodologies developed were influenced by the scale of analysis, the availability of input data, and the required details of the hazard map (Nilsen et al., 1979; Brabb, 1984; Varnes, 1984; Wagner et al., 1988; Pachauri and Pant, 1992; Sarkar et al., 1995; Mehrotra et al., 1996). These methods are based on the integration of information about the spatial distribution of the factors identified to be important in assessing slope instability. The selection of variables with a major role in landslide susceptibility analysis can be very difficult. Factors must not be redundant or arising from a combination of others (Ayalew et al., 2005; Yalcin, 2008). Blanc and Cleveland (1968) prepared LHZ maps by combining geological formations of different lithologic groups with slope categories, below and above the critical. Brabb et al. (1972) rated slope stability of geological units on the basis of the percentage of outcrop area of a formation occupied by landslide debris in combination with slope categories. Nilsen and Brabb (1972) used geological formations, slope ranges, and landslide debris to prepare zonation maps. Radbruch and Crowther (1973) classified instability on the basis of lithology and the number of landslides present. Radbruch et al. (1976) considered the frequency of slope failure in different groups of geologic units. Rodriguez et al. (1978) used a grouping of lithology and mass movement. The basic factors used by Varnes (1980) to prepare landslide susceptibility maps were slope, soil thickness, land use practice, and drainage. Takie (1982) used the types of rock fracturing, weathering characteristics, springs, vegetation, valley slopes, etc. to describe methods for making debris flow hazard maps. Brabb (1984) provided a useful review of development of landslide hazard mapping. To prepare a quantified landslide risk map Kawakami and Saito (1984) used valley density, elevation, slope angle, and formations. Wagner et al. (1987) prepared risk maps for road alignment using geologic, structural, slope, and geomorphic factors. They also prepared maps for rock and debris slides. A slope ranking system mainly for adopting preventive measures during excavations was given by Koirala and Watkins (1988). A relationship of landslides with geomorphic and geological features was worked out by Fugita (1994).

To evaluate the combined effect of the factors, the use of GIS in the modeling of landslide hazards using many different parameter maps was attempted by several researchers (Carrara et al., 1991; Kingsbury et al., 1992; van Westen, 1994; Nagarajan et al., 1998; Gupta et al., 1999; Dhakal et al., 2000). Over the past few decades RS and GIS technologies has gained significant importance for spatial data analysis. It has proved to be a very powerful tool for landslide study. Researchers have exploited RS and GIS technologies to process and analyze data that are relevant in evaluation of natural hazards (Carrara, 1983; Carrara et al., 1991; Soeters et al., 1991). Using RS data and techniques for land surface change detection has gained increasing attention in the recent past. Cheng et al. (2003) evaluated RS techniques for locating landslides using multi-temporal satellite imagery. Ohlmacher and Davis (2003) used multiple logistic regression and GIS technology to predict landslide hazard. Logistic regression relates predictor variables to the occurrence or nonoccurrence of landslides within geographic cells and uses the relationship to produce a map showing the probability of future landslides, given local slopes and geologic units. Today, with the availability of RS data and various commercial GIS technologies, hazard mapping has become a means towards logical solution, allowing earth science data to be analyzed efficiently and cost-effectively.

In India, many workers have attempted LHZ mapping taking into account the various factors of the terrain. Seshagiri and Badrinarayan (1982) carried out hazard zonation of the Nilgiri hills using numerical ratings of slope, land use, soil cover, and drainage depending on the frequency of landslides. The Central Road Research Institute (1989) took up zonation mapping on the basis of nature and characteristics of rock and soil materials, the overall stability of slope constituting formations, slope angle, condition of slope surface, hydrological features, and toe erosion which were assessed quantitatively. In this study the overall rating of slope stability was divided into three categories, viz., very good, good, and fair. Choubey and Litoria (1990) constructed a LHZ map of the Garhwal Himalaya considering slope, lithology, structure, and earthquake epicentres. Using a GIS approach Gupta and Joshi (1990) worked in the Himalayas, giving index values to factors like land use, lithology, major tectonic features, and azimuth of landslides. An empirical approach for LHZ mapping based on a landslide susceptibility index using factors like lithology, slope angle, distance from major thrusts and faults, land use pattern, and drainage density in relation to frequency of existing landslides was attempted by Mehrotra et al. (1992). Based on slope, lithology, structure, relative relief, land use and land cover, and groundwater conditions Anbalagan (1992) carried out mapping of the Kathgodam-Nainital area in the Kumaon Himalaya in which a LHEF rating scheme was proposed. It involves demarcation of facets, preparation of thematic maps, estimation of LHEF ratings, calculation of TEHD values and construction of a LHZ map of the area. Owing to the paucity of data on topography, climate, geology, hydrogeology, seismicity, and anthropogenic activity and their components or variables Thigale et al. (1998) stress that difficulties does exist in preparing LHZ maps. Aier (2005) prepared a LHZ map along the NH 29 between Chumukedima and Kohima and proposed some mitigation measures. Walling (2005) studied instability in Kohima town and prepared a LHZ map using RS and GIS and recommended mitigation measures for some weak zones. Hiese (2005) prepared a risk map of Kohima town and its surrounding. Deva and Srivastava (2006) suggested a grid-based approach for classifying the terrain into five categories using three factors that include lithology, ruggedness number, and land use

/ land cover. Pachauri et al. (2006) attempted risk zonation of an area in the Garhwal Himalaya and concluded that rock fall velocity modeling can be useful in landslide risk zonation of an area. Pachauri (2007), based on LHZ mapping carried out in the Chamoli area of Uttarakhand, concluded that facet-based LHZ is a very effective tool for landslide mapping and is cost effective in high relief areas of the Himalayan region.

Hazard mapping of the study area is studied following Anbalagan (1992) and the recommendations of the Department of Science and Technology (1994) and Bureau of Indian Standards (1998). The present effort of LHZ mapping takes into account the slope morphometry, lithology, relationship of structural discontinuities with slope, groundwater condition, and land use and land cover. Thematic maps are generated for slope, lithology, groundwater condition, and land use and land cover. The LHEF is assigned for each causative factor. The LHEF rating scheme of Anbalagan is a numerical system governed by the major causative factors of slope instability which helps determine landslide vulnerability of a slope. The thematic maps generated are then superimposed to provide the required data for the LHZ map by a combination of the thematic layers in a GIS platform. A LHZ map is generated on the basis of the distribution of the TEHD values. The landslide hazard map plays a significant role in minimizing loss of life and property, unstable areas can be avoided, or appropriate mitigation or remedial measures adopted. Hence, they provide a boost to development and safety.

6.2 LANDSLIDE HAZARD ZONATION MAPPING

The LHZ map delineates the area of investigation into four classes comprising low, moderate, high, and very high hazard zones (Fig. 6.1a). Low hazard zones occupy an area of 0.73 sq km. This represents 5.23% of the total area of study. Moderate hazard areas cover 4.93 sq km which is 35.51%. High hazard areas occupy 49.88% covering 6.93 sq km, while very high hazard areas occupy 1.30 sq km, which is 9.38% of the total area. Ratings for the various hazard zones are generated (Table 5.1). Table 6.1 shows the frequency of landslides on the various hazard classes. The pie charts show the distribution of hazard zones and the frequency of landslide incidences on hazard zones (Figs. 6.1b).

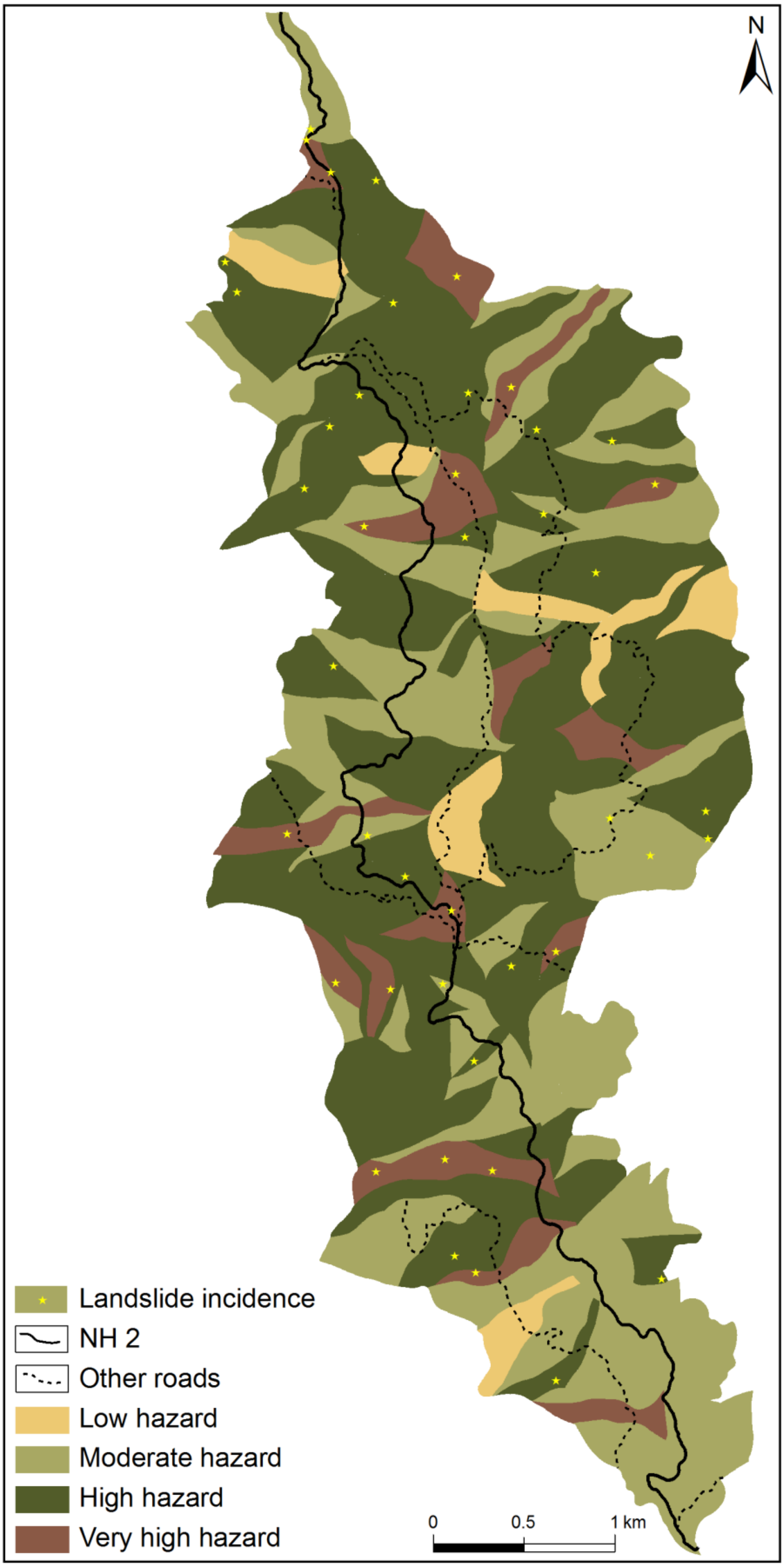

Fig. 6.1a. Landslide hazard zonation map

Table 6.1. Frequency of landslide incidences on hazard zones

Category	Area		Landslides		Frequency
	km^2	%	No	%	No/km^2
Low hazard	0.73	5.23	-	-	-
Moderate hazard	4.93	35.51	5	11.63	1.01
High hazard	6.93	49.88	22	51.16	3.17
Very high hazard	1.30	9.38	16	37.21	12.31

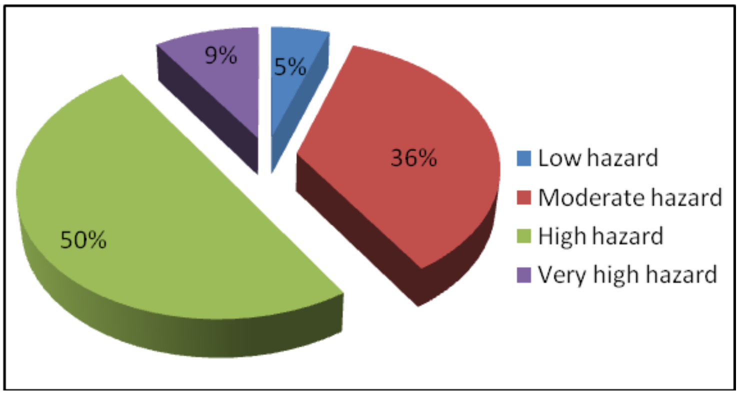

Fig. 6.1b. Distribution of hazard zones

CHAPTER 7

RISK ANALYSES

Landslides and other forms of surface instability have posed major challenges to the country in recent years. Slope failure is common in most mountainous terrains. Such phenomena affect life and economy of both urban and rural areas and also disturb the ecosystem. Topography, lithology, geologic structures, and groundwater are important initiators of landslides. Anthropogenic factors such as haphazard and unscientific developmental activities worsen existing stability conditions.

For sustainable development in structurally disturbed hilly terrain, study of cut-slopes is of prime importance. To ensure stability of slopes, particularly along highways, excavations require an evaluation of the structures affecting rocks. Rock and soil cuts along highways should be made with appropriate safety designs in place to avoid accidents. Excavated slopes, particularly those cut during the dry season, are initially stable but will gradually deteriorate with time. Wherever slopes are steep, safety designs should be rational and economical.

Nagaland being a mountainous terrain is prone to landslides. Due to under-thrusting of the Indian plate beneath that of the Burmese, rocks in the region have been uplifted to form a very mountainous terrain. Hill ranges trend approximately NE-SW and are more or less parallel to each other. In this region the rocks are complexly folded, jointed, and faulted, which leads to surface instability.

Road construction in Nagaland is extremely poor. This is because a very thin veneer of road tar is often pasted over a thin layer of road metal. The resulting roads are thus very weak and quickly deteriorate by surface flows and vehicles plying over hillside debris straying onto roads. Every monsoon potholes quickly develop with the aid of rock and soil debris from the upper slopes. This emphasizes the requirement of good roadside drains to enhance the longevity of roads in such terrain.

The former State Highway No. 1 was taken over by the National Highways Authority of India (NHAI) and thus was re-designated NH 61. This was again recently renamed NH 2. Consequently, widening of this narrow highway has begun to that of Four-lane category. However, slope excavations have been taken up very indiscriminately without any engineering considerations. As such, some sections of this highway between Kohima and Zhadima junction, and those beyond, are vulnerable to various forms of mass wasting. Similarly, the approach road leading to the Nagaland University Campus is affected by long stretches of small, but continuous debris slides.

The NH 2 and the Nagaland University approach road run through thick piles of Disang shale intercalated with thin beds of flaggy sandstone and siltstone. These rocks are sheared and crumpled to varying degrees. The weakened shales are commonly weathered to clays. Such weak rocks, besides adverse hydrogeological conditions and heavy and prolonged rainfall are the major causes of instability. Clays are highly cohesive but during the monsoon water absorption and retention get too high. This leads to build-up of pore pressure and a consequent drop in the degree of cohesion, which is responsible for continued subsidence of portions of roads during the monsoon.

Excavations for widening the highway and other roads are being undertaken without consideration for mitigation measures resulting in some slopes being left as high as 10-18 m and at angles of 70º-80º without any support. It is thus, for such reasons that portions of these roads are weak or affected by debris slides. Due to the importance of this highway and high risk in parts of the study area, studies have been carried out to determine the causes of failure in the affected areas and probable modes of failure in the zones that are still stable, with a view to recommend appropriate mitigation and/or preventive measures.

In the study area fresh cut slopes do not have adequate roadside drainage. Moreover, continued debris slides and falls litter the roads leading to rapid deterioration of the bitumen. So roadside drains and favorably modified slopes or slopes with adequate support that prevent debris from straying down into the drains or onto roads are important.

PART - A

NATIONAL HIGHWAY 2

The study takes into consideration thirteen weak sections along the highway between Kohima and Zhadima junction. Each section is thoroughly analyzed and appropriate measures provided based on the causes or the probable modes of failure.

7.1 LOCATION 1 (6.45 km Junction)

7.1.1 Introduction

This rock and debris slide is part of SoI toposheet no. 83 K/2 NW and lies between 25°42'39" N latitudes and 94°04'22.41" E longitudes covering about 230 sq m west of the Indoor Stadium. This slide has also affected a 40 m stretch of the NH 2 (Fig. 7.1). Small rock and debris slides are very common along this section of the highway.

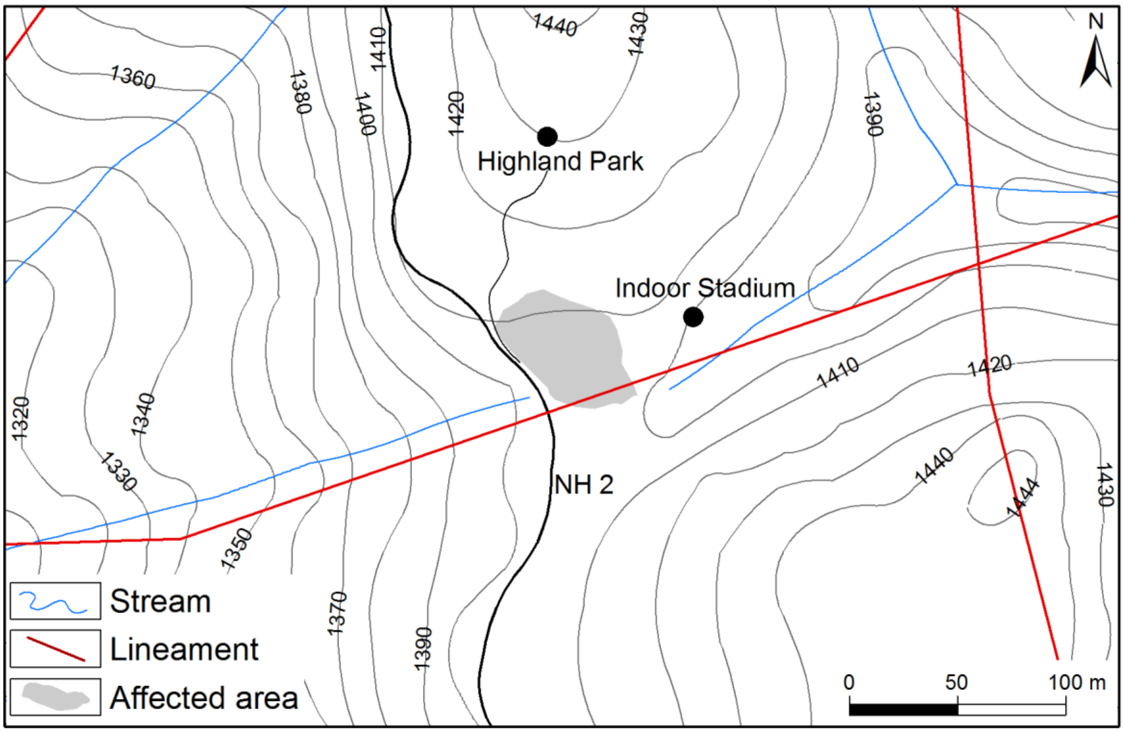

Fig. 7.1. Map of location 1

7.1.2 Geology and structure

The Disang rocks of this area have been severely affected by tectonism as inferred in the field by severe geological deformations. The slope is made up of partially weathered to crumpled shale which has been folded, jointed, and crumpled (Plate 7.1a); this is overlain by debris and newer soil. The general trend of the slope varies from 25°-32° in a WSW direction. The rocks exhibit three prominent sets of joints. The first set of joints dipping at an angle of 45°, trends NW-SE. The second set dip 76° and trend NE-SW. The third set dips at 69° and trends ENE-WSW. A NE-SW trending lineament cuts through the area.

7.1.3 Causes and effects

Excavation of the road leading to the Highland Park has left the weak slope as high as 12 m with an average angle of 55º. The highly sheared and jointed rocks combined with anthropogenic activity are the cause of the slide. Slide material had choked the drain (Plate 7.1b) leading to damage of the road. This has led to water retention and subsurface saturation during the monsoon. This may initiate large-scale landsliding in the area. The brick wall above the slide zone has also been partially damaged. The process also leads to overflow of water, debris, and mud which further deteriorate the road.

7.1.4 SMR and KA

The SMR technique for assessment of slope stability is used in the delineation of weak areas. Forty rock samples are collected from the site to determine the strengths of rocks using a PLIT from which values are (Table 7.1). An RMR rating of 44 is obtained location which indicates more or less weak rocks. SMR values falling in Class IV indicate unstable slope conditions due to planar and wedge failure. This requires extensive corrective measures.

Table 7.1. Slope mass rating

	Value or Condition	**Rating**
1. Point Load Test	1.40 MPa	4
2. RQD	49%	8
3. Spacing of joints	50 mm	10
4. Condition of joints	Slightly rough; separation <1 mm; soft joint wall rock	12

5. Groundwater condition	Dry	10
RMR	*(1+2+3+4+5)*	***44***
6. $F_1 = (1-\mathrm{Sin}\lvert\alpha_j - \alpha_s\rvert)^2$	10°	0.70
7. $F_2 = \mathrm{Tan}^2\beta_j$ or $F_2 = 1$ for toppling	40°	0.85
8. $F_3 = \lvert\beta_j - \beta_s\rvert$ for plane failure $= \lvert\beta_j + \beta_s\rvert$ for toppling where β_s= dip/angle of slope	-10°	-50
9. F_4 = Adjustment factor	Pre-splitting	10
SMR *= RMR+(F_1xF_2xF_3)+F_4*	*44+{0.70x0.85x(-50)}+10*	***24.25***
10. Class	IV	
11. Description	Unstable; planar or large wedges	

Kinematic analyses have been performed for determination of mode of failure in jointed rock masses. About 165 joint attitudes taken in the field are plotted in pole (Fig. 7.1a) and contour diagrams (Fig. 7.1b). From the contour diagrams, three dominant joint sets are identified (J_1: 45°→217°, J_2: 69°→300°, J_3: 76°→159°), which are plotted against slope (50°→230°) in a stereographic projection (Fig. 7.1c).

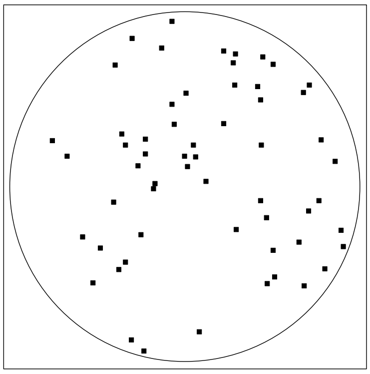

Fig. 7.1a. Pole diagram

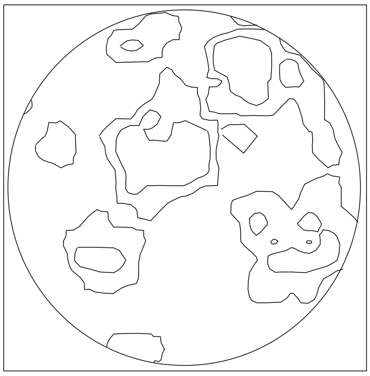

Fig. 7.1b. Contour diagram

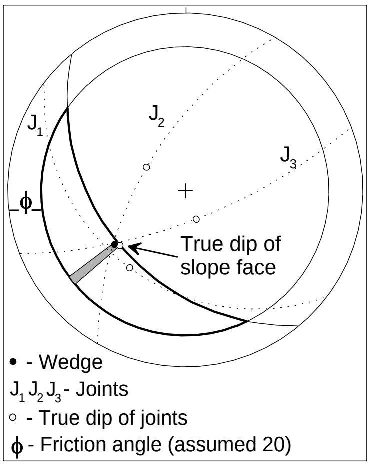

Fig. 7.1c. Stereogram

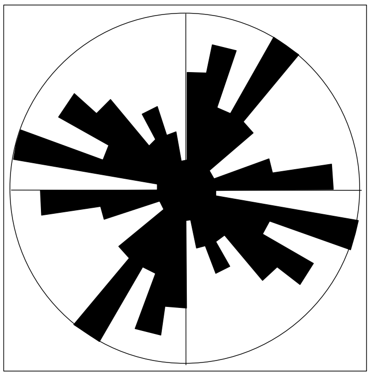

Fig. 7.1d. Rosette

Plate 7.1a. Folded and crumpled Disang shale

Plate 7.1b. Choked drain

The true dips of the joint planes J_2 and J_3 lie outside the shaded region. Here double plane wedge type of failure is inferred. Analyses of the intersections of these joints indicate that wedges form small blocks in the rocks. J_1 plotted against slope shows planar failure. It is therefore concluded that both planar and wedge failure have occurred and are likely in the future. Heavy structures in the vicinity may initiate rock slides. A rosette is constructed from the joint data to understand the orientation of lineaments with respect to the general regional trend (Fig. 7.1d). The orientation of joints shows all components of structural deformation which suggest that the rocks of the area are highly sheared, besides being affected by small faults.

7.1.5 Recommendations

i. Surface runoff around the IG Stadium should be channelized effectively by a good roadside drain to control seepage into the vulnerable subsurface.

ii. An appropriately designed retaining wall of about 2 m height along the road is necessary to prevent the slope mass from sliding down.

iii. Further heavy constructions should be prevented in the vicinity, on the down slope side of the slide zone.

7.2 LOCATION 2 (7.00 km Junction)

7.2.1 Introduction

The is a comparatively small area located at 25°42'47" N latitudes and 94°05'18.09" E longitudes and is incorporated in the of SoI toposheet no. 83 K/2 NW. The road in this area is prone to water logging during monsoon due to debris choking the drain. The length of road affected is about 56 m (Fig. 7.2).

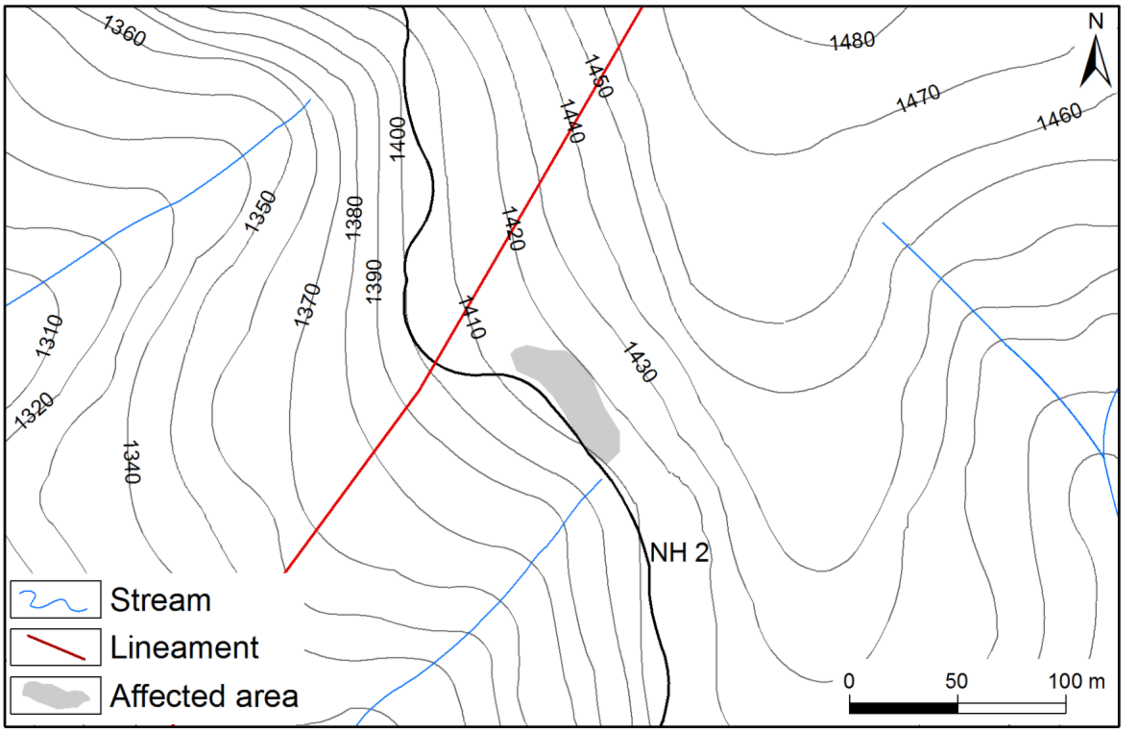

Fig. 7.2. Map of location 2

7.2.2 Geology and structure

Disang rocks in the area, comprising abundant shale, make up the sediments of this area. The bedrocks are weathered shale, brown to dark gray, and often interbedded with minor siltstone. The brown color of the shale is due to iron oxidation. These rocks are highly crumpled and exhibit three prominent sets of joints, viz. 74°→210°, 77°→246°, and 72°→283° (Plate 7.2a) and one set of bedding joints. The clayey soils are mixed with rock fragments. The bedrocks are overlain by thick piles of regolith (about 5 m). The trend of the rocks is NE-SW to N-S with varying degrees of dips.

Plate 7.2a. Highly jointed Disang shale

Plate 7.2b. Water logging during monsoon

7.2.3 Causes and effects

The rocks are highly jointed and soils loose due to which water seepage is high in the upper slopes. This has caused water to concentrate in the road. The drains are choked by debris due to unscientific road construction and lack of breast walls to hold back the debris of the upper slopes. Human activities like concrete fencing on the down slope side of the road have further dammed the outlet for water. Water logging during the monsoon is very high, particularly along the road (Plate 7.2b). This has damaged the road causing large potholes. Such activities along weak slopes of about 60° pose great risk in triggering major slide in the future. The entire road may fail if the ground is allowed to be continuously saturated.

7.2.4 SMR and KA

Forty five rock samples are collected from the site to determine their strengths. Point load test data indicates low value for the rocks (Table 7.2). RMR values of 46 indicate fair stable rocks. SMR values fall in Class III, which indicates partially stable slope conditions that requires systematic maintenance.

Table 7.2. Slope mass rating

	Value or Condition	**Rating**
1. Point Load Test	1.75 MPa	4
2. RQD	65.5%	13
3. Spacing of joints	66 mm	10
4. Condition of joints	Slightly rough; separation <1 mm; soft joint wall rock	12
5. Groundwater condition	Moist (interstitial water)	7
RMR	*= (1+2+3+4+5)*	***46***
6. $F_1 = (1\text{-Sin}I\alpha_j - \alpha_s I)^2$	40°	0.15
7. $F_2 = \text{Tan}^2\beta_j$ or $F_2 = 1$ for toppling	45°	0.85
8. $F_3 = I\beta_j - \beta_s I$ for plane failure $= I\beta_j + \beta_s I$ for toppling where β_s= dip/angle of slope	-15°	-60
9. F_4 = Adjustment factor	Pre-splitting	10
SMR *= $RMR+(F_1xF_2xF_3)+F_4$*	*44+{0.70x0.85x(-50)}+10*	***48.36***
10. Class	III	
11. Description	Fair rock; partially stable; some joints or many wedges	

200 joint attitudes are taken in the field for KA to determine the probable mode of failure. From the joint analyses pole density (Fig. 7.2a) and contour diagrams (Fig.

7.2b) are constructed, from which three dominant joint sets are identified. These are plotted against slope attitude in a stereographic projection (Fig. 7.2c).

1. Slope : 77°→246°
2. J_1 : 74°→210°
3. J_2 : 77°→246°

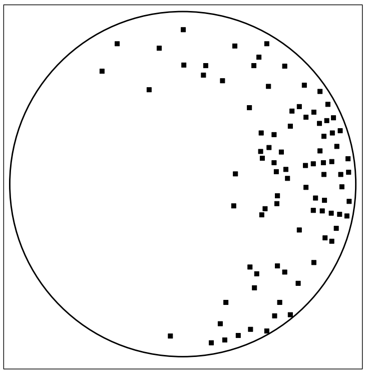

Fig. 7.2a. Pole diagram

Fig. 7.2b. Contour diagram

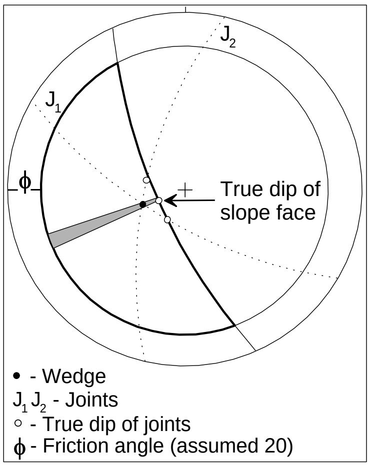

Fig. 7.2c. Stereogram

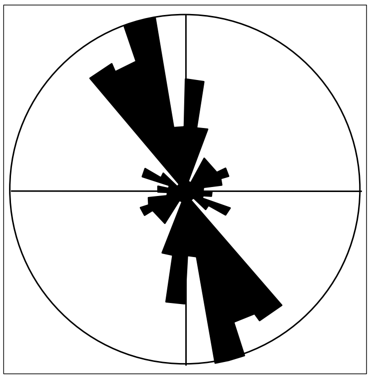

Fig. 7.2d. Rosette

The stereogram shows that both the true dips of the joint planes J_1 and J_2 lie outside the shaded region. In such cases double plane failure takes place (Yoon et al., 2002). It is therefore concluded that double plane wedge failure may occur along this portion of the highway. A rosette is constructed from the joint data (Fig. 7.2d). The orientation of joints indicates the prominence of antithetic shear stresses.

7.2.5 Recommendations

i. Retaining walls about 1 m in height are needed to protect the slope.
ii. Surface runoff should be effectively channelized via a good roadside drain to check seepage into the subsurface.
iii. The road should be so constructed as to tilt towards the drain to prevent water logging and subsequent ground saturation.

7.3 LOCATION 3 (7.12 km Junction)

7.3.1 Introduction

This location is part of SoI toposheet no. 83 K/2 NW and located at 25°42'50.30" N latitudes and 94°05'16.94" E longitudes. A debris slide has affected about 110 m of the highway (Fig. 7.3). Such road blockage is very common during the monsoon.

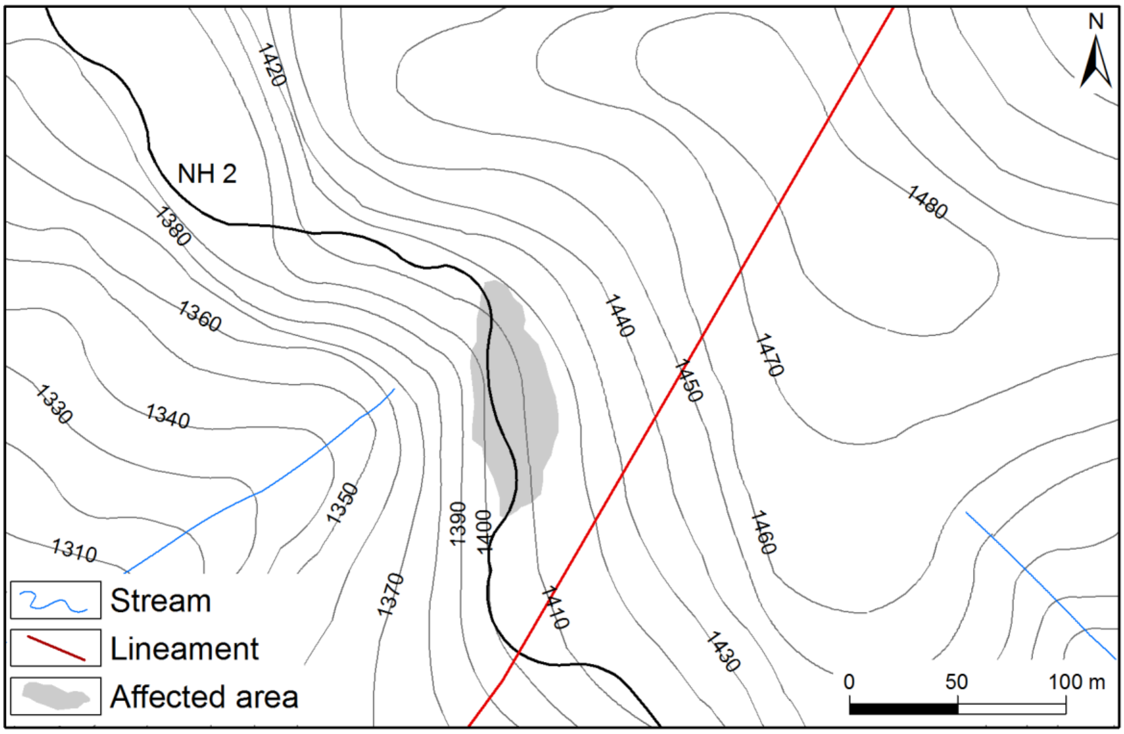

Fig. 7.3. Map of location 3

7.3.2 Geology and structure

This area is predominantly made up of Disang shale. These rocks are jointed, fractured (Plate 7.3a), and weathered. They comprise black, buff, and brown shale with minor siltstone. A lineament trending NE-SW, traverses this area. Rock dips are variable due to local structural disturbances. Three prominent sets of joints with varying trends are noted.

7.3.3 Causes and effects

The rocks are jointed and fragmented due to which debris slides are a continuous phenomenon along this part of the highway. The bedrocks are covered with soil and debris. This is covered by trees on the upper portion of the slopes. The slope varies in

Plate 7.3a. Jointed and weathered shale

Plate 7.3b. Choked drain

height from 6 to 15 m and has been left at an angle of about 80°. The jointed rocks allow water seepage into the subsurface during the monsoon. Debris and plants had completely blocked the drain and part of the highway in August 2011 (Plate 7.3b).

7.3.4 SMR and KA

Point load data indicates low values (Table 7.3) of the forty rock samples collected along the affected site. RMR values have a rating of 38.6, which indicate poor rock quality. SMR values fall in Class IV which is indicative of an unstable slope that will suffer from planar or large wedge failure.

Table 7.3. Slope mass rating

	Value or Condition	**Rating**
1. Point Load Test	1.75 MPa	4
2. RQD	55.6%	13
3. Spacing of joints	55 mm	10
4. Condition of joints	Slightly rough; separation <1 mm; soft joint wall rock	12
5. Groundwater condition	Dry	10
RMR	*= (1+2+3+4+5)*	***49***
6. $F_1 = (1\text{-Sin}I\alpha_j - \alpha_s I)^2$	25°	0.40
7. $F_2 = \text{Tan}^2\beta_j$ or $F_2 = 1$ for toppling	45°	0.85
8. $F_3 = I\beta_j - \beta_s I$ for plane failure $= I\beta_j + \beta_s I$ for toppling where β_s= dip/angle of slope	-35°	-60
9. F_4 = Adjustment factor	Pre-splitting	10
SMR *= RMR+(*$F_1 x F_2 x F_3$*)+*F_4	*49+{0.40x0.85x(-60)}+10*	***38.6***
10. Class	IV	
11. Description	Poor rock; unstable; planar or large wedges	

Kinematic analyses have been performed from 200 joint attitudes taken in the field to determine the probable mode of failure. From joint analyses, pole density (Fig. 7.3a) and contour diagrams (Fig. 7.3b) are constructed and from which three dominant joint sets are identified. These are plotted against slope attitude in a stereographic projection (Fig. 7.3c).

1. Slope : 80°→265°
2. J_1 : 74°→236°
3. J_2 : 75°→249°
4. J_3 : 81°→310°

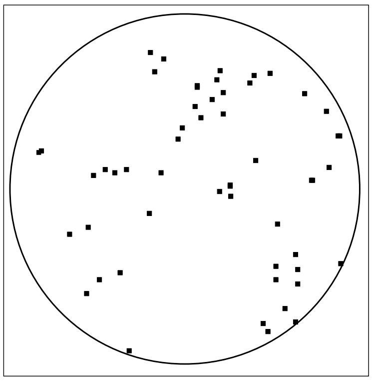

Fig. 7.3a. Pole diagram

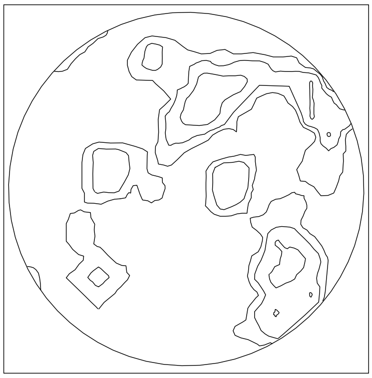

Fig. 7.3b. Contour diagram

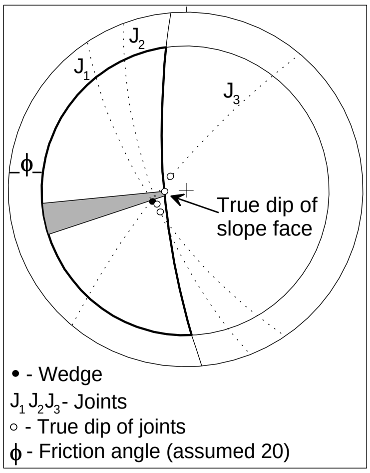

Fig. 7.3c. Stereogram

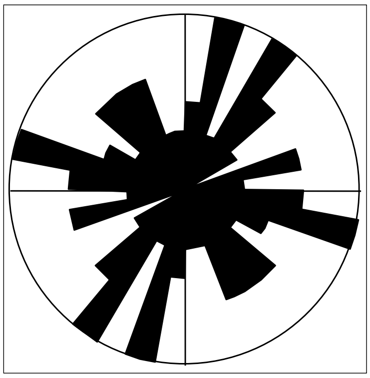

Fig. 7.3d. Rosette

The true dips of the joint planes J_1 and J_3 lies outside the shaded region between the true dip of the slope and the line of intersection of the two joint planes (J_2 and J_3). J_2 plotted against slope shows probability of planar failure. Analyses of joint intersections (J_2 and J_3) indicate that wedges form small blocks in the rocks. It is concluded that both planar and wedge failure may occur along this portion of the highway. A rosette constructed from joint data (Fig. 7.3d) indicates complex structural deformations which have sheared the rocks.

7.3.5 Recommendations

i. The inclination of the slope should be reduced.

ii. The present retaining should be built higher (Plate 7.3b) and requires to be extended through the entire length of the affected area.

iii. A roadside drain should be constructed and properly maintained.

iv. No trees should be planted on the upper slopes, while those already planted should be removed to improve slope stability.

7.4 LOCATION 4 (7.30 km Junction)

7.4.1 Introduction

This location is a very high and steep slope located at 25°42'54.01" N latitudes and 94°51'13.28" E longitudes. Rock and debris slides are very common in this section of the road which stretches for about 120 m (Fig. 7.4).

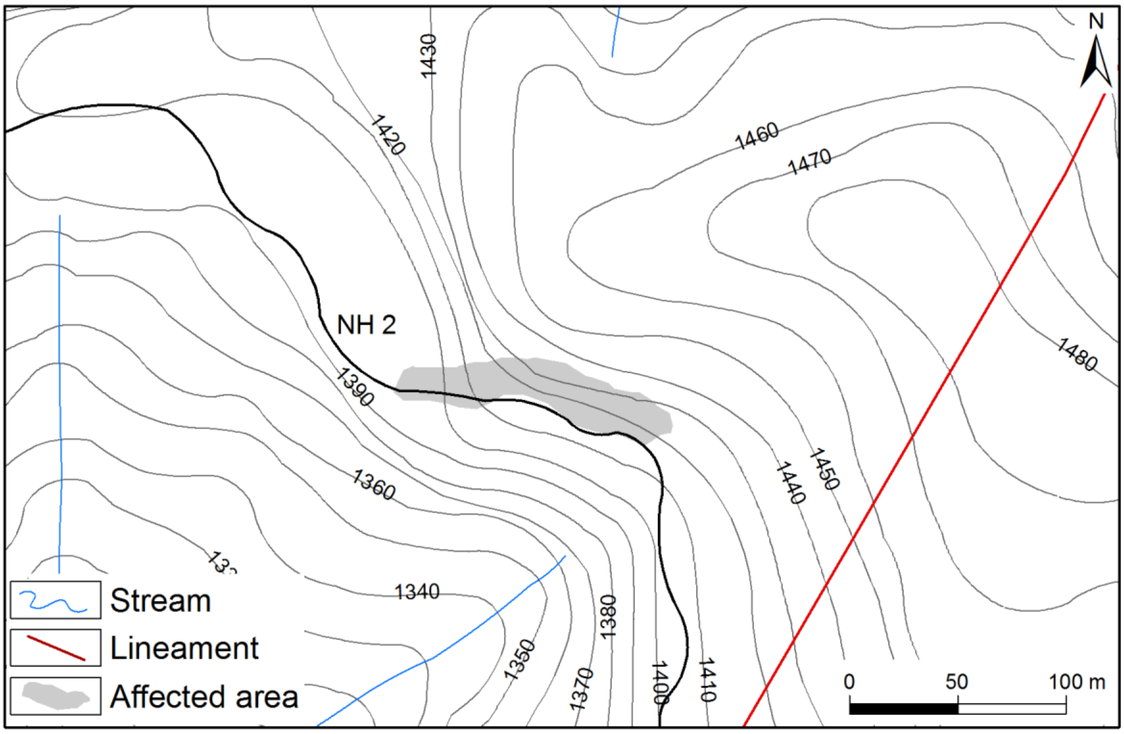

Fig. 7.4. Map of location 4

7.4.2 Geology and structure

The rocks exposed in the area comprise jointed and fractured Disang shale intercalated with minor siltstone (Plate 7.4a) that are brown, buff, and gray in color. The bedrocks dip 70° towards 55°NE. A local fault striking N60°E and S240°W breaks the continuity of the beds (Plate 7.4b). The rocks exhibit three prominent sets of joints with varying trends. The first set of joints trends WNW-ESE with moderate dips towards SSW. The second set trends NW-SE with almost vertical dips towards SW. The third set trends NNE-SSW with near vertical dips towards the SE.

Plate 7.4a. Jointed and fractured rocks

Plate 7.4b. Local fault in Disang

7.4.3 Causes and effects

Lithology and structures on nearly vertical and steep slopes are the cause of slope failure. The exposure comprises highly jointed shale of 15-20 m height with slopes averaging 75°. Slope material is prone to failure by heavy or continued rainfall. The bedrocks are displaced by a local fault along which debris slides are noted. Talus cones forming at the base of slopes completely block the drains (Plate 7.4a) causing overflow of water which litters the road during the monsoon to deteriorate road condition.

7.4.4 SMR and KA

Forty rock samples are collected along the affected site to determine their strengths. Point load test data indicates low values for the rocks (Table 7.4). A rating of 39 is estimated for the RMR which indicates poor rock quality. SMR values for this slope fall in Class V which indicates very unstable slope conditions with large planar or soil-like types of failure.

Table 7.4. Slope mass rating

	Value or Condition	**Rating**
1. Point Load Test	1.45 MPa	4
2. RQD	42.4%	8
3. Spacing of joints	45.4 mm	5
4. Condition of joints	Slightly rough; separation <1mm; soft joint wall rock	12
5. Groundwater condition	Dry	10
RMR	*= (1+2+3+4+5)*	***39***
6. $F_1 = (1\text{-Sin}I\alpha_j - \alpha_s I)^2$	20°	0.70
7. $F_2 = \text{Tan}^2\beta_j$ or $F_2 = 1$ for toppling	40°	0.85
8. $F_3 = I\beta_j - \beta_s I$ for plane failure $= I\beta_j + \beta_s I$ for toppling where β_s= dip/angle of slope	-35°	-60
9. F_4 = Adjustment factor	Pre-splitting	10
SMR *= RMR+(F_1xF_2xF_3)+F_4*	*39+{0.70x0.85x(-60)}+10*	***13.3***
10. Class	V	
11. Description	Planar or soil like	

215 joint attitudes are taken for kinematic analyses. From the joint analyses data pole density (Fig. 7.4a) and contour diagrams (Fig. 7.4b) are constructed and from which the dominant joint (J_1: 63°→188°) is identified. These are plotted against slope attitude (75°→200°) in a stereographic projection (Fig. 7.4c).

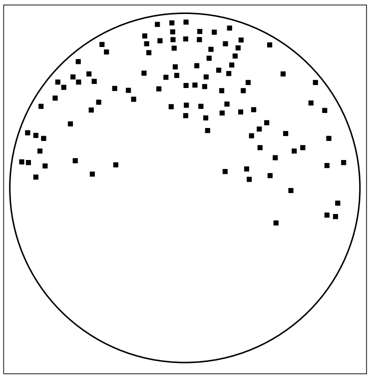

Fig. 7.4a. Pole diagram

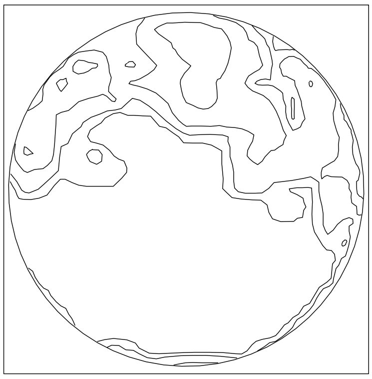

Fig. 7.4b. Contour diagram

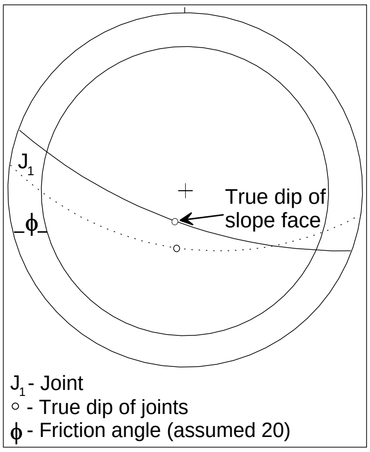

Fig. 7.4c. Stereogram

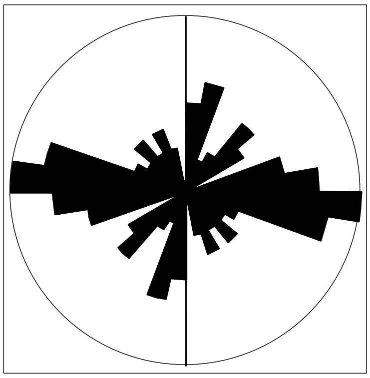

Fig. 7.4d. Rosette

The true dip of the joint plane J_1 lies at an angle of ±12° with respect to the true dip of the slope face. According to Hoek and Bray (1981) such relationship indicates planar mode of failure. It is therefore concluded that planar or soil like failure is likely to occur here. A rosette constructed from joint data (Fig. 7.4d) indicates synthetic shearing of rocks.

7.4.5 Recommendations

i. A retaining wall of 2 m height will help protect the slope in the vulnerable areas.

ii. Proper roadside drain and regular maintenance are necessary.

iii. It is advisable to treat some of the vertical exposed rock surfaces with GI wire netting to prevent debris falls.

7.5 LOCATION 5 (7.80 km Junction)

7.5.1 Introduction

A debris slide was triggered during the monsoon of 2011 which damaged a 50 m stretch of the highway (Fig. 7.5). This section is part of SoI toposheet no. 83 K/2 NW that is located at 25°42'59.15" N latitudes and 94°05'5.50" E longitudes.

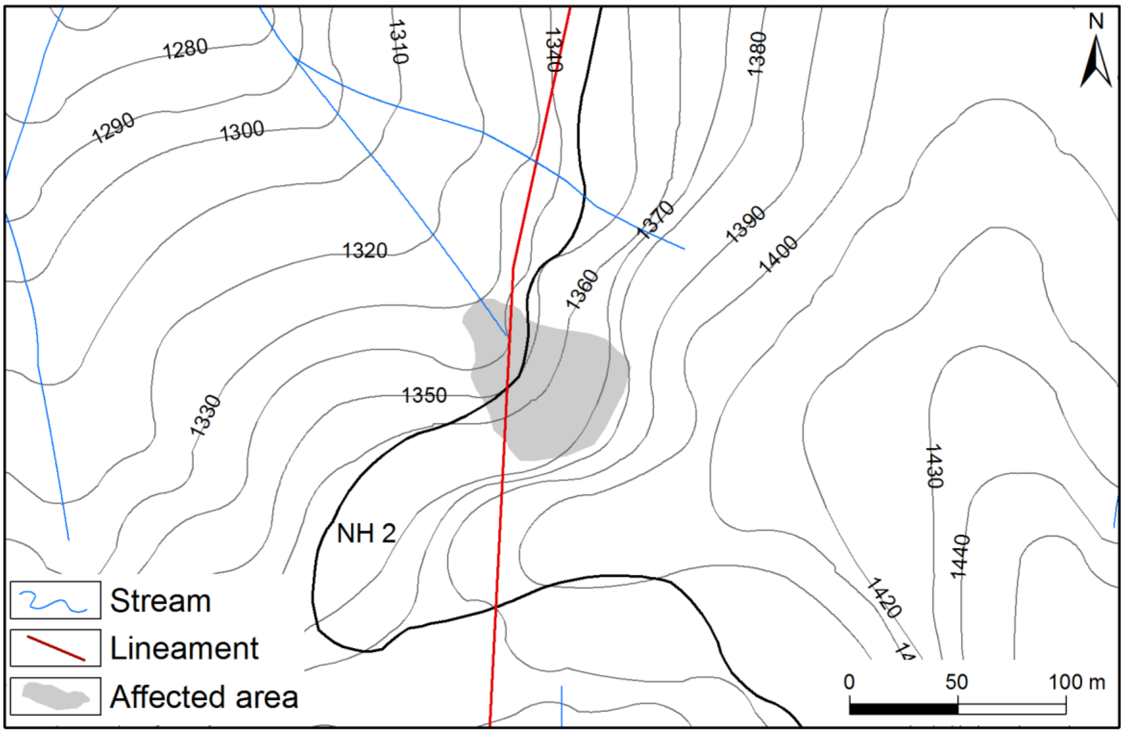

Fig. 7.5. Map of location 5

7.5.2 Geology and structure

The Disang comprising abundant shale make up the rock type of this area. The rocks are highly crumpled and weathered due to which debris slides are common (Plate 7.5a). The shale is splintery and brown to dark gray in color. The bedrocks in the affected area are highly crumpled. Outcrops in the vicinity exhibit a number of joints dipping in various directions. Three prominent sets of joints with varying trends are noted. The first set trends WNW-ESE and dips 70° towards the SSW. The second set trends NW-SE with almost vertical dips towards the SW. The third set trends NE-SW and dips 33° towards the NW.

Plate 7.5a. Debris slide

Plate 7.5b. Blocked roadside drain

7.5.3 Causes and effects

Lithology, structure, and rainfall are the main causes of the failure at this location. The outcrops are crumpled and weathered shale that are capped by loose debris on a 75° slope, the height of which is approximately 10 m. Water entering through the joints and loose debris during the monsoon saturates the slope material. The upper portion of the area is clad with trees which add to the load on the weak slope. These factors combine to cause debris slides along this portion of the highway. Debris and vegetation completely blocked the roadside drain and part of the highway during the monsoon of 2011 (Plate 7.5b).

7.5.4 SMR and KA

Forty rock samples are collected along the affected site to determine their strengths. Point load test data indicate low values for the rocks. The RMR value indicates weak rock (Table 7.5). SMR values for this slope fall in Class IV which indicates unstable slope conditions; under such conditions planar or large-wedge failure is expected.

Table 7.5. Slope mass rating

	Value or Condition	**Rating**
1. Point Load Test	1.45 MPa	4
2. RQD	39.1%	8
3. Spacing of joints	43.4 mm	5
4. Condition of joints	Slightly rough; separation <1 mm; soft joint wall rock	12
5. Groundwater condition	Dry	10
RMR	*= (1+2+3+4+5)*	***39***
6. $F_1 = (1\text{-Sin}I\alpha_j - \alpha_s I)^2$	10°	0.70
7. $F_2 = \text{Tan}^2\beta_j$ or $F_2 = 1$ for toppling	30°	0.40
8. $F_3 = I\beta_j - \beta_s I$ for plane failure $= I\beta_j + \beta_s I$ for toppling where β_s= dip/angle of slope	-45°	-60
9. F_4 = Adjustment factor	Pre-splitting	10
SMR *= RMR+(F_1xF_2xF_3)+F_4*	*39+{0.70x0.40x(-60)}+10*	***32.2***
10. Class	IV	
11. Description	Unstable; planar or large wedges	

For the determination of the probable mode of failure, about 200 joint attitudes are taken for kinematic analyses. Joints are analyzed to construct pole density (Fig. 7.5a) and contour diagrams (Fig. 7.5b), from which three dominant joint sets are identified. These are plotted against slope attitude in a stereographic projection (Fig. 7.5c).

1. Slope : 75°→320°
2. J_1 : 70°→20°
3. J_2 : 80°→253°
4. J_3 : 33°→305°

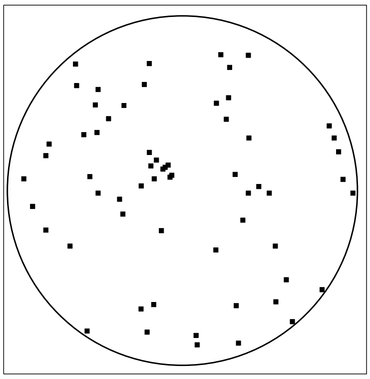

Fig. 7.5a. Pole diagram

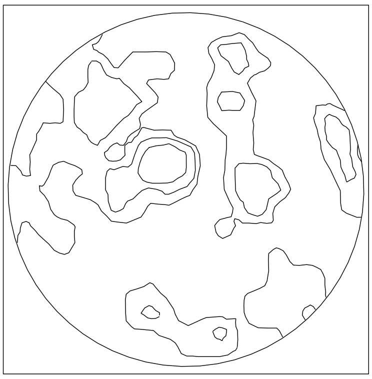

Fig. 7.5b. Contour diagram

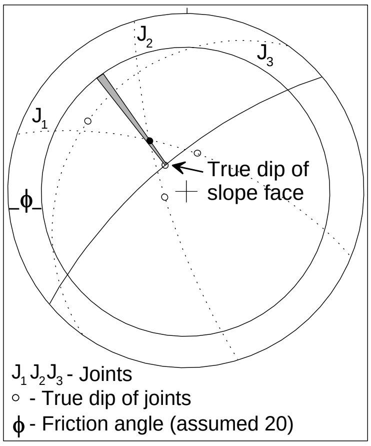

Fig. 7.5c. Stereogram

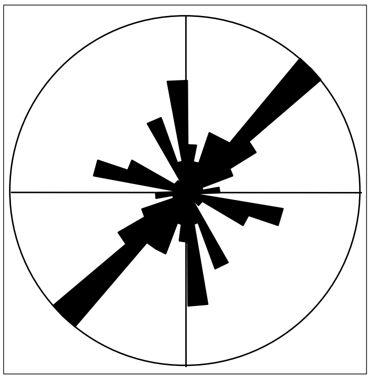

Fig. 7.5d. Rosette

The true dips of the joint planes J_1 and J_2 lie outside the shaded region as seen in the diagram. This indicates double plane wedge failure. Analyses of joint intersections (J_1 and J_2) indicate that wedges form small blocks in the rocks. J_3 plotted against slope shows the probability of planar failure. It is therefore concluded that both planar and wedge failure are likely to occur along this section of the road. The rosette of this location shows that the lineaments are in conformity with that of the general trend of the region that is affected by F_1 folds. The rocks are also faulted along this plane (Fig. 7.5d). Antithetic and synthetic shearing stresses have also played a role in rock deformation.

7.5.5 Recommendations

i. Appropriately designed and higher retaining walls are necessary.
ii. Proper roadside drain and regular maintenance is a must.
iii. Heavy loads should be removed from the upper slope.

7.6 LOCATION 6 (8.60 km Junction)

7.6.1 Introduction

This slide, about 50 m in length (Fig. 7.6), is located at 25°43'19.36" N latitudes and 94°05'1.84" E longitudes. Rock quarrying has destabilized the slope and littered the road.

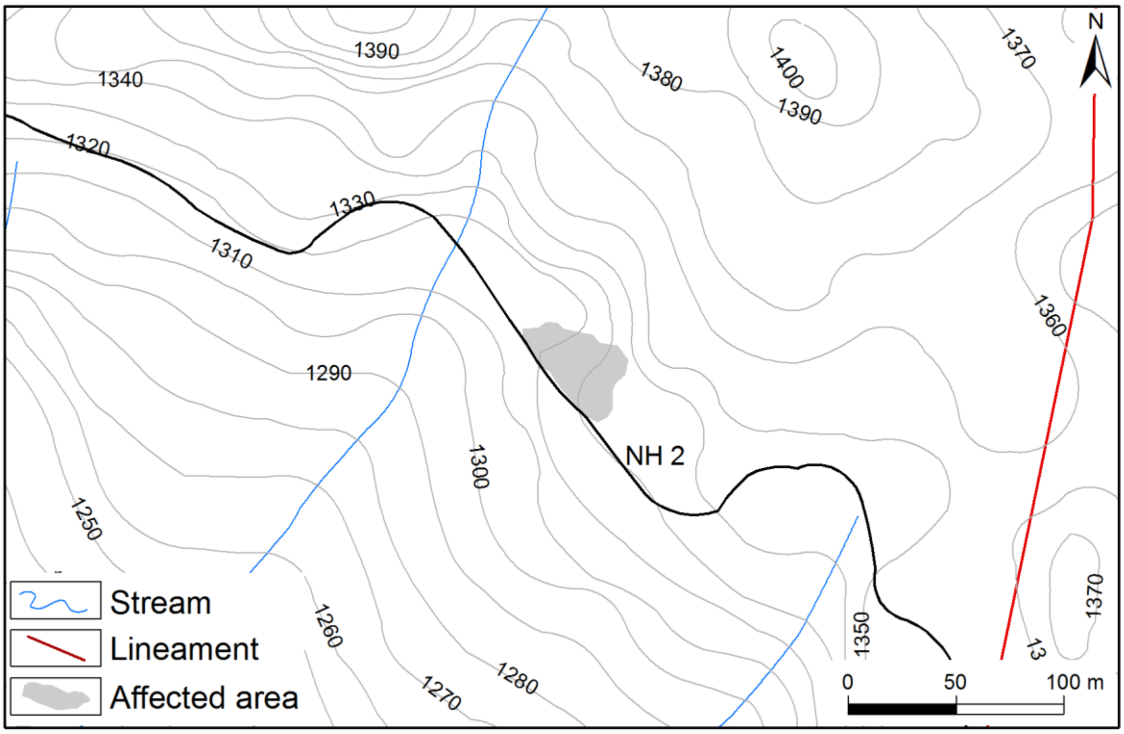

Fig. 7.6. Map of location 6

7.6.2 Geology and structure

The area is predominantly made up of weathered shale intercalated with fine grained, brownish sandstones. The rocks are highly deformed due to local faulting (Plate 7.6a). Slickensides provide evidence of the direction of movement. These rocks exhibit three prominent sets of joints. The first set trends NE-SW and dips 75° SW. The second set trends WNW-ESE with dips of 54° towards SSW. The third set trends NNW-SSE with steep dips of 69° towards SW.

Plate 7.6a. Local deformation of rocks

Plate 7.6b. Drainage blockage by debris

7.6.3 Causes and effects

The factors responsible for failure are unfavorable joints on steep slopes that are capped by unstable soils along an 85º slope which is about 18 m high. The exposures along the highway are highly jointed shale and sandstone. Localized excavation for rocks has altered the stability of the natural slope causing the jointed rocks and weak soils to collapse. The debris due to quarrying spreads over the highway and blocks the drain and litters the road (Plate 7.6b).

7.6.4 SMR and KA

Forty six rock samples were collected from the site for determination of their strengths. Point load test data indicates low values of 1.01 MPa for the rocks. RMR value indicates fair rock quality (Table 7.6). However SMR values for this slope fall in Class V which indicates very unstable slope conditions; in such slopes planar failure is likely.

Table 7.6. Slope mass rating

	Value or Condition	**Rating**
1. Point Load Test	1.01 MPa	4
2. RQD	55.6%	13
3. Spacing of joints	55.5 mm	10
4. Condition of joints	Slightly rough; separation <1 mm; soft joint wall rock	12
5. Groundwater condition	Dry	10
RMR	*= (1+2+3+4+5)*	***49***
6. $F_1 = (1\text{-Sin}I\alpha_j - \alpha_s I)^2$	5°	0.85
7. $F_2 = \text{Tan}^2\beta_j$ or $F_2 = 1$ for toppling	40°	0.85
8. $F_3 = I\beta_j - \beta_s I$ for plane failure $= I\beta_j + \beta_s I$ for toppling where β_s= dip/angle of slope	-45°	-60
9. F_4 = Adjustment factor	Pre-splitting	10
SMR *= $RMR+(F_1xF_2xF_3)+F_4$*	*49+{0.85x0.85x(-60)}+10*	***15.65***
10. Class	V	
11. Description	Large planar or soil type	

For kinematic analyses about 200 joint attitudes are taken. The joint data are used to construct pole density (Fig. 7.6a) and contour diagrams (Fig. 7.6b) and from which three dominant joint sets are identified and plotted against slope attitude in a stereographic projection (Fig. 7.6c).

1. Slope : 85°→200°

2. J_1 : 75°→144°
3. J_2 : 54°→184°
4. J_3 : 69°→256°

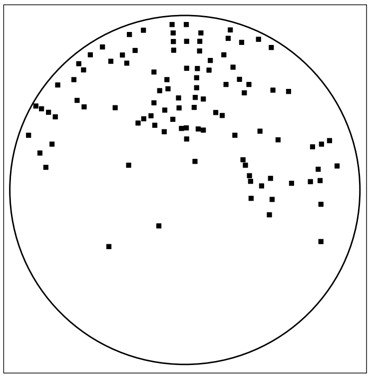

Fig. 7.6a. Pole diagram

Fig. 7.6b. Contour diagram

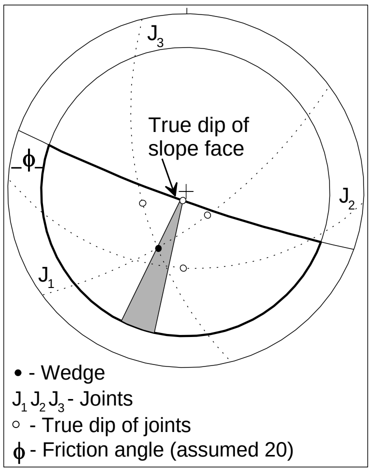

Fig. 7.6c. Stereogram

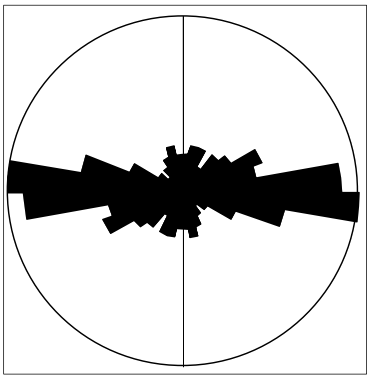

Fig. 7.6d. Rosette

The true dips of the joint planes J_1 and J_3 lie outside the shaded region indicating double plane wedge failure. J_2 plotted against slope shows the probability of planar failure. Therefore both planar and wedge failure are likely to occur along this portion of the highway. Analyses of joint intersections (J_1 and J_3) indicate that wedges form small blocks in the rocks. The rosette of this location shows the dominant role of synthetic shears (Fig. 7.6d).

7.6.5 Recommendations

i. Proper roadside drain and periodic maintenance is important.
ii. A retaining wall should be constructed in the soil covered area.
iii. Further quarrying should be prevented in the area.

7.7 LOCATION 7 (8.85 km Junction)

7.7.1 Introduction

A debris slide that was triggered by rainfall, took place in July 2011 (Fig. 7.7). This area is located at 25°43'23.17" N latitudes and 94°04'55.09" E longitudes and is part of SoI toposheet no. 83 K/2 NW. The affected road section is about 45 m (Plate 7.7a).

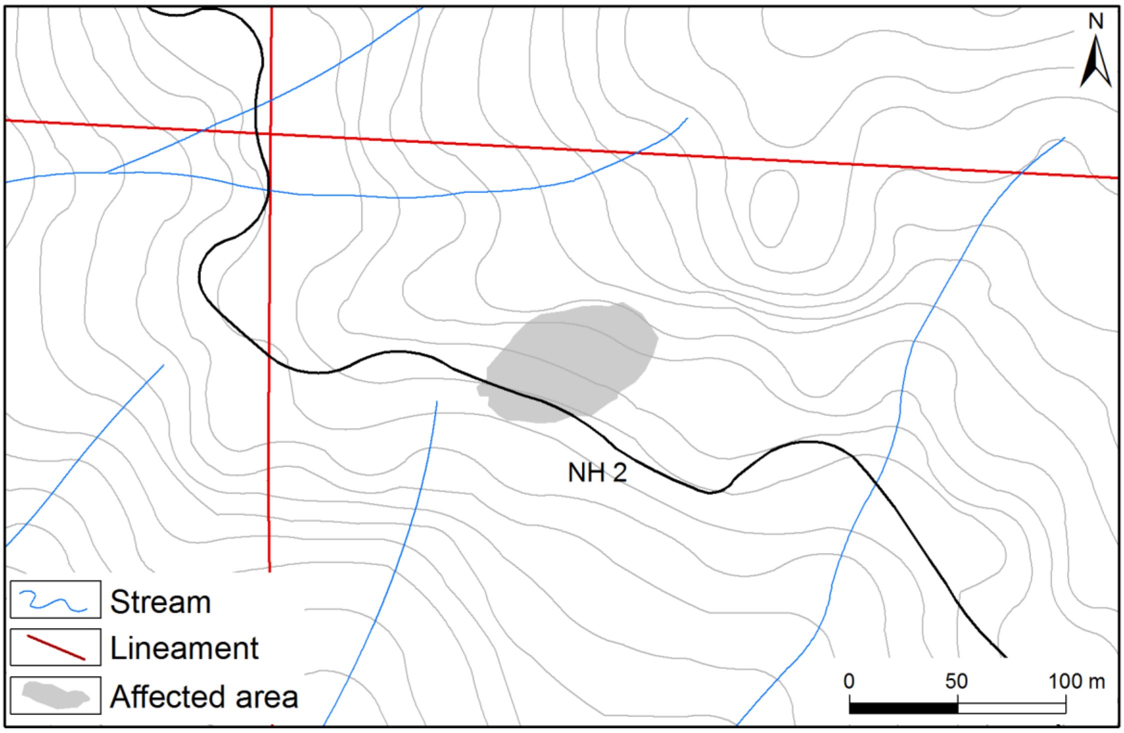

Fig. 7.7. Map of location 7

7.7.2 Geology and structure

The Disang shale making up the rock type of this area is splintery, brown to dark gray, and often interbedded with minor siltstone. The shale is highly susceptible to weathering and disintegrates on exposure to air. Bedding is very poor in the outcrops due to weathering and crumpling of the rocks. However, stable rock outcrops in the vicinity of the slide zone exhibit a number of joints. These are overlain by about 5 m of loose debris. The rocks exhibit three prominent sets of joints. The first set of joints trends NE-SW and dips 73° NW. The second set trends E-W, dipping 182° S, while the third set trends NNW-SSE and dips 72° SSW.

Plate 7.7a. View of debris slide scar

Plate 7.7b. Drain blocked by debris

7.7.3 Causes and effects

Heavy rainfall on the unfavorable slope of loose debris triggered the slide. Water saturated the loose debris in the upper slopes which caused it to slide down and block the drain (Plate 7.7b). The height of the slope is >20 m with an inclination of 75°. Such unfavorable slopes composed of weathered shale and loose debris are easily affected by water. The slide material completely blocked the poorly constructed drain leading to overflow of water and deterioration of road condition.

7.7.4 SMR and KA

Forty rock samples are collected from the site to determine their strengths (Table 7.7) using a PLIT. These are used to calculate the RQD. The RMR value of 44 indicates moderately weak rocks. SMR values which fall in Class IV indicate unstable slope conditions where failure may be planar or wedge type.

Table 7.7. Slope mass rating

	Value or Condition	**Rating**
1. Point Load Test	1.02 MPa	4
2. RQD	49%	8
3. Spacing of joints	50 mm	10
4. Condition of joints	Slightly rough; separation <1 mm; soft joint wall rock	12
5. Groundwater condition	Dry	10
RMR	*= (1+2+3+4+5)*	***44***
6. $F_1 = (1\text{-Sin}I\alpha_j - \alpha_s I)^2$	10°	0.70
7. $F_2 = \text{Tan}^2\beta_j$ or $F_2 = 1$ for toppling	30°	0.40
8. $F_3 = I\beta_j - \beta_s I$ for plane failure $= I\beta_j + \beta_s I$ for toppling where β_s= dip/angle of slope	-45°	-60
9. F_4 = Adjustment factor	Pre-splitting	10
SMR *= RMR+(F_1xF_2xF_3)+F_4*	*44+{0.70x0.40x(-60)}+10*	***37.2***
10. Class	IV	
11. Description	Planar or large wedges	

Kinematic analyses have been performed for determination of possible failure mode. 205 joint attitudes taken in the field are analysed to construct pole density (Fig. 7.7a) and contour diagrams (Fig. 7.7b) and from which three dominant joint sets are identified. These are plotted against slope attitude in a stereographic projection (Fig. 7.7c).

1. Slope : 75°→265°
2. J_1 : 73°→320°
3. J_3 : 72°→253°

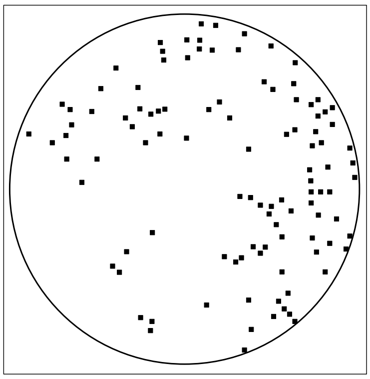

Fig. 7.7a. Pole diagram

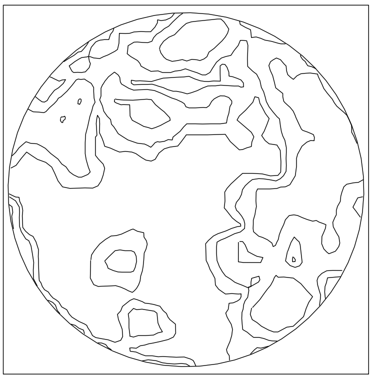

Fig. 7.7b. Contour diagram

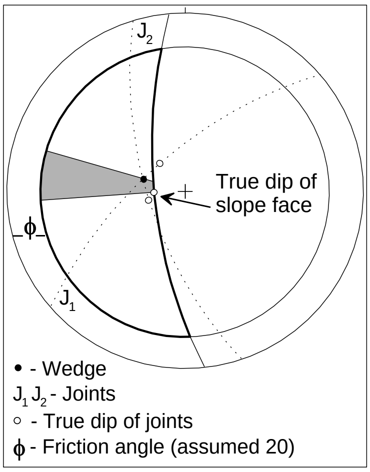

Fig. 7.7c. Stereogram

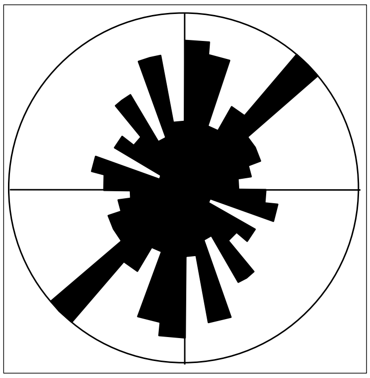

Fig. 7.7d. Rosette

True dips of joint planes J_1 and J_2 lie outside the shaded region which indicates that double plane wedge failure is likely in this area. Analyses of joint intersections (J_1 and J_2) indicate that small blocks of wedges are common in the rocks. The rosette (Fig. 7.7d) shows that the lineaments are parallel to the F_1 folds and thrusts of the region, so squeezing of rocks in the compression direction would have crumpled them to a great extent causing weakness of the slope forming material.

7.7.5 Recommendations

i. A proper roadside drain and periodic maintenance is necessary.
ii. A retaining wall, about 2-2.5 m height, is required.
iii. Trees on the upper slope should be felled.

7.8 LOCATION 8 (9.30 km Junction)

7.8.1 Introduction

This area is located at 25°43'37.8" N latitudes and 94°04'46.95" E longitudes and is part of SoI toposheet no. 83 K/2 NW. A very high and steep slope has been left due to road widening which is vulnerable to slope failure (Fig. 7.8). The affected length of the road is about 40 m along a bend.

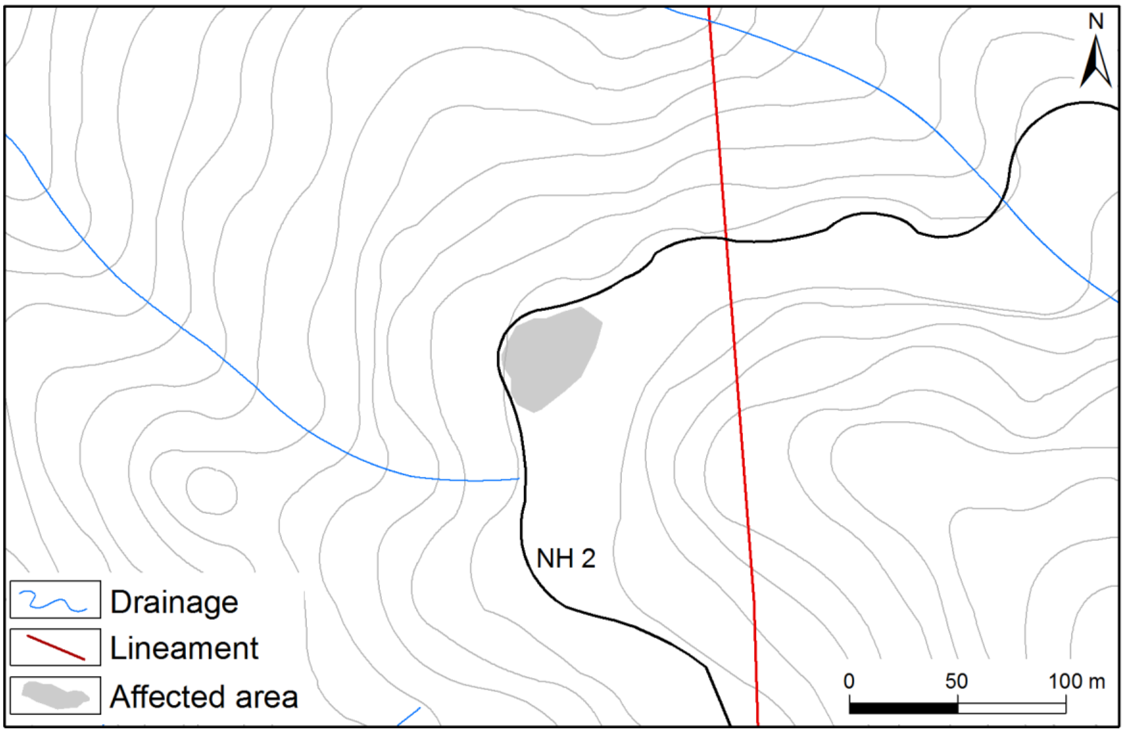

Fig. 7.8. Map of location 8

7.8.2 Geology and structure

This area is predominantly made up of brown Disang shale (Plate 7.8a) intercalated with minor siltstone. The rocks are jointed and crumpled, portions being highly weathered. The rocks dip at angles of 45° towards SW. These jointed shales are also affected by prominent fissures of about 3-6 cm (Plate 7.8b). The rock exhibits three prominent sets of joints. The first set trends NW-SE and dips 60° SW. The second set trends N-S, dipping towards the west at angles of 69°, while the third set dips 75° towards SSW.

Plate 7.8a. Brown Disang shale

Plate 7.8b. Fissures in Disang shale

7.8.3 Causes and effects

Excavations for widening of the highway without consideration for stability left the slopes as high as 12 m at angles of 75º without any support. Weathered shale and loose debris on unfavorable slope are prone to sliding. It is for such reasons that small debris slides have been triggered along this highway. Debris partially blocked the roadside drain.

7.8.4 SMR and KA

Forty rock samples collected from the site were subject to point load test to determine rock strength. RMR value obtained is 39 (Table 7.8) which indicates weak rocks. SMR values fall in Class V, which points to unstable slope conditions with potential for large planar or soil-like types of failure.

Table 7.8. Slope mass rating

	Value or Condition	**Rating**
1. Point Load Test	1.00 MPa	4
2. RQD	39.1%	8
3. Spacing of joints	43.4 mm	5
4. Condition of joints	Slightly rough; separation <1 mm; soft joint wall rock	12
5. Groundwater condition	Dry	10
RMR	*= (1+2+3+4+5)*	***39***
6. $F_1 = (1\text{-Sin}I\alpha_j - \alpha_s I)^2$	5°	0.85
7. $F_2 = \text{Tan}^2\beta_j$ or $F_2 = 1$ for toppling	45°	0.85
8. $F_3 = I\beta_j - \beta_s I$ for plane failure $= I\beta_j + \beta_s I$ for toppling where β_s= dip/angle of slope	-5°	-50
9. F_4 = Adjustment factor	Pre-splitting	10
SMR *= RMR+(F₁xF₂xF₃)+F₄* → $SMR = RMR+(F_1 x F_2 x F_3)+F_4$	*39+{0.85x0.85x(-50)}+10*	***12.8***
10. Class	V	
11. Description	Very unstable; planer or soil-like	

Kinematic analyses are performed for determination of possible failure mode. 190 joint attitudes are plotted for pole density (Fig. 7.8a) and contour diagrams (Fig. 7.8b) from which three dominant joint sets are identified. These are plotted against slope attitude in a stereographic projection (Fig. 7.8c).

1. Slope : 75°→210°
2. J_1 : 60°→222°

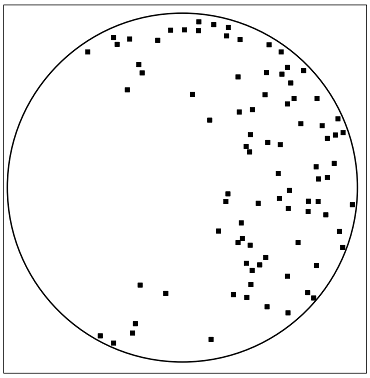

Fig. 7.8a. Pole diagram

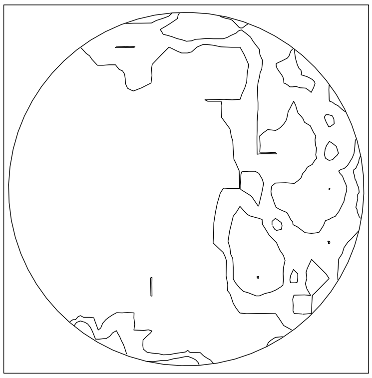

Fig. 7.8b. Contour diagram

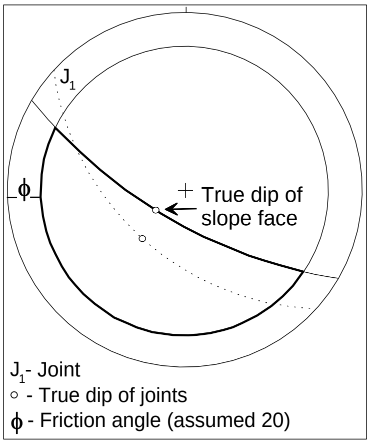

Fig. 7.8c. Stereogram

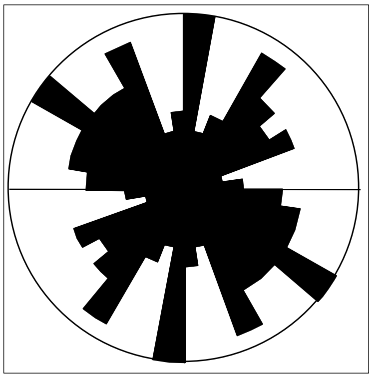

Fig. 7.8d. Rosette

The true dip of the joint plane J_1 lies with at angle of ±12° with respect to that of the slope face indicating planar mode of failure. It is therefore concluded that along this portion of the highway planar or soil-like failure is likely to occur. The rosette (Fig. 7.8d) shows complex deformation leading to folding and high degree of shearing of the rocks.

7.8.5 Recommendations

i. Slope gradient should be reduced.

ii. A retaining wall of 2 m height will protect slope material from sliding down.

iii. Proper roadside drain and periodic maintenance is recommended.

7.9 LOCATION 9 (11.65 km Junction)

7.9.1 Introduction

This area is located at 25°44'12.41" N latitudes and & 94°04'59.52" E longitudes and is part of SoI toposheet no. 83 K/2 NW. Debris falls and slides are common in this section of the highway (Fig. 7.9). Mass wasting affected 110 m of the road in 2007.

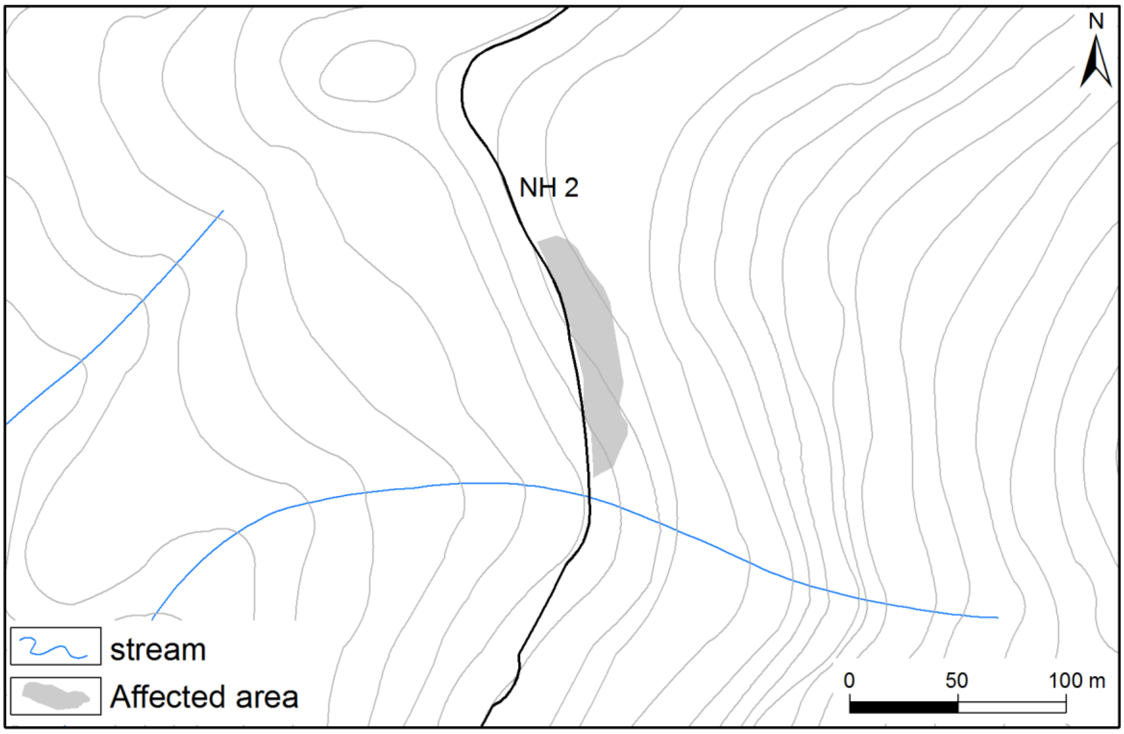

Fig. 7.9. Map of location 9

7.9.2 Geology and structure

This area is made up of partially weathered shale capped by weak soil, the thickness of which ranges from 2 to 3 m (Plate 7.9a). The rocks are jointed, fragmented, and weathered due to which debris continuously slides downhill to block the roadside drain (Plate 7.9b). The bedrocks dip about 30° towards 135° SE. Three prominent sets of joints are noted. The first set of joints trends NW-SE dipping at angles of 45° towards SW. The second set trends N-S, dipping towards 270° W and the third set trends NNE-SSW, dipping 72° NNW.

Plate 7.9a. Partially weathered shale capped by weak soil

Plate 7.9b. Debris along the road section

7.9.3 Causes and effects

The triggering factor for instability in this section of the highway is a combination of steep slope, adverse lithology, and structures. The height of the unstable slope here is about 10 m at an inclination of 75º. Such slopes made up of partially weathered shale overlain by loose debris and soil are highly prone to slope failure. Slide materials frequently block the drain during the monsoon thereby affecting the road.

7.9.4 SMR and KA

Forty five rock samples are collected from the site for determination of their strengths. The RMR value of 39 (Table 7.9) obtained indicates weak rock. SMR values fall in Class IV indicating unstable slope conditions. This indicates potential planar or large wedge-type failure.

Table 7.9. Slope mass rating

	Value or Condition	**Rating**
1. Point Load Test	1.53 MPa	4
2. RQD	32.5%	8
3. Spacing of joints	40 mm	5
4. Condition of joints	Slightly rough; separation <1 mm; soft joint wall rock	12
5. Groundwater condition	Dry	10
RMR	***= (1+2+3+4+5)***	***39***
6. $F_1 = (1\text{-Sin}I\alpha_j - \alpha_s I)^2$	30°	0.40
7. $F_2 = \text{Tan}^2\beta_j$ or $F_2 = 1$ for toppling	35°	0.70
8. $F_3 = I\beta_j - \beta_s I$ for plane failure $= I\beta_j + \beta_s I$ for toppling where β_s= dip/angle of slope	-30°	-60
9. F_4 = Adjustment factor	Pre-splitting	10
***SMR** = RMR+(F_1xF_2xF_3)+F_4*	*39+{0.40x0.70x(-60)}+10*	***32.2***
10. Class	IV	
11. Description	Unstable; planar and/or large wedges	

200 joint attitudes taken in the field are used to construct pole density (Fig. 7.9a) and contour diagrams (Fig. 7.9b) and from which three dominant joint sets are identified, which are plotted in a stereographic projection against slope (Fig. 7.9c).

1. Slope : 65°→230°
2. J_1 : 45°→210°
3. J_2 : 75°→292°

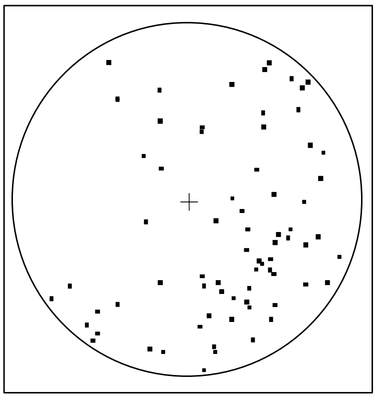

Fig. 7.9a. Pole diagram

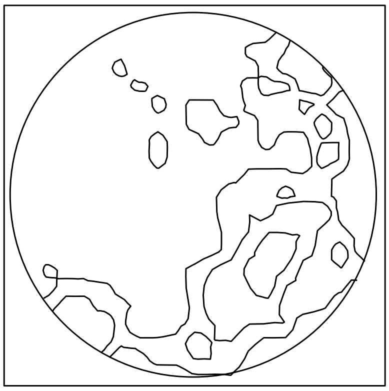

Fig. 7.9b. Contour diagram

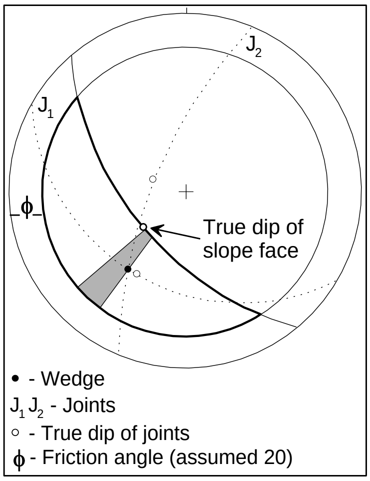

Fig. 7.9c. Stereogram

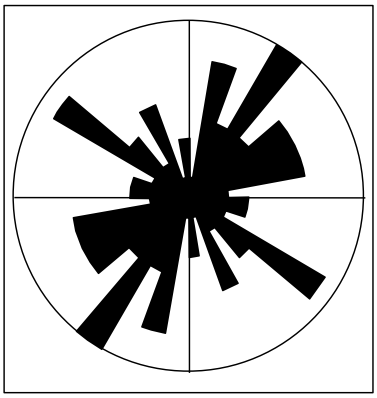

Fig. 7.9d. Rosette

Two sets of joints are found to lend instability to the slope. The figure shows the development of a distinct wedge due to the intersection of these two joint sets. Both the true dips of these joints lie outside the shaded area. The intersection of J_1 and J_2 forms a double plane wedge. A rosette (Fig. 7.9d) data indicates F_1 folds and possible tensile fractures affecting the rocks.

7.9.5 Recommendations

i. Reduction of slope angle in the upper soil horizon and removal of 3 m of the top soil is recommended (Fig. 7.9e).

ii. A geotextile cover and grass plantation on the excavated soil will greatly help.

iii. About 100 m length of the rock section treated with GI wire netting will provide stability to the slope.

iv. Proper roadside drainage and maintenance is necessary.

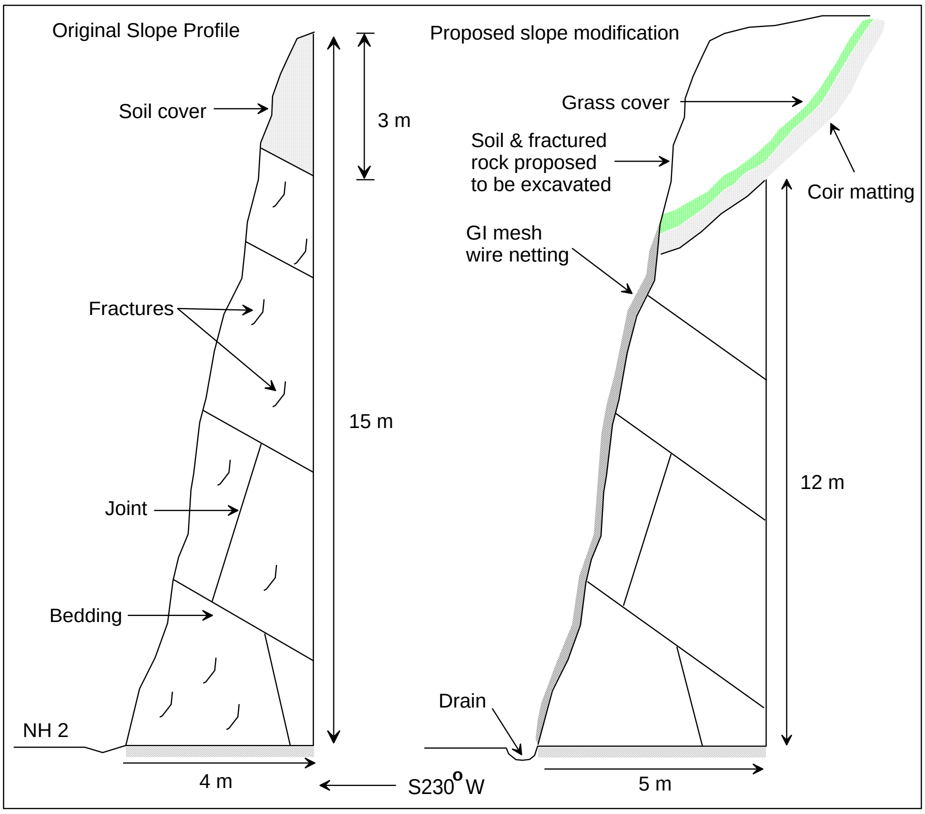

Fig. 7.9e. Proposed slope modification / mitigation measures

7.10 LOCATION 10 (11.75 km Junction)

7.10.1 Introduction

This area located at 25°44'18.08" N latitudes and 94°05'1.05" E longitudes, is part of SoI toposheet no. 83 K/2 NW. This location (Fig. 7.10) was affected by minor but continuous debris slides (Plate 7.10a). Accidents are also likely as this area is a sharp and blind bend (Plate 7.10b).

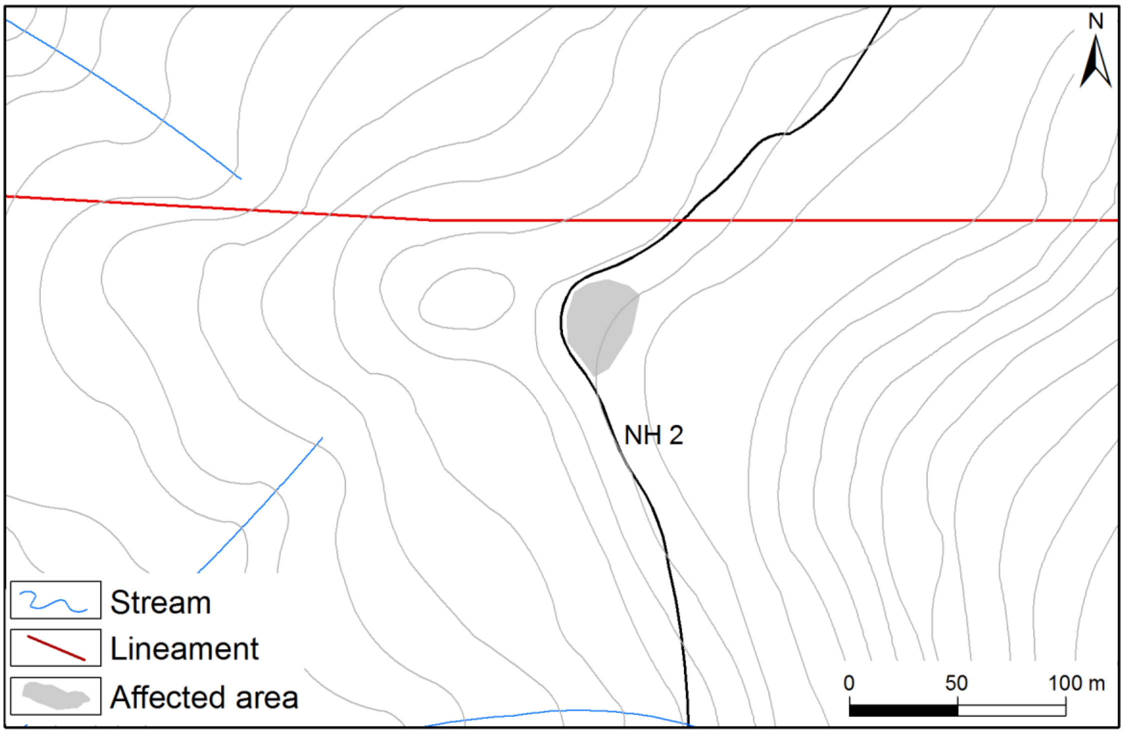

Fig. 7.10. Map of location 10

7.10.2 Geology and structure

The slope of this area is made up crumpled Disang shale. The upper horizons comprise debris and loose soil. Bedrocks are not exposed along the section but outcrops in the vicinity show a number of joints. Two prominent sets of joints control rock behavior. The first set of joints trends ENE-WSW, dipping at an angle of 54° towards NNW. The second set trends N-S and dip 53° towards the west.

7.10.3 Causes and effects

The cause of this instability is due to weak lithology on a high and steep slope with a gradient of 70º. This slope is approximately 10 m in height.

Plate 7.10a. Weak hill slope

Plate 7.10b. Blind bend

7.10.4 SMR and KA

Forty rock samples are collected from the site for strength determination. RMR value obtained is 46 which indicate fair rock quality. SMR values fall in Class III which is indicative of partially stable slope conditions (Table 7.10).

Table 7.10. Slope mass rating

	Value or Condition	**Rating**
1. Point Load Test	1.88 MPa	4
2. RQD	49%	10
3. Spacing of joints	50 mm	10
4. Condition of joints	Slightly rough; separation <1 mm; soft joint wall rock	12
5. Groundwater condition	Dry	10
RMR	*= (1+2+3+4+5)*	***46***
6. $F_1 = (1\text{-}\mathrm{Sin}\mathrm{I}\alpha_j - \alpha_s\mathrm{I})^2$	0.85	0.85
7. $F_2 = \mathrm{Tan}^2\beta_j$ or $F_2 = 1$ for toppling	0.70	0.70
8. $F_3 = \mathrm{I}\beta_j - \beta_s\mathrm{I}$ for plane failure $= \mathrm{I}\beta_j + \beta_s\mathrm{I}$ for toppling where β_s= dip/angle of slope	4	-6
9. F_4 = Adjustment factor	Pre-splitting	10
***SMR** = RMR+(F₁xF₂xF₃)+F₄*	*46+{0.85x0.70x(-6)}+10*	***52.43***
10. Class	III	
11. Description	Partially stable; some joints or many wedges	

200 joint attitudes are analyzed and two sets of joints are deciphered from pole (Fig. 7.10a) and contour diagrams (Fig. 7.10b) to cause instability to the slope due to interference.

1. Slope : 70°→284°
2. J_1 : 54°→272°
3. J_2 : 53°→320°

The stereographic projection shows the development of a distinct wedge due to the intersection of these two joint sets. The true dip of both J_1 and J_2 lie outside the slide envelope (Fig. 7.10c). Cruden (1978) suggests double plane wedge failure in such cases. The rosette (Fig. 7.10d) suggests complex deformation including shearing of the rocks.

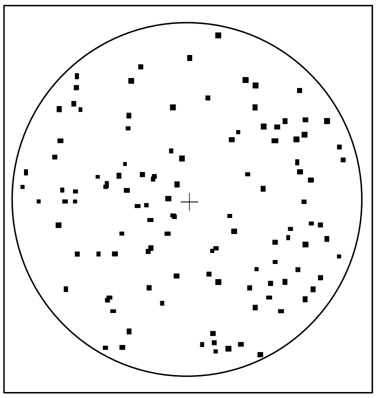

Fig. 7.10a. Pole diagram

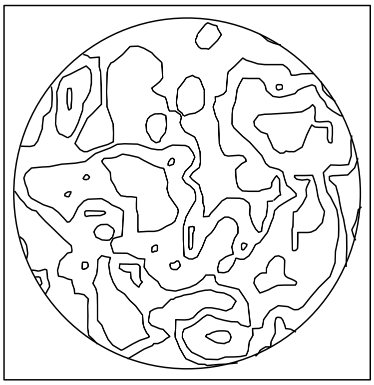

Fig. 7.10b. Contour diagram

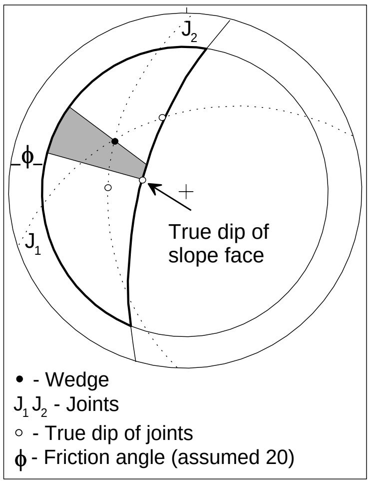

Fig. 7.10c. Stereogram

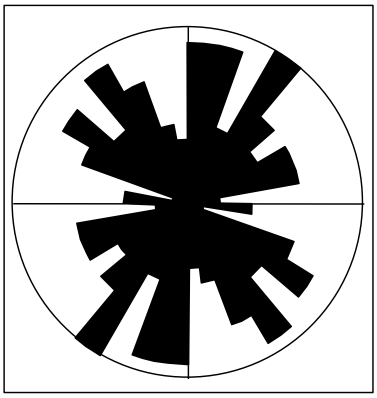

Fig. 7.10d. Rosette

7.10.5 Recommendations

i. The free face of the slope is steeply inclined hence, benching is recommended to increase stability (Fig. 7.10e). The following are the proposed parameters:

Base of bench	- 1.5 m
Height of bench	- 3 m
Length of bench	- 80 m

ii. A carpet of grass planted on the exposed surface will serve to prevent excess seepage of water into the soil.

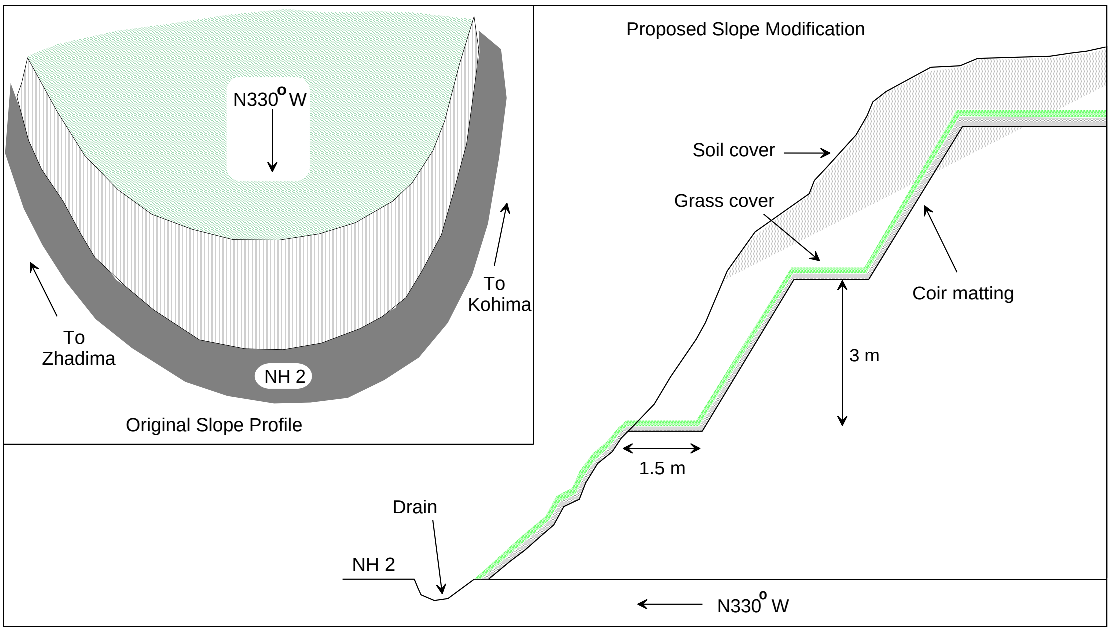

Fig. 7.10e. Proposed slope modification / mitigation measures

7.11 LOCATION 11 (14.80 km Junction)

7.11.1 Introduction

The slide is located at 25°45'22.54" N latitudes and 94°04'45.83" E longitudes and is part of SoI toposheet no. 83 K/1SW. The bypass from Dimapur to Wokha via Peducha meets the NH 2 at this location (Fig. 7.11). This is a comparatively small area but sliding of debris is a continuous process (Plate 7.11a).

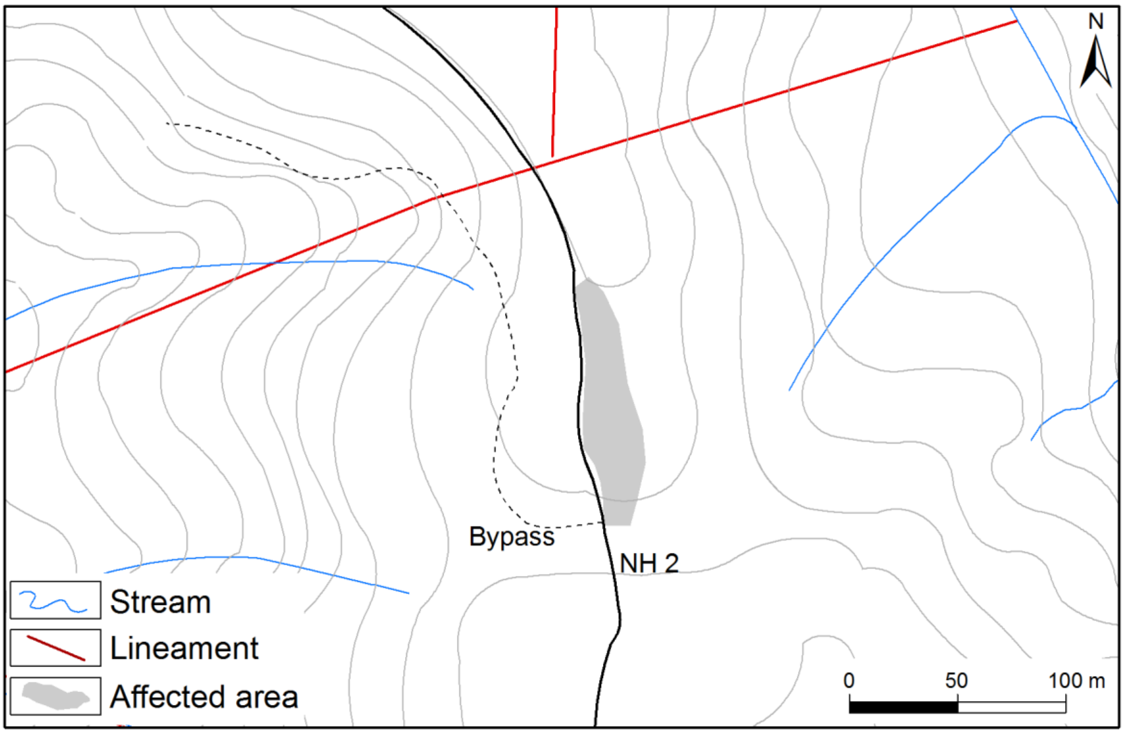

Fig. 7.11. Map of location 11

7.11.2 Geology and structure

This slope is made up of partially weathered Disang shale and unsorted debris. Joint data have been collected from the surroundings. The rocks exhibit three prominent sets of joints. Two lineaments cutting across this area are intimately associated with these joints. The lineament towards the north traverses along an ENE-WSW direction, while the other lineament trends N-S.

7.11.3 Causes and effects

Road widening has destabilized the slope. The process left the slope without any support, as high as 8 m and at an angle of about 70º. The weak materials on these steep

Plate 7.11a. Minor debris slide

Plate 7.11b. Unstable steep slope between NH 2 and Bypass

slopes are susceptible to sliding during the monsoon. Such slide material block drains and damage roads. The excavation of the bypass without proper mitigation measures has left a very steep slope between the two roads (Plate 7.11b) which may be destabilized in the future.

7.11.4 SMR and KA

Forty rock samples are collected from the site for point load test. Data shows an average value of 1.68 MPa (Table 7.11). RMR rating of 44 indicates moderately weak rock condition. SMR values falling in Class IV indicate unstable slope conditions and probable wedge failure.

Table 7.11. Slope mass rating

	Value or Condition	**Rating**
1. Point Load Test	1.68 MPa	4
2. RQD	49%	8
3. Spacing of joints	50 mm	10
4. Condition of joints	Slightly rough; separation <1 mm; soft joint wall rock	12
5. Groundwater condition	Dry	10
RMR	*= (1+2+3+4+5)*	***44***
6. $F_1 = (1\text{-Sin}I\alpha_j - \alpha_s I)^2$	10°	0.85
7. $F_2 = \text{Tan}^2\beta_j$ or $F_2 = 1$ for toppling	25°	0.40
8. $F_3 = I\beta_j - \beta_s I$ for plane failure $= I\beta_j + \beta_s I$ for toppling where β_s= dip/angle of slope	-45°	-60
9. F_4 = Adjustment factor	Pre-splitting	10
SMR *= RMR+(F_1xF_2xF_3)+F_4*	*44+{0.85x0.40x(-60)}+10*	***33.6***
10. Class	IV	
11. Description	Unstable; large wedges	

About 160 joint attitudes are taken for kinematic analyses. Three joint sets are identified from pole (Fig. 7.11a) and contour diagrams (Fig. 7.11b), which are plotted against slope attitude in a stereographic projection. Wedge mode of failure is inferred by the plot (Fig. 7.11c).

1. Slope : 70°→256°
2. J_1 : 29°→259°
3. J_2 : 44°→229°

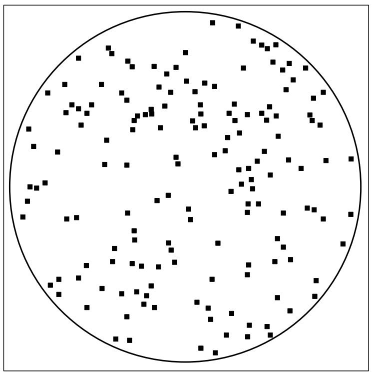

Fig. 7.11a. Pole diagram

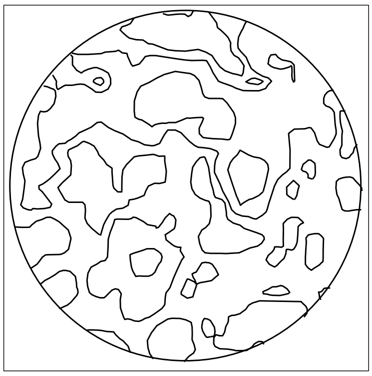

Fig. 7.11b. Contour diagram

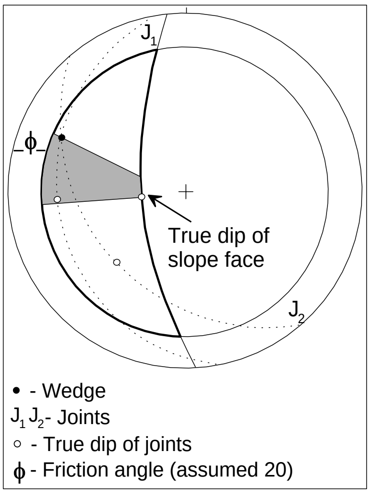

Fig. 7.11c. Stereogram

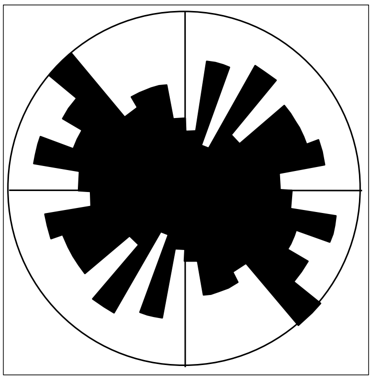

Fig. 7.11d. Rosette

True dips of joint planes J_1 and J_2 lie outside the shaded region. It is therefore concluded that double plane wedge failure is likely to occur here where wedges will be large. Analyses of joint intersections (J_1 and J_2) indicate that wedges form small blocks in the rocks. Deformation in this location will primarily be of sheared nature (Fig. 7.11d) with other complex deformation.

7.11.5 Recommendations

i. The top of the ridge should be trimmed to about 5 m for a length of 100 m (Fig. 7.11e).
ii. Electric poles on the ridge crest should be relocated.
iii. A reduction of slope gradient is recommended.
iv. A cover of grass along the modified slope will lend stability to the slope.
v. Proper maintenance of the roadside drain is required.

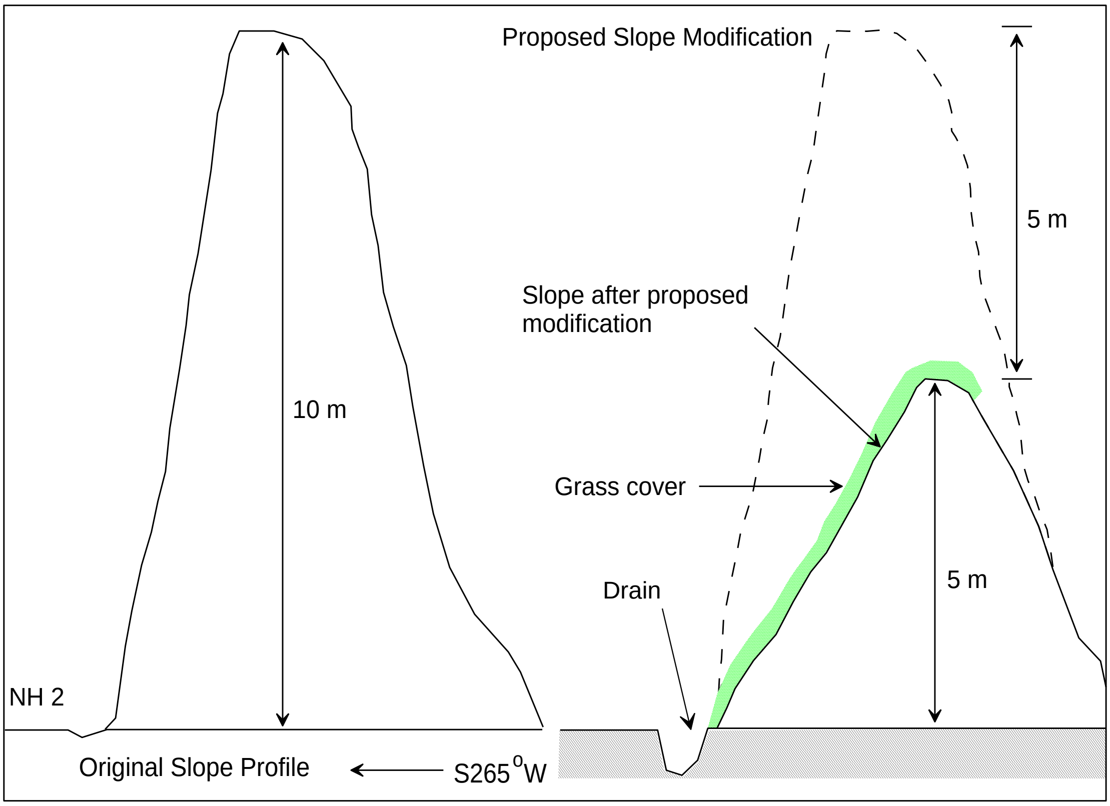

Fig. 7.11e. Proposed slope modification / mitigation measures

7.12 LOCATION 12 (15.80 km Junction)

7.12.1 Introduction

This debris slide is located at 25°45'36.21" N latitudes and 94°04'41.81" E longitudes and is part of SoI toposheet no 83 K/1. This is a steep slope along which a debris slide took place in the monsoon of 2007 (Fig. 7.12). The portion of the slope face above the highway is unstable (Plate 7.12a) and has affected about 120 m of the road.

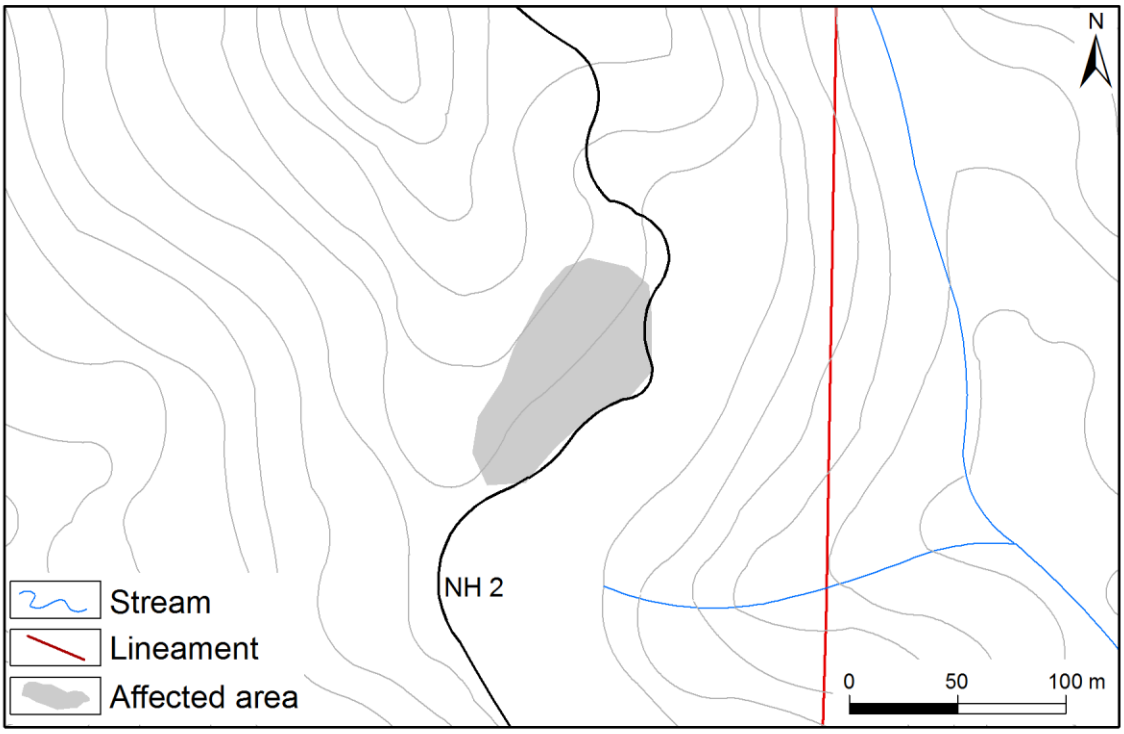

Fig. 7.12. Map of location 12

7.12.2 Geology and structure

The Disang rocks making up the area comprise splintery shale interbedded with minor siltstone. The base of the hill along the highway is made up of partially sheared shale. Above this is crumpled and weathered debris that is prone to saturation. The probability of wedge failure exists due to the interference of two local faults which have weakened the slope material (Plate 7.12b). The outcrops exhibit three prominent sets of joints affecting the rocks. The first set trending NNW-SSE, dips 47°. The second set trends NNE-SSW and dips 65°. The third set dips 47° and trends in an almost NE-SW direction. One of the faults in the area is associated with the third set of joints while the other fault trends N-S.

Plate 7.12a. Critical condition of slope

Plate 7.12b. Probability of wedge failure due to local faults

7.12.3 Causes and effects

The debris slide was triggered by rainfall in August 2007. The rocks comprising partially sheared shale dipping towards the road, is overlain by crumpled and weathered materials. These rocks are easily saturated by water and hence, are prone to erosion. The slope has been left as high as 18 m at an angle of about 75º without any support which is the reason for the debris slide. The debris moreover blocked the drain and damaged a good portion of the road which affected vehicular movement.

7.12.4 SMR and KA

Forty five rock samples were collected from this site for point load test. RMR values indicate moderately weak rocks. SMR values falling in Class IV and indicating unstable slope conditions point to planar and wedge failure (Table 7.12).

Table 7.12. Slope mass rating

	Value or Condition	**Rating**
1. Point Load Test	1.07 MPa	4
2. RQD	55.6%	13
3. Spacing of joints	50.55 mm	10
4. Condition of joints	Slightly rough; separation <1 mm; soft joint wall rock	12
5. Groundwater condition	Dry	10
RMR	*= (1+2+3+4+5)*	***49***
6. F1 = (1-SinIαj - αsI)2	10°	0.85
7. F2 = Tan2βj or F2 = 1 for toppling	35°	0.70
8. F3 = Iβj - βsI for plane failure = Iβj + βsI for toppling where βs= dip/angle of slope	-40°	-60
9. F4 = Adjustment factor	Pre-splitting	10
***SMR** = RMR+(F1xF2xF3)+F4*	*49+{0.85x0.85x(-50)}+10*	***23.30***
10. Class	IV	
11. Description	Unstable; planar and/or large wedges	

Kinematic analyses have been performed using about 165 joint attitudes that are plotted in pole (Fig. 7.12a) and contour diagrams (Fig. 7.12b), from which three joint sets (J_1: 47°→143°, J_2: 65°→75°, and J_3: 47°→114°) affecting the rocks are identified. These joints are plotted against slope attitude (75°→160°) in a stereographic projection (Fig. 7.12c).

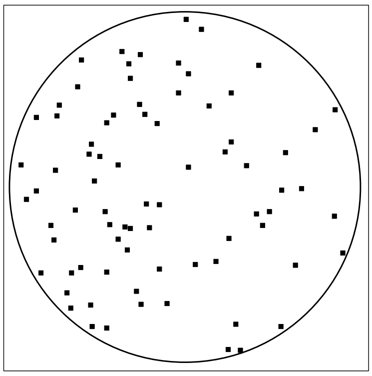

Fig. 7.12a. Pole diagram

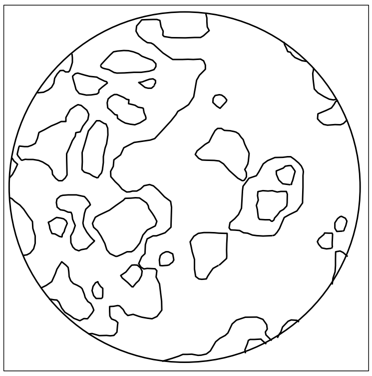

Fig. 7.12b. Contour diagram

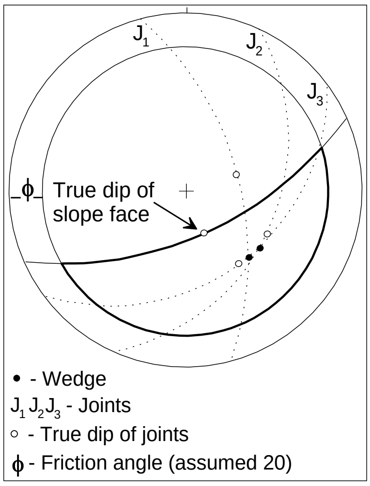

Fig. 7.12c. Stereogram

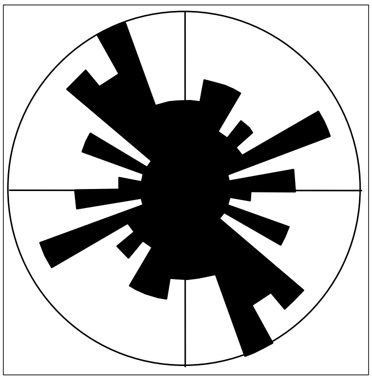

Fig. 7.12d. Rosette

The diagram shows the development of two distinct wedges due to the intersection of these joint sets. The intersection of J_1, J_2, and J_3 forms a number of wedges. It is inferred that single plane wedge failure will occur as the true dip of one of the joint planes lies in the slide envelope. J_1 plotted against slope shows probable planar failure. Therefore, any slope failure will involve both planar and wedge types. The rosette constructed from joints (Fig. 7.12d) indicates extensive shearing, particularly antithetic, of the rocks besides tensile fractures and folding.

7.12.5 Recommendations

i. A cantilever wall with the following specification along the toe of the slope is recommended (Fig. 7.12e).

   Height - 2.5 m
   Length - 120 m

ii. Drainage of subsurface water through perforated pipes is necessary to prevent buildup of pore pressure.

iii. It is also advisable to trim 4 m of the ridge crest.

iv. The drain at the base should be regularly maintained.

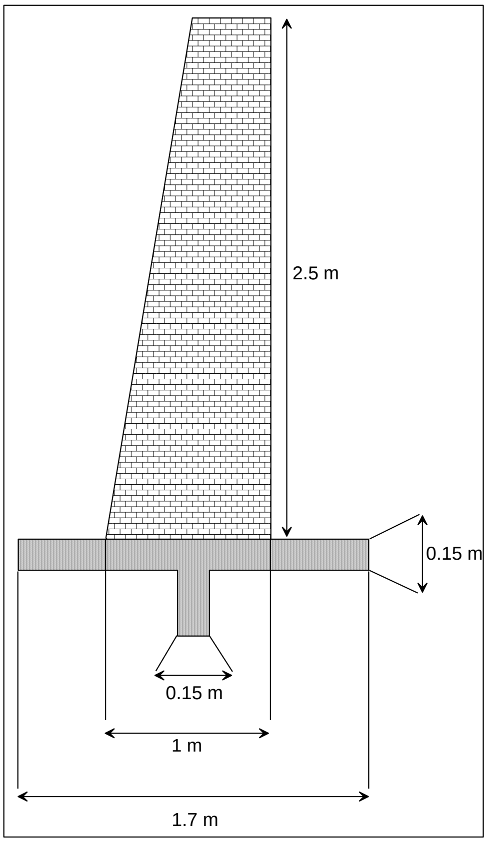

Fig. 7.12e. Proposed cantilever wall

7.13 LOCATION 13 (16.10 km Junction)

7.13.1 Introduction

This area located at 25°44'51.97" N latitudes and & 94°04'36.71" E longitudes, is part of SoI toposheet no. 83 K/2 SW. A very high and steep slope has been left due to road widening (Fig. 7.13). This section is very dangerous for a length of about 110 m for vehicular movement along the road (Plate 7.13a). The opposite side of the road is also dangerous due to weak material that has led to subsidence of portions of the highway (Plate 7.13b).

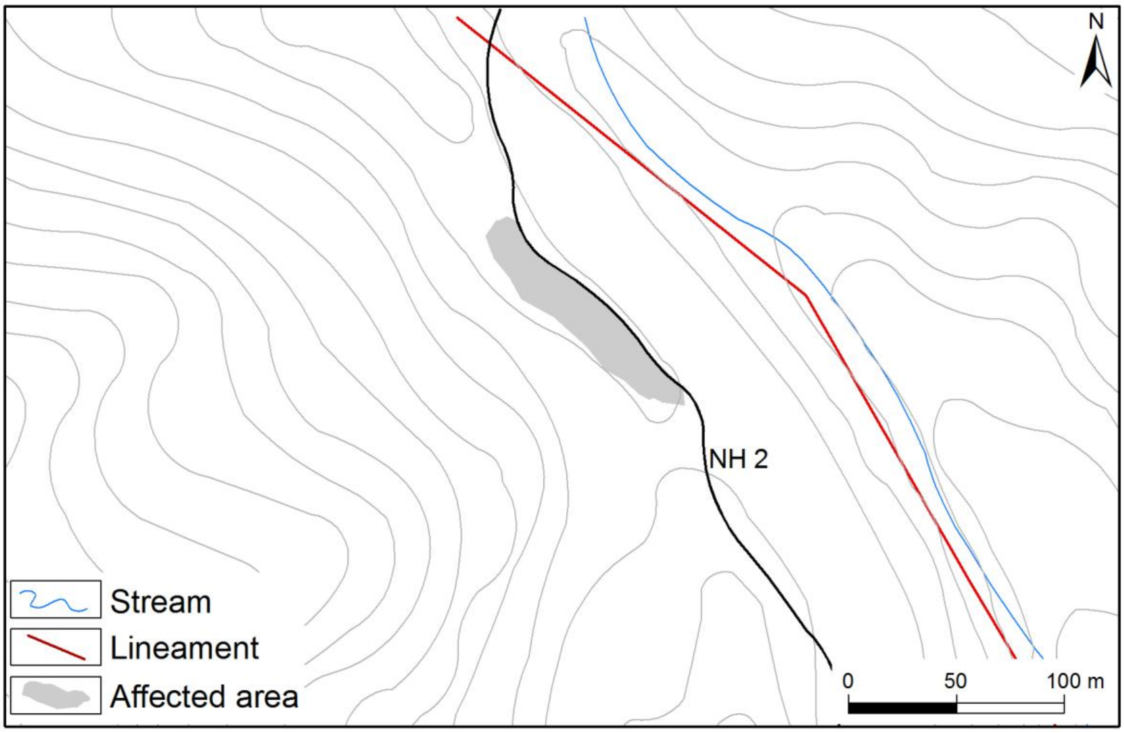

Fig. 7.13. Map of location 13

7.13.2 Geology and structure

The Disang rocks making up the area are brown to dark gray splintery shale with intercalations of thin siltstone. The outcrops exhibit three prominent sets of joints. The first set trending NW-SE dips at an angle of 60°; the second set dips 24° towards NNW-SSE, while the third set dips 79° with an almost N-S trend. A fault, trending NW-SE, traverses this area. This lineament is parallel to the first set of joints.

Plate 7.13a. High and steep slope

Plate 7.13b. Subsidence of portion of highway

7.13.3 Causes and effects

Road widening has left the slope as high as 12 m with an average inclination of 80°, without any support. Highly jointed shales exposed on such unfavorable slopes are susceptible to collapse. The poor drain constructed along this section of the road is always completely blocked by debris. The waters flowing over to the other side of the road saturated the lower slopes leading to the development of tension cracks and causing subsidence of the road.

7.13.4 SMR and KA

Forty rock samples are collected from the site and RMR value derived. SMR values fall in Class IV indicating unstable slope conditions (Table 7.13). This area suffers from potential planar or wedge type of failure.

Table 7.13. Slope Mass Rating

	Value or Condition	**Rating**
1. Point Load Test	1.44 MPa	4
2. RQD	32.5%	8
3. Spacing of joints	40 mm	5
4. Condition of joints	Slightly rough; separation <1 mm; soft joint wall rock	12
5. Groundwater condition	Dry	10
RMR	*= (1+2+3+4+5)*	***39***
6. $F_1 = (1\text{-Sin}I\alpha_j - \alpha_s I)^2$	15°	0.70
7. $F_2 = \text{Tan}^2\beta_j$ or $F_2 = 1$ for toppling	25°	0.40
8. $F_3 = I\beta_j - \beta_s I$ for plane failure $= I\beta_j + \beta_s I$ for toppling where β_s= dip/angle of slope	-55°	-60
9. F_4 = Adjustment factor	Pre-splitting	10
SMR *= RMR+(F_1xF_2xF_3)+F_4*	*39+{0.70x0.40x(-60)}+10*	***32.2***
10. Class	IV	
11. Description	Unstable; planar and/or large wedges	

175 joint attitudes are used for kinematic analyses. Three sets of joints as deciphered from pole (Fig. 7.13a) and contour diagrams (Fig. 7.13b), which point to possible instability of the slope material.

1. Slope : 80°→75°
2. J_1 : 60°→45°
3. J_2 : 24°→60°
4. J_3 : 79°→84°

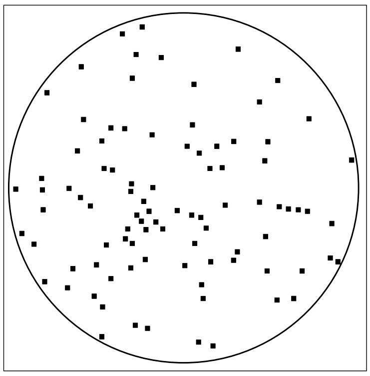

Fig. 7.13a. Pole diagram

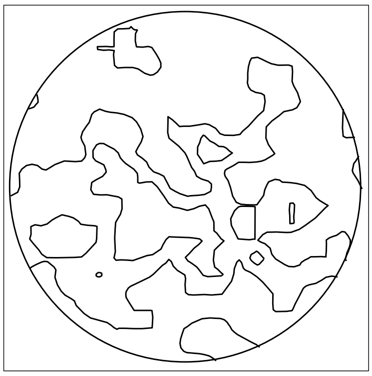

Fig. 7.13b. Contour diagram

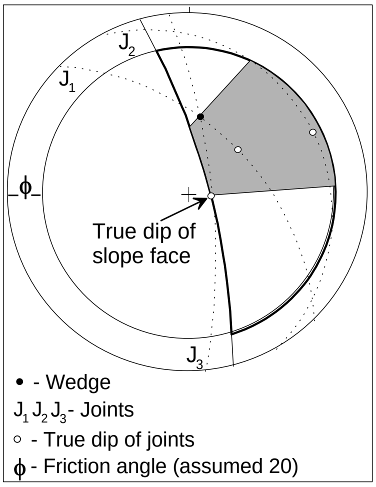

Fig. 7.13c. Stereogram

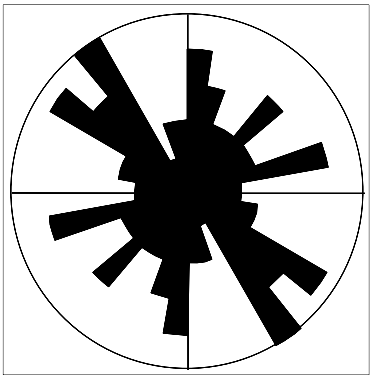

Fig. 7.13d. Rosette

The stereographic projection (Fig. 7.13c) shows development of both wedge and planar failure which are inferred from the intersection of the joint sets. One of the true dips of the joint planes lies within the shaded region between the true dip of the slope and the line of intersection of the two joint planes. Planar and/or wedge failure are likely to occur along this portion of the highway. Analyses of joint intersections indicate that wedges form small blocks in the rocks; joint 3 will cause planar mode of failure. The rosette (Fig. 7.13d) indicates high structural deformation including tensile fractures.

7.13.5 Recommendations

i. About 115 m of part of the top of the ridge, 6 m above the highway, should be trimmed (Fig. 7.13e). Benching of the slope with the following specifications is recommended:

Base - 1.5 m
Height - 3 m
Inclination - 60º

ii. A geotextile cover should be placed in the debris covered areas and grass planted.

iii. Proper roadside drainage at the base of the slope is important.

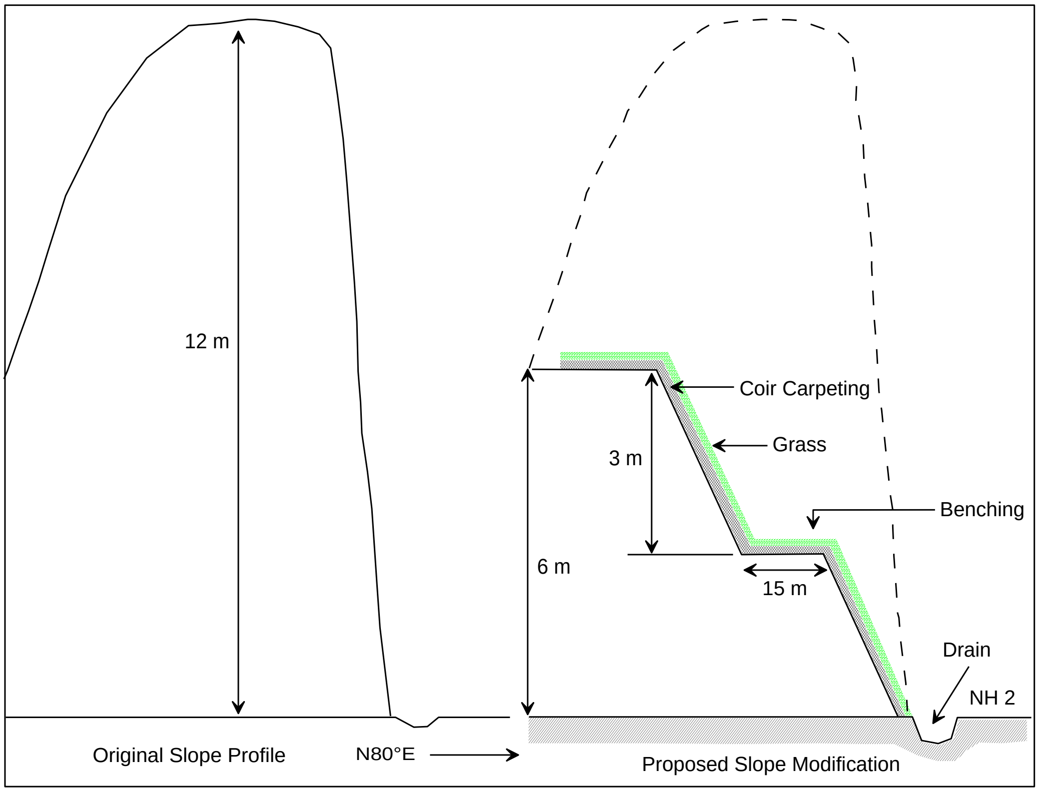

Fig. 7.13e. Proposed slope modification / mitigation measures

PART - B

NAGALAND UNIVERSITY APPROACH ROAD

7.14 LOCATION 14

7.14.1 Introduction

The location is part of SoI toposheet no. 83 K/2 NW that is located at 25°43'26.25" N latitudes and 94°05'29.26" E longitudes. The road leading to the Nagaland University Campus (Fig. 7.14) is scarred by a debris slide and subsidence due to road widening. The slope had been cut and left untreated which is the reason for the instability.

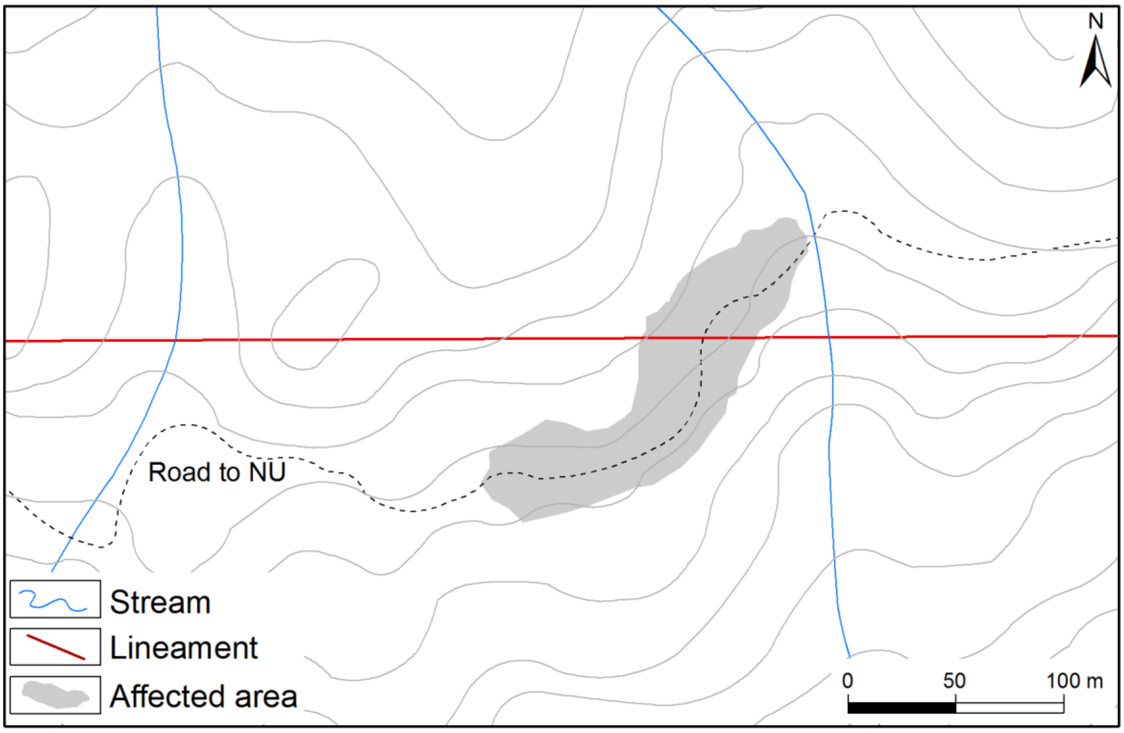

Fig. 7.14. Map of location 14

7.14.2 Geology and structure

The rocks here are, for the most part, weathered, fractured, and crumpled shale that is topped by loose debris and soil, the average thickness of which is about 1 m. The crumpled and weathered horizons are prone to saturation during the monsoon. The outcrops exhibit two prominent sets of joints which affect the rocks. The first set trending NE-SW dips at an angle of 24° while the second set trends almost N-S and dips 39°. A major lineament trending E-W, traverses the area.

7.14.3 Causes and effects

This section is made up of weak shales that are crumpled and weathered to varying degrees (Plate 7.14a). About 210 m of this road section is adversely affected by debris slides due to road widening (Plate 7.14b). The height of the unstable slope under study prior to sliding was about 15 m at an inclination of about 75º. During prolonged rainfall in the monsoon of 2010 part of the road was also affected by a subsidence up to 2 m. To raise the road level, debris from the upper slopes was excavated and dumped on the subsidence zone which aggravated the situation. To rectify this problem a pit was excavated on the down-slope side. All water from the uphill side flowed into the pit thereby saturating the material and seeping through the debris. Such seepage will ultimately lead to washing away of the down-slope side of the road and a major portion of it.

7.14.4 SMR and KA

Forty rock samples were collected from this site for point load tests. RMR values at 36 indicate weak rocks. SMR values fall in Class IV indicating unstable slope conditions (Table 7.14). Planar and/or wedge failure is likely here.

Table 7.14. Slope mass rating

	Value or Condition	**Rating**
1. Point Load Test	1.49 MPa	4
2. RQD	42.45%	8
3. Spacing of joints	45.5 mm	5
4. Condition of joints	Slightly rough; separation <1 mm; soft joint wall rock	12
5. Groundwater condition	Moist only (interstitial water)	7
RMR	*= (1+2+3+4+5)*	***36***
6. $F_1 = (1\text{-Sin}I\alpha_j - \alpha_s I)^2$	15°	0.70
7. $F_2 = \text{Tan}^2\beta_j$ or $F_2 = 1$ for toppling	30°	0.40
8. $F_3 = I\beta_j - \beta_s I$ for plane failure $= I\beta_j + \beta_s I$ for toppling where β_s= dip/angle of slope	-30°	-60
9. F_4 = Adjustment factor	Pre-splitting	10
SMR *= RMR+(*$F_1xF_2xF_3$*)+*F_4	*36+{0.70x0.40x(-60)}+10*	***29.2***
10. Class	IV	
11. Description	Unstable; large wedges	

Kinematic analyses have been performed for determination of possible mode of failure. About 150 joint attitudes are taken and plotted in pole (Fig. 7.14a) and contour diagrams (Fig. 7.14b) from which two joint sets affecting the rocks are identified.

1. Slope : 60°→145°
2. J_1 : 24°→170°
3. J_2 : 39°→84°

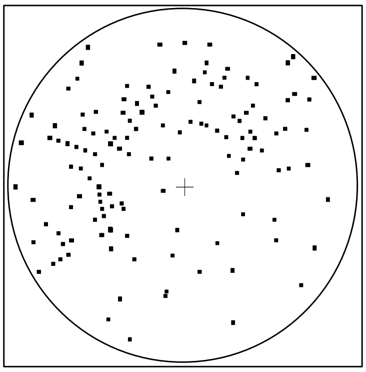

Fig. 7.14a. Pole diagram

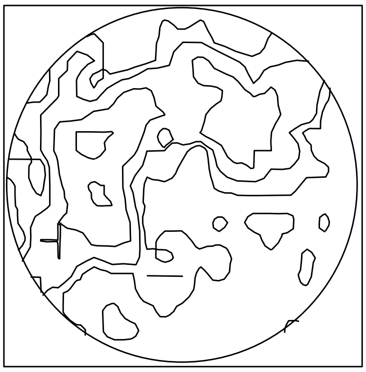

Fig. 7.14b. Contour diagram

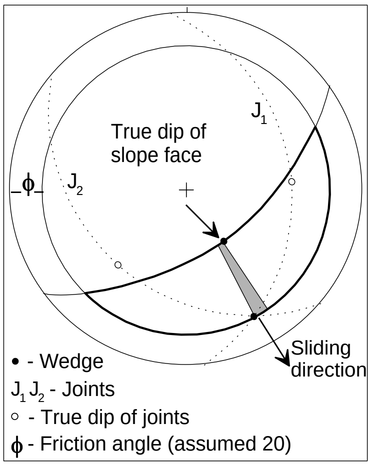

Fig. 7.14c. Stereogram

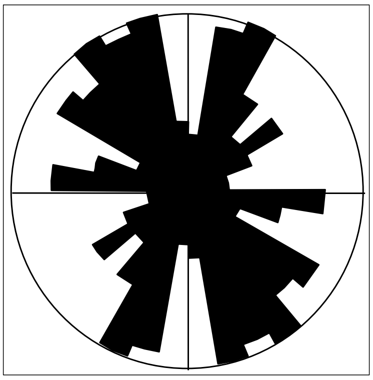

Fig. 7.14d. Rosette

These joints are plotted against slope attitude in a stereographic projection (Fig. 7.14c). The diagram shows a distinct wedge due to the intersection of joints J_1 and J_2. Cruden (1978) suggests double-plane wedge failure in such cases as both the true dips of the two joints lie outside the shaded area. Development of planar failure cannot be ascertained as none of the strikes of joints have a parallelism value of ±20° against the strike of the slope as opined by Hoek and Bray (1981). Field observations also rule out planar failure. The rosette (Fig. 7.14d) indicates extensive shearing and folding of the rocks, and possibly the action of a thrust.

Plate 7.14a. Deformed shales

Plate 7.14b. Debris slide

7.14.5 Recommendations

i. A terrace should be cut at a height of 8 m above and along the road for a length of 90 m to reduce the head load (Fig. 7.14e).

ii. The slope along the section should be reduced to 50° above and below the terrace.

iii. An appropriately designed retaining wall of 2 m height along the road will help protect the upper slope material from sliding down. (Fig.7.14f).

iv. The pit should be filled up with the material excavated from the uphill slope. This filled area should slope 20° away from the road and be covered with a grass carpet.

v. As the upper slope generally consists of loose soils, a thick carpet of grass will help stabilize the same.

vi. The roadside drain should be well plastered along the slide zone to prevent water from seeping into the subsurface.

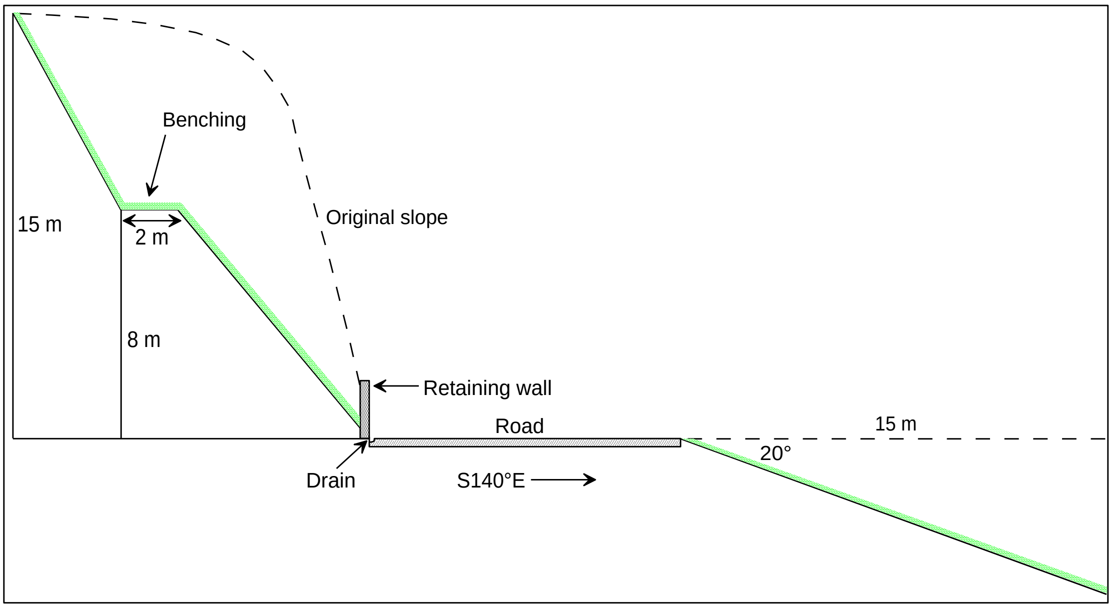

Fig. 7.13e. Proposed slope modification / mitigation measures

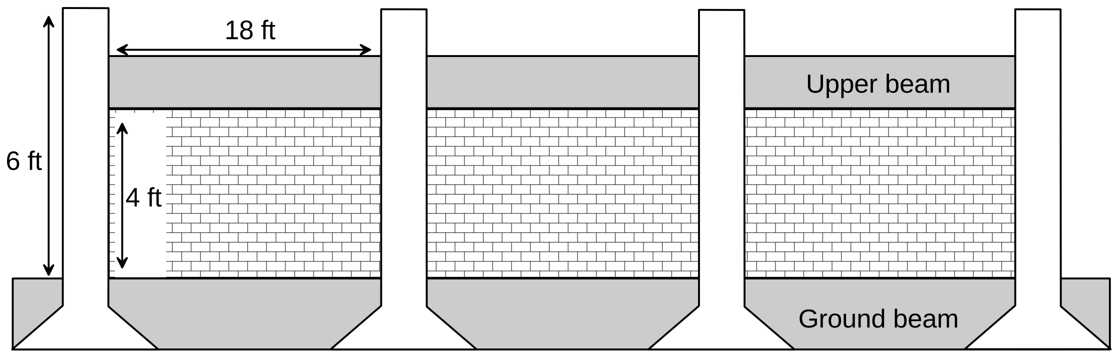

Fig. 7.14f. Proposed retaining wall

CHAPTER 8

DISCUSSION AND CONCLUSIONS

8.1 DISCUSSION

Rapid urbanization and development in hilly areas has underlined the importance of understanding the geological factors promoting instability. This requires careful and comprehensive assessment of factors that lead to initial and subsequent failure. Assessments involve detailed field investigations for geology, soils, hydrology, topography, rainfall, and human factors which collectively cause slope instability. Assessments may conclude with recommendations for methods and procedures for mitigation of existing landslides, immediate landslide hazards, as well as the identification of more detailed geotechnical analysis and monitoring of selected landslides.

Landslides and other forms of mass wasting have posed major challenges to the mountainous terrains of the country. It is a natural hazard of significant impact worldwide, and affects at least 15 percent of the land surface of India, an area that exceeds 0.49 million km^2 (National Institute of Disaster Management, 2009). Landslides may occur almost anywhere, from manmade slopes to natural, pristine ground. It occurs independently or aided by human activity. They typically result from extreme natural events such as heavy rainfall, volcanic eruptions, earthquakes, etc. which can be combined with factors related to human activities such as deforestation and intensive exploitation of land for agricultural use and other developmental activities. Landslides have caused large numbers of casualties and huge economic losses in hilly and mountainous areas.

Geological investigations of land instability have been attempted to derive the spatial variation and distribution of slope instability in the study area. Geomorphology, geological features, lithology, land use / land cover, groundwater, and rainfall are important initiators of landslides. Human interventions such as haphazard and unscientific developmental activities worsen existing stability conditions. The present study is carried out to evaluate the factors responsible for land instability and to generate a LHZ map for the study area as developmental activities and expansion of Kohima town are taking place or are being proposed in this area. In addition risk analyses has been carried out along the NH 2 and the approach road to the NU campus, which are being widened, to provide mitigation measures against possible landslides and those areas along the highway that are affected by landslides.

More than 90 percent of the surface area of Nagaland state is hilly. Due to under-thrusting of the Indian plate below that of the Burmese, most rocks of the region is highly deformed. The deformation is primarily in the form of large scale folding, faulting, and shearing. Large scale jointing has also affected the rocks; due to stresses along various directions the rocks are commonly fractured. The region receives abundant rainfall which has aided rapid weathering of the already weakened rocks. All these processes together have played a very significant role in causing much surface instability in the study area and region as a whole.

The study area represents high denudational hills made up of rocks belonging to the Disang and Barail groups. The Disang make up the bulk of the rocks of the study area. They are very weak, being made up primarily of shale with thin alternations of sandstone and siltstone. These are overlain by the younger Barail made up dominantly of sandstone with minor intercalations of shale. The unmappable Barail are confined to the upper ridges as irregular blocks along the flanks of some slopes due to faulting. The rocks of this area are commonly affected by two to four sets of joints. Faults too are fairly common in the study area, though most are of local extent. The weak Disang are jointed, fractured, and crumpled to varying extents and have been affected by the weathering processes aided by prolonged monsoonal rains.

Studies have been carried out for landslide hazard microzonation mapping of the study area. Data on geoenvironmental parameters such as slope, structural features, lithology, groundwater, and land use / land cover are derived from various sources through the analysis of SoI toposheet and satellite imagery and extensive fieldwork. These parameters are converted into digital format in ArcGIS 9.2 and databases are generated for road network, facet, slope morphometry, land use / land cover, drainage network, groundwater, lithology, structure, and landslide incidences employing visual interpretation and digital techniques.

In the study area surface instability is noted even in gentle slopes. This is due to local steepness of these slopes and the weak rocks and soils that make up the area. Hence, it was felt justifiable to raise the rating of lithology for this area to 2.5 from the recommended 2.0 of the Bureau of Indian Standards (1998). Similarly the rating for land use / land cover is reduced to 1.5 from 2.0 as the relative effect of this parameter is not as significant as that of lithology. Relative relief as a factor in instability studies in this area is insignificant. It is therefore proposed not to use relative relief, as this parameter bears no impact in this study. The TEHD value is therefore reduced to 9.0 from the 10.0 proposed by the Bureau of Indian Standards (1998). However, the total value for the different zones is preserved as percentages of the original value of 10.0. Based on computed TEHD values the hazard zones of the study may be classified under four categories, viz. low, moderate, high, and very high. Slopes are generally gentle to moderate in this area. Most steep and very steep slopes are confined to the north. The rocks are commonly partially weathered, crumpled, and weathered shale which are responsible for the general weakness of the slopes. Landslide incidences maps generated in ArcGIS are laid over the thematic and LHZ maps to ascertain their relationship with the various categories of the themes and hazard zones.

All five categories of slopes are noted in the study area. A large number of slopes are mapped as gentle but much of these are locally moderate to steep along stream channels, being areally too small to be categorized as individual facets. Hence, in the overall analyses these slopes are given the ratings of the general slope in that facet. Slides normally occur in areas of locally steep slopes. With relation to slope, 2.33% of slides occur on very steep slopes, 6.98% on steep slopes, 44.19% on moderately steep slopes, and 46.50% on gentle slopes. Very gentle slopes constitute a small portion of the area, these slopes being more or less stable. The frequency of landslides in the very steep slopes is naturally high while that of the steep slopes is also high. The moderately steep slopes also show reasonably high values. The frequency of landslides on the gentle slopes is appreciably low. However, the reason that landslides have affected this category as well, besides locally steepness of slopes, is attributed to the weak lithology, faulting in the area, and erosive activity of streams.

The lithological map of the study area shows the distribution of the various litho-units. Here, 34.88% of the slides occur in weathered shale and the same in loose debris, 25.58% in crumpled shale, and 4.65% in partially weathered shale. The other litho-units, being more stable are not affected by landslides. Another reason is that the slopes of some of these areas are gentler. The frequency of slide distribution indicates that the loose debris areas are most prone to landslides. This is natural as debris slopes possess very low shearing strengths, being mixed with clays and hence, collapse easily in the presence of water. The high frequency of slides in the weathered horizons is due to the abundance of water from rainfall during the monsoon when the shearing strengths of clays are reduced. The 2.21 frequency of the crumpled shale also point to the same reasons, besides rampant slope cutting.

Most of the surface area in this study is dry. The largest percentage of slides has occurred in wet areas (46.51) followed by the dry areas (34.88). The damp areas show negligible percentages (18.60) of landslides. However, the frequency of landslides in wet areas (9.30) is high while damp areas also show relatively higher values (2.24) compared to the dry areas.

The area has been classified under five categories of land use / land cover. The populated areas made up of some small villages are located in geologically more stable areas and as such do not suffer from landslide activity. Moreover, indiscriminate earth cutting and unscientific land use practices such as construction of large and heavy structures is not resorted to in such areas. Most wet cultivation for paddy is confined to old landslides. In these areas the water retention during the growing season increases the pore-water pressure tremendously leading to continued subsidence and/or damage of hill slopes and roads. The moderately and sparsely vegetated areas are usually geologically weak with unfavorable slopes and hence, have been affected by 18.60% and 16.28% of landslides respectively. Densely vegetated areas also are affected by landslides which are ascribed to structural disturbances and weak lithology. Hence, the frequency of landslides is also high.

The LHZ map delineates the study area into four classes comprising low, moderate, high, and very high hazard zones. The low hazard zones are free of landslides. 11.63% slides occur in moderate hazard zones, 51.16% in high hazard zones, and 37.21% in very high hazard zones. The very high hazard zones have a frequency of 12.31 and high hazard zones 3.17. The moderate hazard zones have a comparatively low frequency of 1.01%. Results indicate that the very high hazard zones are highly unstable. The high hazard zones too are unstable. Much of the areas identified as moderate hazard zones are more or less stable as long as external factors such as large earthquakes, cloudbursts, excessive anthropogenic activity, etc. do not disturb the equilibrium.

Structure and lithology are the main geologic factors contributing to slope instability in the area. These rocks are commonly affected by local folds (Plate 8.1) and are cut across by two to four sets of joints. Thrusts too are probably present in the Disang. However, due to the monotonous nature of the Disang sediments it is difficult to map such thrusts. Joints, shear zones, fault planes, and weathered horizons in this area facilitate erosion, particularly with the aid of surface runoff. Surface runoff is responsible for removal of most top soil. The joints are responsible for imparting the splintery nature to some of the Disang shales (Plate 8.2). The shales in this area are highly fissile, which is another cause of their weakness. The fissile nature of the shales coupled with the joint planes have made this terrain highly susceptible to mass wasting. Folding and faulting in the area have crumpled and fractured the shales to a great extent (Plate 8.3). These crushed zones comprise debris of various materials that are thoroughly mixed with clayey and sandy soils.

Numerous well-defined lineaments are very prominent in satellite imagery of the area. Some streams have cut deep channels along such planes. Steep gullies have formed due to base erosion by streams flowing along fault planes. Trellis drainage patterns are common in the study area. Other drainage patterns include parallel, some dendritic, and intermediate forms. Most of these patterns indicate structural control. The lower order streams generally follow major joint patterns. These channels meet larger streams at various angles forming irregular branches. Toe erosion by streams is active along the lower flanks of the hills of this area. This has facilitated well developed tension cracks.

Plate 8.1. Folding in shale

Plate 8.2. Splintery Disang shale

Joint data obtained from the field are plotted to generate a rose diagram (Fig. 1.4). The rosette shows concentration of one set of plots along NE-SW, which is parallel to the regional trend that is related to F_2 movements. Another set of joints trend NW-SE. These joints are due to tensile or shear stresses that are concentrated around the regional NW-SE compression corresponding to F_3 movements. As a consequence hybrid fractures have developed in the terrain due to the interplay of these stresses causing extensive deformation of the rocks. Jointing and fracturing have considerably weakened the rock masses thereby initiating extensive weathering to produce thick mantles of waste, making the area susceptible to sliding, particularly during the monsoon.

Studies reveal that the major triggering factors of landslides in the area are anthropogenic activity and excessive rainfall received during the monsoon. One of the factors for slope destabilization in the terrain is the removal of slope support for widening of roads. This is particularly true in areas where topographic slopes and dips of beds are in conformity, with beds dipping at equal or lesser amounts than hill slopes. The overloading of slopes or removal of lateral support by human interference is a prime concern for slope failure in many areas. Soil cover in the area permits luxuriant growth of vegetation but urbanisation and other human activities have disturbed the natural processes thereby exposing the soil to water action which ultimately results in extensive surface erosion and slope instability. Terrace cultivation for paddy is commonly practiced in old landslide areas rich in silt and clay. In such areas water is trapped in the terraces during the planting season whereby extreme pore pressure is generated. Such terraces are found in patches along the NH 2. On either side of the highway water logging leads to continuous subsidence and damage of the road during the monsoon (Plate 8.4). The area experiences high monsoon precipitation which causes abundant percolation of rainwater through the porous soils and highly jointed and fractured rocks. With the high saturation due to excess water the weathered and crumpled shales become unstable leading to mud and debris flows. However, the area is generally dry after the monsoon. During this period landslide activity is not known in Nagaland. Most landslides take place during the peak of monsoon. This is because the highly porous rocks due to large scale jointing and fracturing does not retain water, but rapid water seepage takes place into the subsurface during the monsoon.

Plate 8.3. Crumpled and fractured shales

Plate 8.4. Damage of road due to terrace cultivation

The abundance and action of water in soils is the major factor for initiation of landslides. However, this is frequently overlooked in soil exploration and safety calculations. Dry surfaces also are not indications of favourable groundwater conditions as groundwater evaporates rapidly during the dry season. It often takes many years until water becomes active (Bishop, 1957; Skempton, 1977; Bauer et al., 1980). Its control and removal are thus very important in the stabilization of slopes. The stabilization of active landslides by controlling drainage has been carried out with full success at numerous landslide zones (Veder and Hilbert, 1980). However size, permeability, and transmissivity of pervious zones and orientation of discontinuities will determine the effectiveness of drains.

As part of the objectives of this study, a report with recommended remedial/mitigation measures for five spots including locations 9, 10, 11, 12, and 13 was submitted to the Government of Nagaland on 26th May 2009 and the same of the debris slide along the Nagaland University road (Location 14) was submitted to the Nagaland University on 14th March 2011.

8.2 CONCLUSIONS

The present study attempts to create a landslide hazard database based on field investigations and using topographical maps and satellite data in a GIS environment. GIS is an effective tool that provides for proper planning and policy and decision-making through data integration and modeling. It is suitable to use these models in this rugged terrain which can be analyzed and viewed in 3D perspective. The LHZ map generated for this area using GIS can serve as a useful management tool. This map gives good indications of stability conditions of the area and clearly defines the various hazard zones. The high and very high hazard zones need to be avoided for any developmental projects. Risk analyses for selected locations along the highway and the NU approach road clearly bring out the weaknesses along these roads. Such areas need to be treated with utmost importance and sincerity to prevent any mishap. On this basis landslide management programmes can be planned to check for possible risk to human lives, property, and roads.

Road making techniques are very poor in the state. The debris from these slopes flowing down onto roads erodes the bitumen rapidly and proves to be a costly affair. Hence, it should be seriously considered to implement mitigation measures that have been provided. Other parts of NH 2 beyond the study area that are weak should also be considered for similar appropriate measures. Detailed geotechnical analyses for appropriate mitigation and/or remedial measures need to be taken up in areas proposed for urban expansion in the high hazard zones.

Fresh cut slopes along the roads are apparently stable at the moment. However, at a number of places they can create havoc if left unattended. Under such circumstances top soil or parts of slope should be removed to reduce the driving forces. Barren upper slopes should be afforested with suitable species. Plantation of fast growing, deep rooted trees such as eucalyptus, alder, cedar, willows like *Salix tetrasperma*, *Salix ichnostachya Lindl* and *Salix sitchensis*, and fir like *Pseudotsuga menziessii* in the lower reaches of slide zones will help control slides. Geo-grids, geo-textile, jute mats, etc. will help hold the rock fragments, debris, and loose soil. In some case benching is recommended depending upon the height and slope forming materials. Buttresses and retaining walls are necessary where slope material is weak.

Surface water is one of the major factors that cause landslides. Thus, appropriate drainage facilities should be provided where slope material is susceptible to erosion, particularly under unfavourable groundwater conditions. As far as possible, water should not be allowed to enter landslide zones, old or new. Surface drainage may be necessary around crowns of present slides to prevent sheet wash from entering landslide areas. It is also necessary to remove excess water from the subsurface so as to reduce pore-water pressure below which can cause slope failure.

The potential to susceptibility of landslides can be predicted with adequate weather forecasting and careful analyses of cumulative rainfall patterns to a reasonable degree of accuracy. The threat of an oncoming storm during the monsoon that may be disastrous in terms of landslide susceptibility should be viewed seriously; public warnings of potential danger should be immediately issued. Attempts were made to correlate landslides with rainfall but the exact temporal relation could not be derived due to paucity of landslide as well as rainfall data. Detailed geotechnical investigations of rocks and soils will be helpful in deriving a threshold rainfall value that triggers landslides in this area.

A strong database is required for the remedy of landslides which involves the determination of appropriate control and preventive measures. Detailed investigations are necessary to assess such factors as the size and shape of unstable masses, the nature and composition of rock types, detailed attitude of joint and bedding planes, and water conditions of the area. Thus, a combination of geologic, geomorphic, and hydrologic studies with soil and rock mechanics is necessary. Mitigation strategies may not be possible in every landslide prone area due to prohibitive costs, engineering and economic feasibility, and social acceptability. However innovations are possible to reduce cost.

The Disaster Management Cell of the Government of Nagaland has recently initiated landslide awareness programs and trainings. Public education and publicity campaigns are also being launched for public awareness on a large scale, for landslide risk and to promote proper understanding of the nature of risk, because public participation in disaster management programs is of utmost importance.

BIBLIOGRAPHY

Abella, E.A.C. and van Westen, C.J., 2008. Qualitative landslide susceptibility assessment by multi-criteria analysis: A case study from San Antonio del Sur, Guantánamo, Cuba. Geomorphology, vol. 94, pp. 453-466.

Acharya, G., Smedt, F., and Long, N.T., 2006. Assessing landslide hazard in GIS: a case study from Rasuwa, Nepal. Bull. Engg. Geol. Environ., vol. 65, pp. 99-107.

Acharyya, S.K., 1986. Tectonostratigraphic history of Naga Hills Ophiolite. Mem. Geol. Surv. India, vol. 199, p. 103.

Agarwal, N.K. and Shukla, R.C., 1996. Kohima urban area. Contri. Environ. Geol., Geol. Surv. India Sp. Publ., vol. 43, p. 150.

Aier, I., 2005. Landslides along the Kohima-Dimapur road: Their causes and possible remedial measures. Unpublished Ph.D. thesis, Nagaland University, Kohima.

Aier, I., Walling, T., Thong, G.T., 2005. Lalmati slide: Causes and mitigation measures. Naga. Univ. Res. Jour., vol. 3, pp. 44-47.

Aier, I. and Thong, G.T., 2006. Geological report on subsidence at the Lumami Campus, Nagaland University. Naga. Univ. Rep.

Aier, I., Supongtemjen, Khalo, M., and Thong G.T., 2009a. Geotechnical assessment of the Mehrülietsa slide (179 km) along NH 39, Kohima, Nagaland. In: Kumar, A., Kushwaha, R.A.S., Thakur, B. (Eds) Earth Sys. Sc. Concept Publishing Company, New Delhi, pp. 81-88.

Aier, I., Supongtemjen, and Thong, G.T., 2009b. Slope mass rating and kinematic analyses along part of NH 61, Nagaland, NE India. Intl. Jour. Earth Sc. Engg. vol. 2, pp. 520-526.

Aier, I., Luirei, K., Bhakuni, S.S., Thong, G.T. and Kothyari, G.C., 2011a. Geomorphic evolution of Medziphema intermontane basin and Quaternary deformation in the schuppen belt, Nagaland, NE India. Z. Geomorph., vol. 55, pp. 247-265.

Aier, I., Pradipchandra, M., Thong, G.T., Soibam, I., 2011b. Instability analyses of Merhülietsa slide, Kohima, Nagaland. Nat. Haz., vol. 60, pp. 1347-1363.

Akgun, A., Dag, S., and Bulut, F., 2008. Landslide susceptibility mapping for a landslide-prone area (Findikli, NE of Turkey) by likelihood frequency ratio and weighted linear combination models. Environ. Geol., vol. 54, pp. 1127-1143.

Aleotti, P., Chowdhury, R., 1999. Landslide hazard assessment: summary review and new perspectives. Bull. Engg. Geol. Environ., vol. 58, pp. 21-44.

Anand, R., 1988. Preliminary geological investigations of landslides along Dimapur-Mao road, Nagaland state, India. Ind. Geol. Assoc. Bull., vol. 21, pp. 199-205.

Anbalagan, R., 1992. Landslide hazard evaluation and zonation mapping in mountainous terrain. Engg. Geol., vol. 32, pp. 269-277.

Anbarasu, K., Sengupta, A., Gupta, S., and Sharma, S.P., 2010. Mechanism of activation of the Lanta Khola landslide in Sikkim Himalayas. Landslides, vol. 7, pp. 135-147.

Arunachalam, A., 1998. Shifting cultivation and soil degradation at lower altitudes of Arunachal Pradesh. Proc. Intl. Conf. Dis. Man., Guwahati, pp. 163-173.

Ayalew, L., Yamagishi, H., Marui, H., and Kanno, T., 2005. Landslides in Sado Island of Japan: Part II. GIS-based susceptibility mapping with comparisons of results from two methods and verifications. Engg. Geol., vol. 81, pp. 432-445.

Badger, C.W., Cummings, A.D., and Whitemore, R.L., 1956. The disintegration of shale. Jour. Inst. Fuel, vol. 29, pp. 417-423.

Barata, F.E., 1969. Landslides in the tropical region of Rio de Janeiro. Proc. Intl. Conf. Soil Mech. Found. Engg., Mexico, vol. 2, pp. 507-516.

Bartarya, S.K. and Valdiya, K.S., 1989. Landslides and erosion in the catchment of the Gaula River, Kumaun Lesser Himalaya, India. Mount. Res. Dev., vol. 9, pp. 405-419.

Barton, N.R. and Choubey, V., 1977. The shear strength of rock joints in theory and practice. Rock Mech., vol. 10, pp. 1-54.

Bauer, G.E., Deschamps, G.P., and Scott, J.D., 1980. The effect of shear strength and pore pressure distribution on the stability of natural slopes. Intl. Symp. Landsl., New Delhi, vol. 1, pp. 297-302.

Beven, K.J. and Kirby, M.J., 1979. A physically based variable contributing area model of basin hydrology. Hydrol. Sci. Bull., vol. 24, pp. 43-69.

Bhandari, R.K., 1984. State-of-the-art report on simple and economical instrumentation and working systems for landslides and other mass movements. Proc. 4th Intl. Symp. Landsl., Toronto, pp. 251-273.

Bhandari, R.K., 1987. Slope instability in the fragile Himalaya and the strategy for development. Ind. Geotech. Jour., vol. 17, pp. 1-77.

Bhattacharjee, C.C., 1991. The Ophiolites of northeast India: a subduction zone Ophiolite Complex of Indo-Burman Orogenic Belt. Tectonophysics, vol. 191, pp. 213-222.

Bhattacharjee, C.C., Rahman, S., Sarmah, R.N., and Thong, G.T., 1998. Landslides and road instability along NH 39, between Kohima and Chumukedima, Nagaland. Proc. Intl. Conf. Dis. Man., Guwahati, pp. 556-568.

Bieniawski, Z.T., 1979. The geomechanic classification in rock engineering application. Proc. 4th Intl. Conf. Rock Mech. ISRM Moutreuse. Balkema, Rotherdam, vol. 2, pp. 51-58.

Bieniawski, Z.T., 1989. Engineering rock mass classifications. Wiley, New York, 251p.

Bishop, A.W., 1957. Some factors controlling the pore pressure setup during construction of earth dams. Proc. 4th Intl. Conf. Soil Mech. Found. Engg., London.

Bishop, D.M. and Stevens, M.F., 1964. Landslides in logged areas in southeast Alaska. For. Ser. Res. Paper, Nor., vol. 7, p. 18.

Blanc, R.P. and Cleveland, G.B., 1968. Natural slope stability as related to geology, San Clemente area, Orange and San Diego Counties, California. Cal. Div. Mines & Geol., Spl. Rep., vol. 98, p. 19.

Blight, G., 1977. Slopes and excavations in the residual soils. Proc. 9th Intl. Conf. Soil Mech. Found. Engg., Tokyo, vol. 2.

Brabb, E.E., 1984. Innovative approaches to landslide hazard and risk mapping. Intl. Symp. Landsl., Toronto, vol. 1, pp. 307-323.

Brabb, E.E., Pameyan, E.H., and Bonilla, M.G., 1972. Landslide susceptibility in San Mateo County, California. USGS Misc. Field Studies Map, MP-360.

Brand, E.W., 1981. Some thoughts on rain induced slope failures. 10th Intl. Conf. Soil Mech. Found. Engg. Stockholm, vol. 3.

Brown, C.B. and Sheu, M.S., 1975. Effects of deforestation on slope. Jour. Geotech. Engg., vol. 101, pp. 147-165.

Brunnschweiler, R.O., 1974. Indo-Burman Ranges. In: Spencer, A.M (Ed.), Mesozoic Cenozoic orogenic belts. Geol. Soc., London, Spl. Publ., vol. 4, pp. 270-299.

Bureau of Indian Standards, 1998. Preparation of landslide hazard evaluation and zonation maps in mountainous terrain. Guidelines, Part 2, Macrozonation: ICS 07.040.54496.

Burroughs (Jr), E.R. and Thomas, B.R., 1977. Declining root strength in douglas fir after felling as a factor in slope stability. US Dept. Agri. For. Ser., Res. Paper, vol. 190, p. 27.

Caine, N., 1980. The rainfall intensity duration control of shallow landslides and debris flows. Geografiska Annaler, vol. 62A, pp. 23-27.

Caine, N. and Mool, P.K., 1982. Landslides and the Kolpu Khola drainage: Middle hills, Nepal. Mount. Res. Dev., vol. 2, pp. 157-173.

Campbell, R.H., 1975. Soil slips, debris flows, and rainstorms in the Santa Monica Mountains and vicinity, Southern California. USGS Prof. paper, 851.

Cardinali, M., Reichenbach, P., Guzzetti, F., Ardizzone, F., Antonini, G., Galli, M., Cacciano, M., Castellani, M., and Salvati, P., 2002. A geomorphological approach to the estimation of landslide hazards and risks in Umbria, Central Italy. Nat. Haz. Earth Sys. Sc., vol. 2, pp. 57-72.

Carrara, A., 1983. Multivariate models for landslide hazard evaluation. Math. Geol., vol. 15, pp. 403-427.

Carrara, A., Cardinali, M., Detti, F., Guzzetti, F., Pasqui, V., and Reichenbach, P., 1991. GIS techniques and statistical models in evaluating landslide hazard. Earth Surf. Proces. Landforms, vol. 16, pp. 427-445.

Central Road Research Institute, 1989. Report on use of coir geogrid for surface erosion control of slopes. Coir Board, GoI.

Central Road Research Institute, 2000a. Preliminary report on correction of landslide at km-174 and km-180 on NH 39 in Nagaland. Rep., pp. 1-6.

Central Road Research Institute, 2000b. Correction of landslides on NH 39 in Nagaland. Suppl. Rep.

Chatterjee, S. and Hotton, N., 1986. The palaeoposition of India. Jour. SE Asian Earth Sc., vol. 1, pp. 145-189.

Chattopadhyay, B., Venkataramana, P., Roy, D.K., Bhattacharya, S., and Ghosh, S., 1993. Geology of Naga Hills Ophiolites. Geol. Surv. India Rec., vol. 112, pp. 59-115.

Chen, H. and Lee, C.F., 2002. A dynamic model for rainfall-induced landslides on natural slopes. Geomorphology, vol. 51, pp. 269-288.

Cheng, K.S., Wei, C., and Chang, S.C., 2003. Locating landslides using multi-temporal satellite images. Advances in Space Research. COSPAR. Elsevier Ltd.

Chi, K.H., Lee, K., and Park, N., 2002. Landslide stability analysis and prediction modeling with landslide occurrences on KOMPSAT EOC imagery. Kor. Jour. Rem. Sen., vol. 18, pp. 1-12.

Choubey, V.D. and Lallenmawia, H., 1987. Landslides and other mass movements in Aizawl, NE India, Mizoram State. 5th Intl. Conf., New Zealand, pp. 113-120.

Choubey, V.D. and Lallenmawia, H., 1989. The structural evolution of northeastern Himalayan zone with special reference to Mizoram region. Current Trends in Geology - XI. Himalayan mountain building. Today & Tomorrow Publishers, N. Delhi, pp. 147-162.

Choubey, V.D. and Litoria, P.K., 1990. Terrain classification and Land hazard mapping in Kalsi-Chakrata area, Garhwal Himalaya, India. ITC Jour., pp. 58-66.

Chung, C.F., Fabbri, A.G., and van Westen, C.J., 1995. Multivariate regression analysis for landslide hazard zonation. In: Carrara, A. and Guzzetti, F. (Eds), Geographical information systems in assessing natural hazards. Kluwer Academic Publishers, Dordrecht, The Netherlands, pp. 107-134.

Comegna, L., Picarelli, L., and Urciuoli, G., 2007. The mechanics of mudslide as a cyclic undrained-drained process. Landslides, vol. 4, pp. 217-232.

Conklin, H.C., 1957. Hunwnoo agriculture in the Philippines. FAO, Rome.

Corominas, J., 2001. Landslides and climate. In: Bromhead, E.N. (Ed), Keynote lectures, 8th Intl. Symp. Landsl., Cardiff.

Corominas, J., Moya, J., and Hürlimann, M.M., 2003. Landslide rainfall triggers in the Spanish eastern Pyrenees. Mediterranean storms, Universitat de les Illes Balears, Spain.

Crosta, G.B., Dal Negro, P., and Frattini, P., 2003. Soil slips and debris flows on terraced slopes. Nat. Haz. Earth Sys. Sc., vol. 3, pp. 31-42.

Crozier, M.J., 1986. Landslide: Causes, environments, and consequences. Croon Helm, London, 252p.

Crozier, M.J., 1989. Landslide hazard in the Pacific islands. In: Brabb, E.E. and Harrod (Eds), Landslides: Extent and economic significance. Balkema, Rotterdam, pp. 357-366.

Crozier, M.J., 1996. The climate-landslide couple: A southern hemisphere perspective. Paleoclim. Res., vol. 19, pp. 329-350.

Crozier, M.J., 1999. Prediction of rainfall-triggered landslides: A test of the antecedent water status model. Earth Surf. Proces. Landforms, vol. 24, pp. 825-833.

Crozier, M.J. and Vaughan, E.E., 1990. Relative instability of colluvium-filled bedrock depressions. Ear. Surf. Proces. Landforms, vol. 15, pp. 329-339.

Cruden, D.M., 1978. Discussion of G. Hocking's paper: A method for distinguishing between single and double plane sliding of tetrahedral wedges. Intl. Jour. Rock Mech. Min. Sci. Geomech. Abstr., vol. 15, pp. 217.

Cruden, D.M. and Varnes, D.J., 1996. Slope movement types and processes. In: Landslides - investigation and mitigation. Spl. Rep. Natl. Acad., Press, Washington, vol. 247, pp. 36-75.

Dadson, S.J., Hovius, N., Chen, H., Dade, B., Lin, J.C., Hsu, M.L., Lin, C.W., Horng, M.J., Chen, T.C., Milliman, J., and Stark, C.P., 2004. Earthquake triggered increase in sediment delivery from an active mountain belt. Geology, vol. 32, pp. 733-736.

Dahal, R.K., Shuichi Hasegawa, S., Minoru Yamanaka, M., Dhakal, S., Bhandary, N.P., and Yatabe, R., 2008. Comparative analysis of contributing parameters for rainfall-triggered landslides in the Lesser Himalaya of Nepal. Environ. Geol., Springer-Verlag.

Dai, F.C., Lee, C.F., and Ngai, Y.Y., 2002. Landslide risk assessment and management: an overview. Engg. Geol., vol. 64, p. 65.

Deere, D.U., Hendron, A.J., Patton, F.D., and Cording, E.J. 1967. Design of surface and near surface construction in rock. In: Fairhurst, C. (Ed.), Failure and breakage of rock. Proc. 8th US Symp. Rock Mech. New York. Soc. Min. Engg, Am. Inst. Min. Metall. Petrol. Engg. pp. 237-302.

Department of Science and Technology, 1994. Methodology for landslide hazard zonation.

DeRose, R.C., 1996. Relationships between slope morphology, regolith depth, and the incidence of shallow landslides in eastern Taranaki hill country, Z. Geomorph., vol, 105, pp. 46-60.

Deva, Y. and Srivastava, M., 2006. Grid-based analytical approach to macro landslide hazard zonation mapping. Jour. Engg. Geol., vol. 33, pp. 60-72.

Dhakal, A.S., Amada, T., and Aniya, M., 2000. Landslide hazard mapping and its evaluation using GIS: An investigation of sampling schemes for a grid-cell based quantitative method. Photogram. Engg. Rem. Sen., vol. 66, pp. 981-989.

Directorate of Geology & Mining, Nagaland, 1978. Misc. Pub. No. 1.

Directorate of Geology & Mining, Nagaland, 1990. A note on the landslide in Alempang ward, Mokokchung town, Nagaland. Geol. Rep.

Directorate of Geology & Mining, Nagaland, 1996. Feasibility studies for groundwater development in the hilly terrain in and around Kohima town, Nagaland. Tech. Rep.

Directorate of Geology & Mining, Nagaland, 2001. Report on geohydrological, geotechnical and geoenvironmental study of Mokokchung town, Mokokchung district, Nagaland. Geol. Rep.

Directorate of Geology & Mining, Nagaland, 2005. A note on the occurrences of landslides at Mokokchung township, Nagaland on 26.05.2005. Geol. Rep.

Directorate of Soil & Water Conservation, 2010. Meteorological Data. Govt. of Nagaland.

Donati, L. and Turrini, M.C., 2002. An objective method to rank the importance of the factors predisposing to landslides with the GIS methodology: Application to an area of the Apennines (Valnerina, Perugia, Italy). Engg. Geol., vol. 63, pp. 277-289.

Dortch, J.M., Own, L.A., Haneberg, W.C., Caffee, M.W., Dietsch, C., and Kamp, U., 2008. Nature and timing of large landslides in the Himalaya and Trans-Himalaya of northern India. Quat. Sc. Rev., doi:10.1016/j.quascirev.2008.05.002.

Endo, T., 1970. Probable distribution of amount of rainfall causing landslides. Ann. Rep. Hokkaido Br. Govt. For. Exptl. Stn., Sapporo, pp. 123-136.

Emelyanova, E.P., 1977. The influence of geological and climatic conditions on the distribution of landslides on Russian Platform. Bull. IAGE., vol. 16, pp. 6-27.

Emmanuel, G.J., Douglas, B.W., Jaakko, P.K., Beth, P.A., and Tank O., 2004. Rainfall thresholds for landsliding in the Himalayas of Nepal. Geomorphology, vol. 63, pp. 131-143.

Evans, P., 1932. Tertiary succession in Assam. Trans. Min. Geol. Inst. Ind., vol. 27, pp. 155-260.

Evans, P., 1964. The tectonic framework of Assam. Jour. Geol. Soc. Ind., vol. 5, pp. 80-96.

Frochlich, W., Starkel, L., and Kasza, I., 1992. Ambootia landslide valley in the Darjeeling hills, Sikkim Himalaya, active since 1968. Jour. Him. Geol., vol. 3, pp. 79-90.

Fugita, T., 1980. Slope analysis of landslides in Sikoku, Japan. Proc. 3rd Intl. Symp. Landsl., New Delhi, vol. 1, pp. 169-174.

Fugita, T., 1994. Characteristics of landslides in southwest Japan based on slope analysis. 7th Intl. IAEG Cong., Lisbon, Portugal, vol. 3, pp. 1415-1424.

Fugita, T., Hirano, M., and Hada, S., 1976. The structural control of landslides in the Kawai area, Tokushima Prefecture, Shekoku, Jisuberi. Jour. Jap. Landsl. Sc., vol. 13, pp. 25-36.

Gahgah, M.M., Akhir, M.J., Rafek, M.A.G., and Abdullah, I., 2009. GIS based assessment on landslide hazard zonation: Case study of Cameron highlands - Gua Musang road Kelantan, Malaysia. Sains Malaysiana, vol. 38, pp. 827-833.

Galster, R.W. and Laprade W.T., 1991. Geology of Seattle, Washington, USA. Bull. Assoc. Engg. Geol., vol. 28, pp. 235-302.

Ghose, N.C., Agrawal, O.P., and Chatterjee, N., 2010. Geological and mineralogical study of eclogite and glaucophane schists in the Naga Hills Ophiolite, Northeast India. Island Arc, vol. 19, pp. 336-356.

Gordon, R.G., DeMets, C., and Argus, D.F., 1990. Kinematic constraints on distributed lithospheric deformation in the equatorial Indian Ocean from present motion between the Australian and Indian plates. Tectonics, vol. 9, pp. 409-422.

Goswami, D.N.D., 1960. Geology of Assam. Dept. Publ., University of Gauhati.

Gray, D.H., 1973. Effects of forest clear-cutting on the stability of natural slopes: Results of field studies. Natl. Sc. Found., Washington, p. 119.

Greenway, D.R., 1987. Vegetation and slope stability. In: Anderson, M.G., Richards, K.S. (Eds.), Slope Stability. Wiley, Chichester, UK, pp. 187-230.

Gudehus, G., Kolymbas, D., and Leninenkugel, H.J., 1976. Zeitverhaltan von Böschungen and Einchnitten. In: Weichem and Steifem (Eds). Proc. 6th Eur. Conf. Soil Mech. Found. Engg., Vienna, vol. 1, pp. 1-51.

Guidicini, G. and Iwasa, D.Y., 1977. Tentative correlation between rainfall and landslides in Mattumid tropical enviroment. Proc. IAEC Symp. Landsl. Mass Move., Prague, pp. 13-18.

Gupta, R.P. and Joshi, B.C., 1990. Landslide hazard zoning using the GIS approach - a case study from the Ramaganga Catchment, Himalayas. Engg. Geol., vol. 28, pp. 119-131.

Gupta, R.P., Saha, A.K., Arora, M.K., and Kumar, A., 1999. Landslide hazard zonation in a part of the Bhagirathi valley, Garhwal Himalayas using integrated remote sensing-GIS. Him. Geol., vol. 20, pp. 71-85.

Gupta, V., Sah, M.P., Virdi, N.S., and Bartarya, S.K., 1993. Landslide hazard zonation in the Upper Sutlej Valley, District Kinnaur, Himachal Pradesh. Jour. Him. Geol., vol. 4, pp. 81-93.

Gurung, N., Haneberg, W.C., Ramana, G.V., and Datta, M., 2011. Engineering geology and stability of the Laprak landslide, Gorkha District, Western Nepal. Envi. Engg. Geosc., vol. 17, pp.23-38.

Guzzetti, F., Peruccacci, S., Rossi, M., and Stark, C.P., 2007. Rainfall threshold for the initiation of landslides. Meteor. Atmos. Phy., doi:10.1007/s00703-007-0262-7.

Havenith, H.B. and Bourdeau, C., 2010. Earthquake-induced landslide hazards in mountain regions: A review of case histories from central Asia. Geologica Belgica, vol. 13, pp. 137-152.

Hiese, N., 2005. Application of remote sensing and GIS on landslide investigation in the Kohima area of Nagaland. Unpublished PhD thesis, Jawaharlal Nehru Technological University, Hyderabad.

Hocking, G., 1976. A method for distinguishing between single and double plane sliding of tetrahedral wedges. Intl. Jour. Rock Mech. Min. Sci. Geomech. Abstr., vol. 13, pp. 225-226.

Hoek, E. and Bray, J.W., 1981. Rock slope engineering. Inst. Min. Metal., London.

Ibsen, M.L. and Casagli, N., 2004. Rainfall patterns and related landslide incidence in the Porretta-Vergato region, Italy. Landslides, vol. 2, pp. 143-150.

Iverson, R. M., 2000. Landslide triggering by rain infiltration. Water Resour. Res., vol. 36, pp. 1897-1910.

Jade, S. and Sarkar, S., 1993. Statistical model for slope instability classifications. Engg. Geol., vol. 36, pp. 71-98.

Jakob, M., 2000. The impact of logging on landslide activity at Clayoquot Sound, British Columbia. Catena, vol. 38, pp. 279-300.

Jelínek, R. and Wagner, P., 2007. Landslide hazard zonation by deterministic analysis (Veľká Čausa landslide area, Slovakia). Landslides, vol. 4, pp. 339-350

Juang, C.H., Lee, D.H., and Sheu, C., 1992. Mapping slope failure potential using fuzzy sets. Geotech. Engg., vol. 118, pp. 475-494.

Jworchan, I. and Nutalaya, P., 1994. Characteristics of landslides in residual soil in Khao Luang Mountain Range in southern Thailand. Proc. Intl. Conf. Landsl., slope stability and the safety of infrastructure, Malaysia.

Kandpal, G.C. and Pant, G., 1995. Geological evaluation of instability along Balia Nala, Dist. UP. Symp. Rec. Adv. Geol. Studies, NE Himalayas, Lucknow, pp. 21-23.

Kanungo, D.P., Arora, M.K., Sarkar, S., and Gupta, R.P., 2006. A comparative study of conventional ANN black box, fuzzy, and combined neural and fuzzy weighting procedure for landslide susceptibility zonation in Darjeeling Himalayas. Engg. Geol., vol. 85, pp. 347-366.

Kawakami. H. and Saito. Y., 1984. Landslide risk mapping by quantification method. Proc. Intl. Symp. Landsl., Toronto, pp. 535-540.

Keefer, D.K., 1984. Landslides caused by earthquakes. Geol. Soc. Am. Bull., vol. 95, pp. 406-421.

Keefer, D.K., 1999. Earthquake-induced landslides and their effects on alluvial fans. Jour. Sed. Res., vol. 69, pp. 84-104.

Kemas, K., Thong, G.T., and Walling, T., 2004. Chokidzü debris slide - A case study. Naga. Univ. Res. Jour., vol. 2, pp. 89-94.

Kingsbury, P.A., Hastie, W.J., and Harrington, A.J., 1992. Regional landslip hazard assessment using GIS. Proc. 6th Intl. Symp. Landsl., Christchurch, New Zealand. A.A. Balkema, Rotterdam, The Netherlands, vol. 2, pp. 995-1000.

Kliche, C.A., 1999. Rock slope stability. SME, Littleton CO.

Koirala, N. and Watkins, A.T., 1988. Bulk appraisal of slopes in Hong Kong. Intl. Symp. Landsl., Lausanne.

Kumar, B., Virdi, N.S., Sahe, M.P., Bartarya, S.K., and Gupta, V., 1995. Landslide hazard zonation between Rampur and Wangtu, H.P. Symp. Rec. Adv. Geol. Studies on NE Himalayas, Lucknow, pp. 324-326.

Larsen, M.C., 2008. Rainfall-triggered landslides, anthropogenic hazards, and mitigation strategies. USGS, 436 National Center, Reston, VA 20192, USA. Adv. Geosci, vol. 14, pp. 147-153.

Lopez-Tello, L.F., 1977. Stabilising effects of plants on slopes. Rev. Obras. Publicas, Madrid, pp. 659-668.

Lotha, K.A., 1994. A note on the geotechnical investigation on landslide at Cheipfütsiepfe, Lower AG colony, Kohima Town, Nagaland. Unpubl. Rep. Geotech. Geoenvir. Cell, DGM, Nagaland.

Mallet, F.R., 1876. On the coalfields of Naga Hills bordering Lakhimpur and Sibsagar Districts, Assam. Geol. Surv. India Mem., vol. 12, pt.2.

Malamud, B.D., Turcotte, D.L., Guzzetti, F., Reichenbach, P., 2004. Landslides, earthquakes, and erosion. Earth Planet. Sc. Let., vol. 229. pp. 45-59.

Mantovani, F., Soeters, R., and van Westen, C.J., 1996. Remote sensing techniques for landslide studies and hazard zonation in Europe. In: Harvey A.M. and Vitek J.D. (Eds), Geomorphology, vol. 15, pp. 213-225.

Markland, J.T., 1972. A useful technique for estimating the stability of rock slopes when the rigid wedge sliding type of failure is expected. Imp. Col. Rock Mech. Res. Rep., vol. 19, p. 10.

Mathewson, C.C. and Clary, J.H., 1997. Engineering geology of multiple landsliding along 1-45 road-cut near Centerville, Texas. In: Coates, D.R. (Ed), Landslides. Geology, vol. 3, pp. 213-223.

Mathur, L.P. and Evans, P., 1964. Oil in India. 22nd Intl. Geol. Cong., N. Delhi.

McElhinny, M.W., 1973. Paleomagnetism and plate tectonics. Cambridge University Press, Cambridge.

McKenzie, D.P. and Sclater, J.G., 1971. The evolution of the Indian Ocean since the Late Cretaceous. Geophys. Jour. Roy. Astron. Soc., vol. 25, pp. 437- 528.

Mehrotra, G.S., Sarkar, S., and Dharamraju, R., 1992. Landslide hazard assessment in Rishikesh-Tehri area, Garhwal Himalaya, India. Proc. 6th Intl. Symp. Landsl., New Zealand.

Mehrotra, G.S., Sarkar, S., and Kanungo, D.P., 1993. Lithotectonic evaluation of landslide and mass movements in Garhwal, Kumaon Himalaya. Jour. Engg. Geol., vol. 22, pp. 19-33.

Mehrotra, G.S., Sarkar, S., Kanungo, D.P., and Mahadevaiah, K., 1996. Terrain analysis and spatial assessment of landslide hazards in parts of Sikkim Himalaya. Jour. Geol. Soc. India, vol. 47, pp. 491-498.

Moghaddas, N.H. and Ghafoori, M., 2007. Investigation of the distributions and causes of landslides in Central Alborz, Iran. World App. Sc. Jour., vol. 2, pp. 652-657.

Montgomery, D.R. and Dietrich, W.E., 1994. A physically based model for the topographic control on shallow landsliding. Water Resour. Res., doi:10.1029/93WR02979.

Muller, L., 1964. The stability of rock bank slopes and the effect of rock water on same. Intl. Jour. Rock Mech. Min. Sc., vol. 1, pp. 475-504.

Nagarajan, R., Mukherjee, A., Roy, A., and Khire, M.V., 1998. Temporal remote sensing data and GIS application in landslide hazard zonation of part of Western Ghat, India. Rem. Sen., vol. 19, pp. 573-585.

Nakamura, H. and Lang, Y.H., 2001. Prediction of hazard area of landslide induced by earthquake. Proc. Intl. Conf. Nat. Haz. Miti. Manage., Amritsar, India, p. 25.

Nandy, D.R., 1976. The Assam syntaxis of the Himalaya: A re-evaluation. Sem. Rec. Geol. Study, Him. Misc. Pub., Geol. Surv. India, vol. 24, pp. 363-368.

Nath, S.K., Singh, K.K., Thingbaijam, and Raj, A., 2008. Earthquake hazard in Northeast India - A seismic microzonation approach with typical case studies from Sikkim Himalaya and Guwahati city. Jour. Earth Syst. Sci. vol. 117, pp. 809-831.

National Disaster Management Guidelines, 2009. Management of landslides and snow avalanches. NDMA Publ., GoI, New Delhi.

Nilsen, T.H. and Brabb, E.E., 1972. Preliminary photo-interpretation and damage maps of landslide and other surficial deposits in northeastern San Jose, Santa Clara County, California. USGS Misc. Field studies Map, MF-361.

Nilsen, T.H., Taylor, F.A., and Brabb, E.E., 1976. Recent landslides in Alameda County, California. USGS Bull., No. 1398, pp. 1-21.

Nilsen, T.H. and Turner, B.L., 1975. Influence of rainfall and ancient landslide deposits on recent landslides (1950-1971) in urban areas of Contra Costa County, California. USGS Bull., No. 1388, pp. 1-18.

Nilsen, T.H., Wright, R.H., Vlasic, T.C., and Spangle, W., 1979. Relative slope stability and landuse planning in the San Francisco Bay region, California. USGS Prof. Paper, vol. 944, p. 96.

Ohlmacher, G.C. and Davis, C. J., 2003. Using multiple logistic regression and GIS technology to predict landslide hazard in northeast Kansas, USA. Engg. Geol., vol. 69, pp. 331-343.

Oldham, R.D., 1883. Report on the geology of parts of Manipur and Naga Hills. Geol. Surv. India Mem., vol. 14, pt. 4.

O'Loughlin, C.L., 1974. A study of tree root strength deterioration following clear felling. Can. Jour. For. Res., vol. 4, pp. 107-113.

Pachauri, A.K., 2007. Facet based landslide hazard zonation maps for the Himalayas: Example from Chamoli Region. Jour. Geol. Soc. Ind., vol. 69, pp. 1231-1240.

Pachauri, A.K., Bhushan, B., and Singh, A.P., 2006. Potential elevation-controlled rock-fall velocity zoning in a part of Garhwal Himalayas and risk perception. Curr. Sc., vol. 90, pp. 1370-1377.

Pachauri, A.K. and Pant, M., 1992. Landslide hazard mapping based on geological attributes. Engg. Geol., vol. 32, pp. 81-100.

Palmström, A. 1982. The volumetric joint count - a useful and simple measure of the degree of rock jointing. Proc. 4th Conf. Intl. Assoc. Engg. Geol., Delhi, vol. 5, pp. 221-228.

Papathanassiou, G., Pavlides, S., and Ganas, A., 2005. The 2003 Lef kada earthquake: Field observations and preliminary microzonation map based on liquefaction potential index for the town of Lef kada. Engg. Geol, vol. 82, pp. 12-31.

Parise, M., 2002. Landslide hazard zonation of slopes susceptible to rock falls and topples. National Research Council - CERIST, Bari, Italy. Jour. Nat. Haz. Earth Sys. Sc., vol. 2, pp. 37-49.

Pascoe, E.H., 1912. Traverse across Naga Hills of Assam from Dimapur to neighbourhood of Saramati Peak. Geol. Surv. India Rec., vol. 13, pt. 4.

Petley, D.N. and Reid, S., 1999. Landscape sensitivity and change at Taroko, eastern Taiwan. In: Smith, B.J., Whalley, W.B., and Warke, P.A. (Eds), Spl. Publ., Geol. Soc. Lond., vol. 162, pp. 179-195.

Petley, D., Dunning, S., Rosser, N., and Kausar, A.B., 2006. Incipient landslides in the Jhelum Valley, Pakistan following the 8th October 2005 earthquake. Disaster mitigation of debris flows, slope failures, and landslides. Universal Academy Press Inc. Tokyo, Japan, pp. 47-55.

Pichler, E., 1957. Aspectos geologicos dos escorregamentos de Santos (Portuguese). Bull. Sociedade Brasilerado Geologia, vol. 6, pp. 69-79.

Pillai, R. Vineetha., Thong, G.T., and Aier, I., (2008) Identification, distribution and significance of clay minerals in the Disang shale of Kohima, Nagaland. Naga. Univ. Res. Jour., Spl. Publ.

Piteau, D.R. and Peckover, F.L., 1989. Engineering of rock slopes. In: Goodman, R.E. (Ed), Introduction to rock mechanics (2nd ed). John Wiley & Sons, 576p.

Radbruch, D.H., Colton, R.B., Davis, W.E., Skipp, B.A., Lucchitta, I., and Varnes, D.J., 1976. Preliminary landslide overview map of the conterminous United States. USGS Misc. Field Studies Map, MP 771.

Radbruch, D.H. and Crowther, K.C., 1973. Map showing areas of estimated relative amounts of landslides in California. USGS Misc. Inv. Map, pp. 1-747.

Raj, T.N., Mohan, V.R., Backiaraj, S., and Muthusamy, S., 2011. Landslide hazard zonation using the relative effect method in south eastern part of Nilgiris, Tamilnadu, India. Intl. Jour. of Engg. Sci. Tech., vol. 3, pp. 3260-3266.

Ramasamy, S.M. and Muthukumar, M., 2008. Geospatial modeling of geosystems and landslides mapping and mitigation, the Nilgiri Mountains, South India. Ind. Landsl., vol. 1, pp. 45-54.

Reichenbach, P., Cardinali, M., De-Vita, P. and Guzzetti, F., 1998. Regional hydrological threshold for landslides and floods in the Tiber River Basin, Central Italy. Env. Geol., vol. 3, pp. 146-159.

Reneau, S.L., Dietrich, W.E., Dorn, R.I., Berger, C.R., and Rubin, M., 1986. Geomorphic and paleoclimatic implications of latest Pleistocene radiocarbon dates from colluvium-mantled hollows, California. Geology, vol. 14, pp. 655-658.

Rodríguez, C.E., Bomer, J.J., and Chandler, R.J., 1999. Earthquake-induced landslides: 1980-1997. Soil Dynam. Eqk. Engg., vol. 18, pp. 325-346.

Rodriguez, O.J.M., Hinojosa, J.A., and Prieto, C., 1978. Regional studies on mass movements in Spain. Intl. Assoc. Engg. Geol., 3rd Intl. Cong., vol. 1, pp. 267-277.

Roering, J.J., Almond, P., Tonkin, P., and McKean, J., 2004. Constraining climatic controls on hillslope dynamics using a coupled model for the transport of soil and tracers: Application to loess-mantled hillslopes, Charwell River, South Island, New Zealand. Jour. Geophy. Res., doi:10.1029/2003JF000034.

Romana, M., 1985. New adjustment ratings for applications of Bieniawski classification of slopes. Intl. Symp. Rock Mech., Zacatecas, pp. 49-53.

Roy, R.K. and Kacker, R.N., 1986. Cenozoic deformation pattern and mechanism in the Belt of Schuppen and their role in hydrocarbon accumulation: Further exploratory concepts for Assam-Arakan Basin. In: Ghose, N.C. and Varadarajan, S. (Eds.). Ophiolites and Indian Plate Margin. Sumna Publishers, Patna, pp.197-221.

Saha, A.K., Gupta, R.P., and Arora, M.K., 2002. GIS-based landslide hazard zonation in the Bhagirathi (Ganga) Valley, Himalayas. Intl. Jour. Rem. Sens., vol. 23, pp. 357-369.

Sahai, B., 1993. Application of remote sensing for environmental management in India. Spa. Envi. Rep. Sp. Plen. Sess., Intl. Astro. Fed., 44th Congress, Garz, Australia.

Sarkar, S., Kanungo, D.P., and Mehrotra, G.S., 1995. Landslide hazard zonation: A case study in Garhwal Himalaya, India. Mount. Res. Dev., vol. 15, pp. 301-309.

Sarmah, R.N., 1989. Clay minerals in Disang-Barail groups of sediments from Kohima, Nagaland. Bull. Ind. Geol. Assoc., vol. 22, pp. 107-111.

Sartori, M., Baillifard, F., Jaboyedoff, M., and Rouiller, J.D., 2003. Kinematics of the 1991 Randa rockslides (Valais, Switzerland). Nat. Haz. Earth Sys. Sc., vol. 3, pp. 423-433.

Sassa, K., 1996. Prediction of earthquake induced landslides. In: Senneset (Ed.), Proceedings on Landslides, pp. 115-131.

Sato, H.P., Hasegawa, H., Fujiwara, S., Tobita, M., Korai, M., Une, H., and Iwahashi, J., 2007. Interpretation of landslide distribution triggered by the 2005 northern Pakistan earthquake using SPOT-5 imagery. Landslides, vol. 4, pp. 113-122.

Schuster, R.L., 1997. Landslides: Effects on the natural environment. Proc. Symp. Engg. Geol. Env. Intl. Assoc. Engg. Geol., Athens, vol. 5.

Schuster, R.L. and Highland, L.M., 2001. Impact of landslides and innovative landslide mitigation measures on the natural environment. USGS Open File Rep. 01-0276, pp. 29-36.

Sengupta, A, Gupta, S, and Anbarasu, K., 2009. Rainfall thresholds for the initiation of landslide at Lanta Khola in north Sikkim, India. Nat. Haz., vol. 52, pp. 31-42.

Serafim, J.L., 1968. Influence of interstitial water on the behaviour of rock masses. In: Zienckiewicz, O.C. and Staag, K.G. (Eds), Rock mechanics in engineering practices. Wiley, New York, pp. 55-97.

Seshagiri, D.N. and Badrinarayan, S., 1982. The Nilgiri landslides. Geol. Surv. India, Misc. Publ. No. 57.

Shah, A.N. and Jadhav, P.C., 1987. Control of slope stability in the Bhinj Rao basin area, Pauri Garhwal Himalaya (UP). Jour. Engg. Geol., vol. 16, pp. 13-22.

Sharda, Y.P. and Bhambay, G.C., 1980. Kohima Town, Nagaland: A decade of environmental geoscientific studies. Geol. Surv. India, Spl. Publ., No. 9.

Sharma, V.K., Sharma, A., and Attre, J.K., 1996. Slope mass rating (SMR) technique in landslide susceptibility evaluation in parts of Nainital area, Kumaon Himalaya. Jour. Engg. Geol., vol. 25, pp. 289-295.

Shimokawa, E., 1984. A natural recovery process of vegetation on landslide scars and landslide periodicity in forested drainage basins. Proc. Symp. Effects of Forest Land Use on Erosion and Slope Stability, East-West Ctr., Honolulu, Hawaii, USA, pp. 99-107.

Sinha, N.K., Chatterjee, B.P., and Satsangi, P.P., 1982. Status of paleontological researches in North Eastern region. Geol. Surv. India Record, No. 112.

Skempton, A.W., 1977. Slope stability cuttings in Brown London Clay. Proc. 9th Intl. Conf. Soil Mech. Found. Engg., Tokyo, vol. 3, pp. 261-270.

Soibam, I., 1998. Structural and tectonic analysis of Manipur with special reference to evolution of the Imphal valley. Unpublished PhD thesis, Manipur University, Imphal, pp. 283.

Soeters, R. and van Westen, C.J., 1996. Slope Instability - recognition, analysis, and zonation. In: Turner, A.K. and Schuster, R.L. (Eds), Landslides - Investigation and mitigation. Transp. Res. Board, Nat. Res. Council, Spl. Rep., vol. 247, pp. 129-177.

Soeters, R., Rengers, N., and van Westen, C.J., 1991. Remote sensing and geographical information systems as applied to mountain hazard analysis and environmental monitoring. Proc 8th Thematic Conf. Geol. Rem. Sen., Denver, USA, vol. 2, pp. 1389-1402.

Sondhi, V.P., 1941. A note on landslips on the Dimapur-Manipur road, Assam. Geol. Surv. India, Unpubl. Rep., Strategic Br.

Sothu, H.N., 2008. Geological investigation of instability along NH 150, between Kohima and Chakabama, Kohima District, Nagaland. Unpublished PhD thesis, Nagaland University, Kohima.

Sridevi, J. and Sarkar, S., 1993. Statistical models for slope instability classification. Engg. Geol., vol. 36, pp. 91-98.

Starkel, L., 1972. The role of catastrophic rainfall in the shaping of the relief of the lower Himalaya (Darjeeling Hills). Geog. Polonica, vol. 21, pp. 103-160.

Swanston, D.N., 1974. Slope stability problems associated with timber harvesting in mountainous regions of the western US. US For. Ser. Gen. Tech. Rep., PNW-21, p. 14.

Swanston, D.N. and Dyrness, C.T., 1973. Stability of steep land. Jour. For., vol. 71, pp. 264-269.

Swanston, D.N. and Dyrness, C.T., 1975. Impact of clear cutting and road construction on soil erosion by landslides in the Western Cascade Range, Oregon. Geology, vol. 3, pp. 393-396.

Swanston, D.N. and Swanson, F.J., 1977. Timber harvesting, mass erosion and steep land forest geomorphology in the Pacific northwest. In: Coates, D.R. (Ed), Geomorphology and engineering. Hutchinson & Ross, Stroudsburg, pp. 199-221.

Takei, A., 1982. Limitation methods of hazard zones in Japan, Kyoto University. Lab. Erosion Contl., Res. Bull., vol. 1, pp. 7-25.

Ter-Stepanian, G., 1974. Depth creep of slopes. Bull. Intl. Soc. Engg. Geol., vol. 9, pp. 97-102.

Terzaghi, K., 1950. Mechanism of landslides. In: Paige, S. (Ed), Application of geology to engineering practice. Geol. Soc. Am. Mem., pp. 83-123.

Terzaghi, K., 1962. Stability of steep slopes in hard unweathered rock. Geotechniques, vol. 12, pp. 251-270.

Thapliyal, B.K., 1998. Disaster management - Preparedness planning. Proc. Intl. Conf. Dis. Man., Guwahati, pp. 55-65.

Thigale, S.S., Khandge, A., Thigale, M., Bhokare, M., and Sawarkar, A., 1998. Causative factors of landslides as applicable to GIS: A case study of western mountain chain of Maharastra, India. Proc. Intl. Symp. Rem. Sen. GIS to Dis. Red., Tsukuba, Japan. Geol. Surv. Japan, pp. 197-213.

Thigale, S.S., 1999. Recommendation on landslide and water scarcity problems of Nagaland with special reference to Kohima. Report.

Thong, G.T. Aier, I., and Walling, T., 2004. Preliminary geological report of Mao slide. BRO Report.

Thong, G.T., Thingo, V., and Walling, T., 2006a. Geotechnical investigations of land instability in Kohima town and along NH 39, between Chumukedima and Kohima. Space Applications Centre (ISRO), Ahmedabad, Project No. 10/4/415, 2002.

Thong, G.T., Deka, G., Thingo, V., and Aier, I., 2006b. Geotechnical investigations of land instability along NH 39, between Kohima and Senapati. DST, New Delhi Project No.DST/Seismo/Jai Vigyan/Landslide/03/2002.

Thong, G.T., Aier, I., and Supongtemjen, 2007. Preliminary geological report on the 179 km slide. BRO Report.

Tiziano, C., 2003. Landslide hazard evaluation: The landslide hazard curves. Jour. Geotech. Geoenviron. Engg., vol. 129, p. 520.

Towhata, I., 2007. New strategy and tools for mitigation of landslide disasters. In: Ayothiraman, R. and Hazarika, H. (Eds), Earthquake hazards and mitigation. Proc. Intl. Workshop Eqk. Haz. Mit., Guwahati, pp. 116-124. I.K. International Publishing House, New Delhi.

Tsai, T.L. and Wang, J.K., 2010. Examination of influences of rainfall patterns on shallow landslides due to dissipation of matric suction. Environ. Earth Sc., Springer-Verlag.

Valdiya, K.S., 1987. Environmental geology: Indian context. Tata-McGraw Hill, New Delhi, 583p.

van Westen, C.J., 1993. Remote sensing and geographic information system for geological hazard mitigation. ITC Publication, No. 15, Enschede, pp. 393-399.

van Westen, C.J., 1994. GIS in landslide hazard zonation: A review, with examples from the Andes of Colombia. In: Price, M.F. and Heywood, D.I. (Eds), Mountain environments and geographical information systems. Taylor & Francis Publishers, London, pp. 135-165.

van Westen, C.J., Rengers, N., and Soeters, R., 2003. Use of geomorphological information in indirect landslide susceptibility assessment. Nat. Haz., vol. 30, pp. 399-419.

Vargas, M., 1971. Effects of rainfall and groundwater levels. Proc. 4th Pan Amer. Conf. SMFE, New York, pp. 135-141.

Varnes, D.J., 1978. Slope movement types and processes, landslides analysis, and control. Spl. Rep., 176. Transportation Research Board, Washington, DC, pp 11-80.

Varnes, D.J., 1980. Landslide hazard zonation. Review of principles and practices. Bull. IAEG.

Varnes, D.J., 1984. Landslide hazard zonation: A review of principles and practice. Nat. Haz., UNESCO, vol. 3, p. 63.

Varshney, R.S., Prakash, S., and Sharma, P.C., 1987. Rock slides in Alakhnanda valley. Jour. Engg. Geol., vol. 16, pp. 1-12.

Veder, C. and Hilbert, F., 1980. Landslides and their stabilization. ISBN, USA.

Verma, R.K., 1985. Gravity field, seimicity, and tectonics of the Indian Peninsula and the Himalaya. Allied Publishers, New Delhi, pp. 155-189.

Wagner, A., Leite, E., and Olivier, R., 1988. Rock and debris slides mapping in Nepal. A user friendly PC system for risk mapping. Proc. 5th Intl. Symp. Landsl., Lausanne, vol. 2, pp. 1251-1258.

Wagner, A., Raymond, O., and Leite, E., 1987. Rock and debris slide risk maps applied to low volume roads in Nepal. Transportation Res. Board, 4th Intl. Conf., Low-volume Roads, Ithaca, USA, pp. 255-267.

Walling, T., 2005. Geological investigation of land instability in Kohima Town, Nagaland. Unpublished PhD thesis, Nagaland University, Kohima.

Walling, T., Lotha, K.A., Thong, G.T., and Aier, I., 2005. Chiepfütsiepfe slide, Kohima, Nagaland - Causes and mitigation measures. Proc. NRDMS (DST) Sem. Landsl. Haz. Miti., NE Ind., pp. 48-54.

Wen, B., Wang, S., Wang, E., and Zhang, J., 2004. Characteristics of rapid giant landslides in China. Landslides, vol. 1, pp. 247-261.

Wu, T.H. and Swanston, D.N., 1980. Risk of landslides in shallow soils and its relation to clearcutting in Southeastern Alaska. For. Sci., vol. 26, pp. 495-510.

Yalcin, A., 2008. GIS-based landslide susceptibility mapping using analytical hierarchy process and bivariate statistics in Ardesen (Turkey): Comparisons of results and confirmations, Turkey. Catena, vol. 72, pp. 1-12.

Yin, K.I. and Yan, T.Z., 1988. Statistical prediction models for slope instability of metamorphosed rocks. Proc. 5th Intl. Symp. Landsl., Lausanne, Switzerland. A.A. Balkema, Rotterdam, The Netherlands, vol. 2, pp. 1269-1272.

Yoon, W.S., Jeong, U.J., and Kim, J.H., 2002. Kinematic analysis for sliding failure of multi-faced rock slopes. Engg. Geol., vol. 67, pp. 51-61.

Zaruba, Q. and Mencl, V., 1969. Landslides and their control. Elsevier, Amsterdam, 205p.

Zezere, J.L., Trigo, R.M., and Trigo, I.F., 2005. Shallow and deep landslides induced by rainfall in the Lisbon region (Portugal): Assessment of relationships with the North Atlantic Oscillation. Nat. Haz. Earth Sys. Sc., vol. 5, pp. 331-344.

Zhang, J., Jiao, J.J. and Yang, J., 2000. Insitu rainfall infiltration studies at a hillside in Hubei Province, China. Engg. Geol., vol. 57, pp. 31-38.

Zuoan, W., Shihai, L., Wang, J.G., and Ling, W., 2006. A dynamic comprehensive method for landslide control. Engg. Geol., 84, pp. 1-11.

PARTICULARS OF CANDIDATE

NAME OF CANDIDATE	: Mr. Supongtemjen
DEGREE	: PhD
DEPARTMENT	: Geology
TITLE OF DISSERTATION	:

Geological investigation of land instability between Kohima and Zhadima

DATE OF ADMISSION	: 24th November 2006
APPROVAL OF RESEARCH PROPOSAL	: 24th November 2006
REGN. NO. & DATE	: **274/2007 (24.11.2006)**

Head

Publications

I. Seminar Proceedings

1. Nokmatongba Jamir, Imtiwapang Aier, **Supongtemjen**, and G.T. Thong (2011). An Appraisal of the Debris Slide in Artang Ward, Mokokchung Town, Nagaland, NE India. *Proceedings of the National Seminar on* Geodynamics, sedimentation and biotic response in the context of India - Asia collision, *Mizoram University*. Memoirs of the *Geological Society of India*, pp. 259-268.

II. Journals

2. Imtiwapang Aier, **Supongtemjen**, and G.T. Thong (2009). Slope Mass Rating and Kinematic Analyses along part of NH 61, Nagaland, NE India. *International Journal of Earth Sciences and Engineering*, vol. 2, No. 6, pp. 520-526.

III. Book Chapters

3. Imtiwapang Aier, **Supongtemjen**, Meniele Khalo and G.T. Thong (2009). Geotechnical assessment of the Mehrülietsa slide in Kohima, Nagaland. In: Kumar, A., Kushwaha, R.A.S., and Thakur, B. (Eds), *Earth System Sciences*, vol. 1, pp. 81-88. Concept Publishing Company, New Delhi.
4. Imtiwapang Aier, G.T. Thong, and **Supongtemjen** (2011). Geological evaluation of surface instability along NH 39 (180 km), west of Raj Bhavan, Kohima, Nagaland. In: Singh, T.N. and Sharma, Y.C. (Eds), *Slope stability - Natural and Man Made Slope*, pp. 192-201. Vayu Education of India, New Delhi.

IV. Abstracts

5. Imtiwapang Aier, **Supongtemjen**, Meniele Khalo and G.T. Thong (2008). RS & GIS applications for landslide investigations in Kohima town and its surrounding, Nagaland, NE India. Organised by Indian Society for Remote Sensing (ISRO) and Nirma University, Ahmedabad.

Conferences Attended

1. Application of RS & GIS for Vulnerability & Risk Assessment related to landslide hazards in Kohima town, Nagaland, NE India. National Seminar on Indo-Myanmar ranges in the tectonic framework of Himalaya and SE Asia, 27-29 November, 2008.
2. Presented paper on landslide hazard zonation mapping of area NNW of Kohima town, Nagaland. 2nd Indian Landslides Congress, 15-16 September, 2011. National Institute of Infotech & Management, Guwahati, Assam.

Geological Reports

1. G.T. Thong, I. Aier, and **Supongtemjen** (2007). Preliminary Geological Report on the 179-km Slide. *Border Roads Organisation Report*.
2. Imtiwapang Aier, **Supongtemjen**, and Glenn T. Thong (2007). Geological report on the southern subsidence of Mehrülietsa colony. *Nagaland Government Report*.
3. G.T. Thong, I. Aier, and **Supongtemjen** (2007). Landslide hazard zonation mapping and instability investigations of Meriema Campus, Kohima, Nagaland University.
4. **Supongtemjen**, Imtiwapang Aier, and G.T. Thong (2011). Risk analysis & mitigation measures along Nagaland University approach road Kohima Campus, Meriema.

Courses/Trainings Attended

1. DST Sponsored "Capacity Building and Training program on Landslide Hazard Mitigations in North Eastern India". Organised by Department of Earth Siences, Manipur University, 1-5 September 2008.
2. DST Sponsored "Brainstorming Session on Landslides of Northeast India". Organised by Department of Geology, Nagaland University, Kohima, 5-6 May 2009.
3. Landslide Risk Management. Conducted by Administrative Training Institute, Government of Nagaland, 11-15 May 2009.

Consultancy

1. Consultant on Remote Sensing & GIS mapping on "An Archaeological investigation at Chungliyimti". Anthropological Society of Nagaland and Department of Art & Culture, Government of Nagaland (2008-2009).
2. Consultant on Remote Sensing & GIS mapping on "Archaeology of early Naga ancestral sites". Anthropological Society of Nagaland and Department of Art & Culture, Government of Nagaland (2009-2010).

Project Fellow

1. Landslide hazard zonation mapping and instability investigations of Meriema Campus, Nagaland University. *Nagaland University, Kohima*, 2009.
2. Landslide hazard zonation mapping and risk assessment of the area between Kohima and Zhadima, Nagaland. *Department of Science & Technology, New Delhi*, 2011.
3. Georesources of Kohima and Dimapur urban areas of Nagaland: Part 1 - Landslide hazard microzonation mapping and risk assessment of major slides of the urban area of Kohima town, 2012.